AHMED RATNANI

ISOGEOMETRIC ANALYSIS: THEORY AND PRACTICE

Contents

Part I

Computer Aided Design

Introduction

Contents

Among the different representations to describe a quarter of circle (of radius 1 and centered at the origin), one can use an implicit form using the equation

$$f(x,y) := x^2 + y^2 - 1 = 0, \quad x \geq 0 \text{ and } y \geq 0$$

In practice, implicit forms are well adapted for unbounded geometries. On the other hand, given a point, it is easy to determine if it is on the curve or a surface. Although, this is an important question, in general, we are interested in geometric manipulations in CAD systems, such as improving the resolution, smoothness and having local control of a given curve or surface. These properties are very difficult to ensure when using an implicit form; at the end, a computer needs discrete values in order to plot or manipulate a CAD object, which is in opposition with the analytical form represented by an equation.

Parametric curves

Another way of representing a quarter of circle is to consider the parametric curve define in 1, where $\theta \in \left[0, \frac{\pi}{2}\right]$

$$\mathcal{C}(\theta) = \begin{bmatrix} x(\theta) \\ y(\theta) \end{bmatrix} = \begin{bmatrix} \cos\theta \\ \sin\theta \end{bmatrix} \tag{1}$$

in which case we can compute its derivative as

$$\mathcal{C}'(\theta) = \begin{bmatrix} -\sin\theta \\ \cos\theta \end{bmatrix} \tag{2}$$

The tangent at $\theta = 0$ and $\theta = \frac{\pi}{2}$ are then given by $\mathcal{C}'(\theta := 0) = \begin{bmatrix} 0 \\ 1 \end{bmatrix}$ and $\mathcal{C}'(\theta := \frac{\pi}{2}) = \begin{bmatrix} -1 \\ 0 \end{bmatrix}$.

Another way to represent the quarter of circle, is to introduce the variable $t := \tan\frac{\theta}{2}$, then we get the following rational form 3, where $t \in [0,1]$,

$$\mathcal{C}(t) = \begin{bmatrix} x(t) \\ y(t) \end{bmatrix} = \begin{bmatrix} \frac{1-t^2}{1+t^2} \\ \frac{2t}{1+t^2} \end{bmatrix} \tag{3}$$

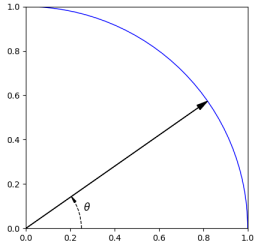

Figure 1: Quarter of circle of radius 1, using polar coordinates.

Exercise 1 *Compare the CPU cost for an evaluation for the presented representations.*

There are different advantages for having a parametric form:

- Extending a 2D curve to 3D,
- Ideal for bounded curves and surfaces,

- Natural orientation of curves and surfaces,
- Appropriate representation for design on a computer. In some particular cases, the coefficients in a parametric form possess interesting geometric significance,
- Computing a point on a curve is easy, while finding its parametric value is a in general a non-linear problem,

Remark 1 *Notice that in some cases, this representation may introduce singularities that are unrelated to the described geometry.*

Remark 2 *Computing the derivatives (tangent or normal vectors at the extremeties) needs an evaluation. We shall be more interested in representation where such informations can be extracted directly from the parametric representations.*

Although one can use any parametric representation for CAD systems, it is important to restrict to a representation that is

- capable of reproducing a *wild class* of curves/surfaces
- easy to implement
- efficient and accurate evaluation
- numerical stable evaluation
- *easy* evaluation of points and their derivatives
- evaluation complexity of the same or comparable order as polynomials
- small memory storage

Power basis form of a curve

If we restrict our representation to polynomials, one naive way would be to use power basis, *i.e.* monomials as in 4

$$\mathcal{C}(t) = \sum_{i=0}^{n} \mathbf{a}_i t^i \tag{4}$$

where $\mathbf{a}_i = \begin{bmatrix} a_i^x \\ a_i^y \\ a_i^z \end{bmatrix}$ are 2D or 3D vectors.
Using the Taylor expansion, we get $\mathcal{C}'(t)|_{t=0} = i!\mathbf{a}_i$, which leads to $\mathbf{a}_i = \frac{\mathcal{C}'(t)|_{t=0}}{i!}$. We then have a direct access to the derivative at $t = 0$, but only at this point.

The evaluation of such a form can be done using the Horner algorithm as described in 5:

$$\mathcal{C}(t) = a_0 + t\,(a_1 + t\,(a_2 + t\,(\cdots + t\,(a_{n-1} + ta_n)))) \tag{5}$$

Exercise 2 *Compute the CPU cost for the Horner algorithm.*

Exercise 3 *Write a Python implementation for the Horner algorithm.*

Exercise 4 (Parallel evaluation) *Let us consider a polynomial P of degree n, defined as $P(t) = \sum_{i=0}^{n} a_i t^i$. Using the form*

$$P(t) = \sum_{j=0}^{k-1} x^j P_j(x^k)$$

as a splitting into k independent parts, write a Python code for the parallel evaluation and compute its complexity.

Remark 3 *The use of power basis form is not suited for shape and geometric design; the coefficients do not have any geoemtric meaning and modifying them do not allow for a good control of a curve or a surface,*

Bézier curves

Contents

Bernstein polynomials

In 1885, Weierstrass proved that the set of polynomial functions on $[0,1]$ is dense in $\mathcal{C}([0,1])$. In 1912, Sergei Bernstein gave a simple proof to this result by introducing the now-famous Bernstein polynomials 6:

$$B_k^n(x) = \binom{n}{k} x^k (1-x)^{n-k}, \quad \text{where} \quad k \in [0,n] \text{ and } x \in [0,1] \tag{6}$$

In figure Fig. 2, we plot Bernstein polynomials of degrees 1 to 5. From these plots, we see that Bernstein polynomials are positive, the first and last polynomials are equal to 1 on the 0 and 1 respectivaly. More properties will be discussed in the sequel.

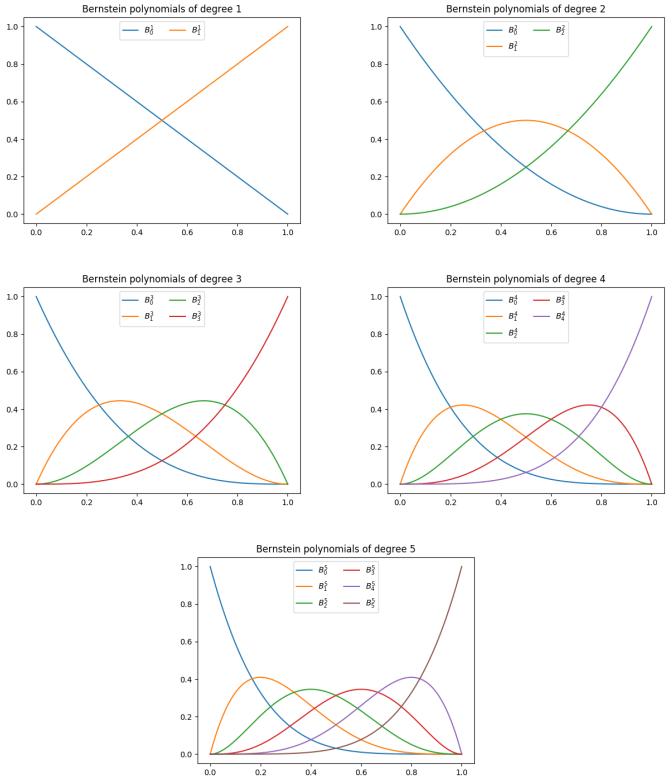

Figure 2: Bernstein polynomials of degree $n = 1, 2, 3, 4, 5$.

Properties of Bernstein polynomials

- $B_k^n(x) \geq 0$, for all $k \in [0,n]$ and $x \in [0,1]$ [positivity]
- $\sum_{k=0}^n B_k^n(x) = 1$, for all $x \in [0,1]$ [partition of unity]
- $B_0^n(0) = B_n^n(1) = 1$

- B_k^n has exactly one maximum on the interval $[0,1]$, at $\frac{k}{n}$
- $\left(B_k^n(x)\right)_{0\leq k\leq n}$ is symmetric with respect to $x=\frac{1}{2}$ [symmetry]
- Bernstein polynomials can be defined recursively using the formulae 7

$$B_k^n(x) = (1-x)B_k^{n-1}(x) + xB_{k-1}^{n-1}(x) \tag{7}$$

  where we assume $B_k^n(x) = 0$ is $k<0$ or $k>n$

- Bernstein derivatives can be computed using the formulae 8

$$B_k^{n\prime}(x) = n\left(B_{k-1}^{n-1}(x) - B_k^{n-1}(x)\right) \tag{8}$$

  using the same assumption as before.

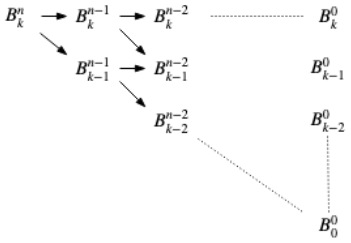

Figure 3: General evaluation triangular diagram for a Bernstein polynomials.

Exercise 5 *Show all Bernstein properties.*

Bézier curves

Rather than taking the power basis as in 4, Pierre Bézier used Bernstein polynomials, in the 1960s while working at *Renault*. This leads to the following definition of a polynomial curve 14

$$\mathcal{C}(t) = \sum_{k=0}^{n} \mathbf{P}_k B_k^n(t) \tag{9}$$

The vector coefficients $(\mathbf{P})_{0\leq k\leq n}$ are called *Bézier points* or **control points**. The reason for this will become clear in the sequel.

Examples

Example 1. A linear ($n=1$) Bézier curve (fig. 4) is defined as

$$\mathcal{C}(t) = \mathbf{P}_0 B_0^1(t) + \mathbf{P}_1 B_1^1(t)$$

which describes a straight line from $\mathbf{P}_0$ to $\mathbf{P}_1$, since $B_0^1(t) = 1-t$ and $B_1^1(t) = t$.

Example 2. A quadratic ($n=2$) Bézier curve (fig. 5) is defined as

$$\mathcal{C}(t) = (1-t)^2\mathbf{P}_0 + 2t(1-t)\mathbf{P}_1 + t^2\mathbf{P}_2$$

We remark that

- the curve starts at $\mathbf{P}_0$ and ends at $\mathbf{P}_2$,
- the curve does not pass through the point $\mathbf{P}_1$,

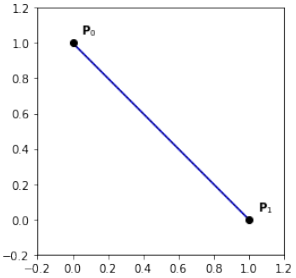

Figure 4: Example of a linear Bézier curve.

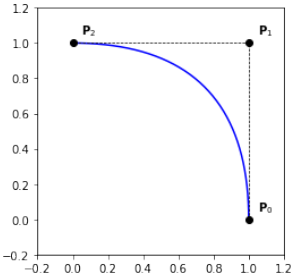

Figure 5: Example of a quadratic Bézier curve.

- the tangent directions to the curves at its extremeties are parallel to $\mathbf{P}_1 - \mathbf{P}_0$ and $\mathbf{P}_2 - \mathbf{P}_1$,
- the curve is contained in the polygone (triangle) formed by $\mathbf{P}_0\mathbf{P}_1\mathbf{P}_2$. This polygone is called the *control polygon* and it approximates the shape of the curve.

Example 3. A cubic ($n = 3$) Bézier curve (figures 6,7,8) is defined as

$$\mathcal{C}(t) = (1-t)^3\mathbf{P}_0 + 3t(1-t)^2\mathbf{P}_1 + 3t^2(1-t)\mathbf{P}_2 + t^3\mathbf{P}_3$$

We remark that

- the curves start at $\mathbf{P}_0$ and end at $\mathbf{P}_3$,
- the curves do not pass through the points $\mathbf{P}_1$ and $\mathbf{P}_2$,
- the tangents directions to the curves at their extremeties are parallel to $\mathbf{P}_1 - \mathbf{P}_0$ and $\mathbf{P}_3 - \mathbf{P}_2$,
- the control polygons approximate the shape of the curves,
- the curves follow the orientation of the control polygons,
- the curves are contained in the convex hulls of their control polygons (*convex hull property*).

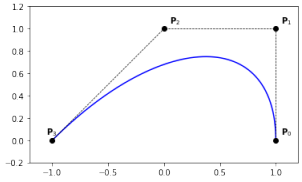

Figure 6: Example of a cubic Bézier curve.

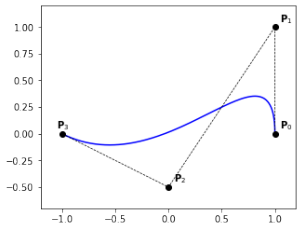

Figure 7: Example of a cubic Bézier curve.

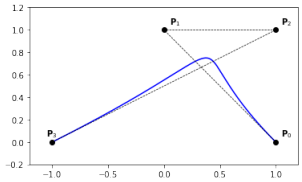

Figure 8: Example of a cubic Bézier curve.

Derivatives of a Bézier curve
Using the formulae 8, we have

$$\mathcal{C}'(t) = \sum_{k=0}^{n} \mathbf{P}_k B_k^{n\prime}(t) = \sum_{k=0}^{n} n\mathbf{P}_k \left(B_{k-1}^{n-1}(x) - B_k^{n-1}(x) \right)$$

by reordering the indices, we get 10

$$\mathcal{C}'(t) = \sum_{k=0}^{n-1} n \left(\mathbf{P}_{k+1} - \mathbf{P}_k \right) B_k^{n-1}(t) \tag{10}$$

Therefor, we get the direct acces to the first order derivatives at the extremeties of a Bézier curve using the formulae 11

$$\begin{cases} \mathcal{C}'(0) = n \left(\mathbf{P}_1 - \mathbf{P}_0 \right) \\ \mathcal{C}'(1) = n \left(\mathbf{P}_n - \mathbf{P}_{n-1} \right) \end{cases} \tag{11}$$

Second derivatives can also be computed directly from the control points using the formulae 12

$$\begin{cases} \mathcal{C}''(0) = n(n-1) \left(\mathbf{P}_0 - 2\mathbf{P}_1 + \mathbf{P}_2 \right) \\ \mathcal{C}''(1) = n(n-1) \left(\mathbf{P}_n - 2\mathbf{P}_{n-1} + \mathbf{P}_{n-2} \right) \end{cases} \tag{12}$$

Properties of Bézier curves

Because of the *symmetry* of the Bernstein polynomials, we have

- $\sum_{k=0}^{n} \mathbf{P}_k B_k^n = \sum_{k=0}^{n} \mathbf{P}_k B_{n-k}^n$

Thanks to the interpolation property, for B_0^n and B_n^n, of the Bernstein polynomials at the endpoints, we get

- $\mathcal{C}(0) = \mathbf{P}_0$ and $\mathcal{C}(1) = \mathbf{P}_n$

Using the partition unity property of the Bernstein polynomials, we get

- any point $\mathcal{C}(t)$ is an *affine combination* of the control points

Therefor,

- Bézier curves are affinely invariant; *i.e.* the image curve $\Phi(\sum_{k=0}^{n} \mathbf{P}_k B_k^n)$ of a Bézier curve, by an affine mapping Φ, is the Bézier curve having $(\Phi(\mathbf{P}_i))_{0 \leq i \leq n}$ as control points.

due to the partition unity of the Bernstein polynomials and their non-negativity,

- any point $\mathcal{C}(t)$ is a *convex combination* of the control points

finally, we get the *convex hull property*,

- A Bézier curve lies in the convex hull of its control points

Rational Bézier curves

We first introduce the notion of Rational Bernstein polynomials defined as, and $w_i > 0, \forall i \in [0, n]$

$$R_k^n(t) := \frac{w_i B_k^n(t)}{\sum_{i=0}^{n} w_i B_i^n(t)} \tag{13}$$

Properties of Rational Bernstein polynomials

- $R_k^n(x) \geq 0$, for all $k \in [0, n]$ and $x \in [0, 1]$ [positivity]
- $\sum_{k=0}^{n} R_k^n(x) = 1$, for all $x \in [0, 1]$ [partition of unity]
- $R_0^n(0) = R_n^n(1) = 1$
- R_k^n has exactly one maximum on the interval $[0, 1]$,
- Bernstein polynomials are Rational Bernstein polynomials when all weights are equal

Definition 1 (Rational Bézier curve)

$$\mathcal{C}(t) = \sum_{k=0}^{n} \mathbf{P}_k R_k^n(t) \tag{14}$$

where $R_k^n(t) := \frac{w_i B_k^n(t)}{\sum_{i=0}^{n} w_i B_i^n(t)}$ *and* $w_i > 0, \forall i \in [0, n]$

Examples

Example 1. We consider the quadratic Rational Bézier curve, where the weights are given by $w_0 = 1$, $w_1 = 1$ and $w_2 = 2$ and the control points are $\mathbf{P}_0 = \begin{pmatrix} 1 \\ 0 \end{pmatrix}$, $\mathbf{P}_1 = \begin{pmatrix} 1 \\ 1 \end{pmatrix}$ and $\mathbf{P}_2 = \begin{pmatrix} 0 \\ 1 \end{pmatrix}$. This leads to a representation of the circular arc, using the parametric form $\mathcal{C}(t) = \begin{pmatrix} \frac{1-t^2}{1+t^2} \\ \frac{2t}{1+t^2} \end{pmatrix}$.

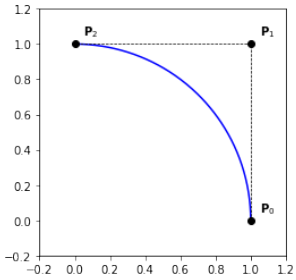

Figure 9: Circular arc using quadratic Rational Bézier curve.

Composite Bézier curves

A composite Bézier curve is a piecewise Bézier curve that is at least continuous at the interpolant control points. An example is given in Fig. 10. The global curve inherit all the nice properties of Bézier curves however, it has a major drawback: when moving an interpolant control point, we must ensure that the associated regularity is not broken, unless it is what we want. This means that a good representation of a curve needs to have the locality control through control points, but also the control points must be associated to some given regularity.
Since Bernstein polynomials are defined locally on the interval $[0, 1]$, and they do not encode any global redularity of the curve, we need another representation, in terms of other functions, while keeping in mind that these functions must be polynomials on every subinterval. Such representation is provided by the Schoenberg spaces, for which B-Splines form a basis. In the next chapter, we will first introduce the uniform Splines, also known as Cardinal Splines, show their advantages and limitations, then we will introduce the general definition of B-Splines.

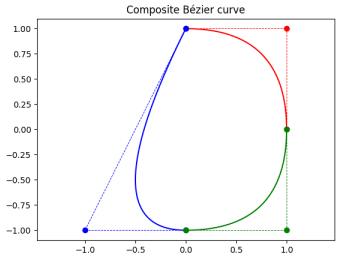

Figure 10: A composite Bézier curve using 3 quadratic Bézier curves.

B-Splines

Contents

In general, one needs to design curves with given regularities at some specific locations. For this purpose, rather than considering piecewise Bézier curves with additional constraints on the control points, we can enforce these constraints on a given space of functions. The Schoenberg spaces [1946] are perfect for this purpose. Before giving more details about Schoenberg spaces, which will be covered in the Approximation Theory part, let us for the moment, use a formal definition, as the following: given a subdivision $\{x_0 < x_1 < \cdots < x_r\}$ of the interval $I = [x_0, x_r]$, the Schoenberg space is the space of piecewise polynomials of degree p, on the interval I and given regularities $\{k_1, k_2, \cdots, k_{r-1}\}$ at the internal points $\{x_1, x_2, \cdots, x_{r-1}\}$.

Given m and p as natural numbers, let us consider a sequence of non decreasing real numbers $T = \{t_i\}_{0 \leqslant i \leqslant m}$. T is called **knots sequence**. From a knots sequence, we can generate a B-splines family using the reccurence formula 15.

Definition 2 (B-Splines using Cox-DeBoor Formula) *The j-th B-spline of degree p is defined by the recurrence relation:*

$$N_j^p = \frac{t - t_j}{t_{j+p} - t_j} N_j^{p-1} + \frac{t_{j+p+1} - t}{t_{j+p+1} - t_{j+1}} N_{j+1}^{p-1}, \tag{15}$$

where

$$N_j^0(t) = \chi_{[t_j, t_{j+1}[}(t)$$

for $0 \leq j \leq m - p - 1$.

Remark 4 *When working with Bernstein polynomials, we introduced the convention* $B_i^n = 0$ *for all* $i < 0$ *or* $i > n$. *For B-Splines, we have a similar convetion* $N_j^p = 0$ *if* $j < 0$ *or* $j > n$. *In addition, we also assume* $\frac{0}{0} = 0$, *when using the formula 15 and* $N_j^0 = 0$ *if* $t_j = t_{j+1}$.

Remark 5 $k = p + 1$ *is called the order of the B-Splines.*

In figure Fig. 12, we plot the quadratic B-Splines functions associated to the knots sequence $\{0, 0, 0, 1, 2, 2, 3, 4, 5, 5, 5\}$. As we can see, there are 8 B-Splines functions and we recover the interpolation property at the first and last knot. In addition, while all the B-Splines are *smooth* at the internal knots, N_3^2 is only $\mathcal{C}^0$ at the grid point 2.
Now if we look for the cubic B-Splines that are associated to the same knots sequence $\{0, 0, 0, 1, 2, 2, 3, 4, 5, 5, 5\}$, we see that the interpolation property is no longer true 13.

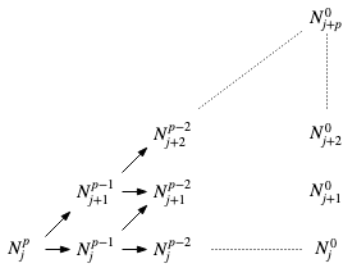

Figure 11: General evaluation triangular diagram for a B-Spline.

Knot vector families

There are two kind of **knot vectors**, called **clamped** and **unclamped**. Both families contains uniform and non-uniform sequences. In figure

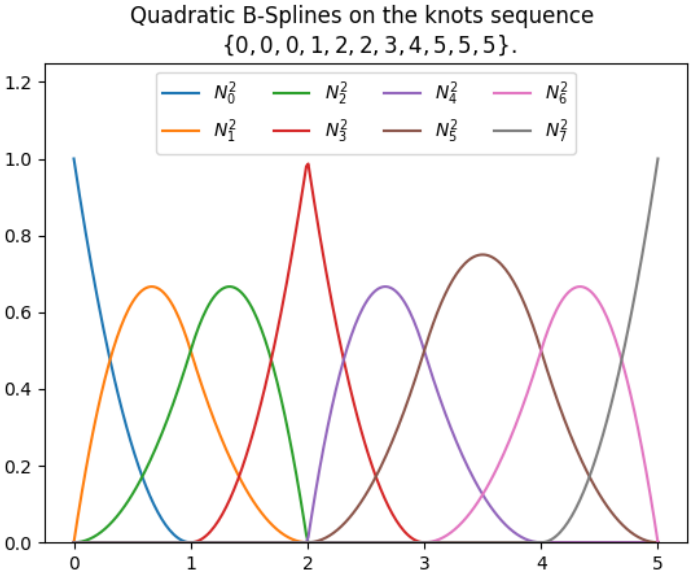

Figure 12: Quadratic B-Splines generated using the knots sequence $\{0, 0, 0, 1, 2, 2, 3, 4, 5, 5, 5\}$.

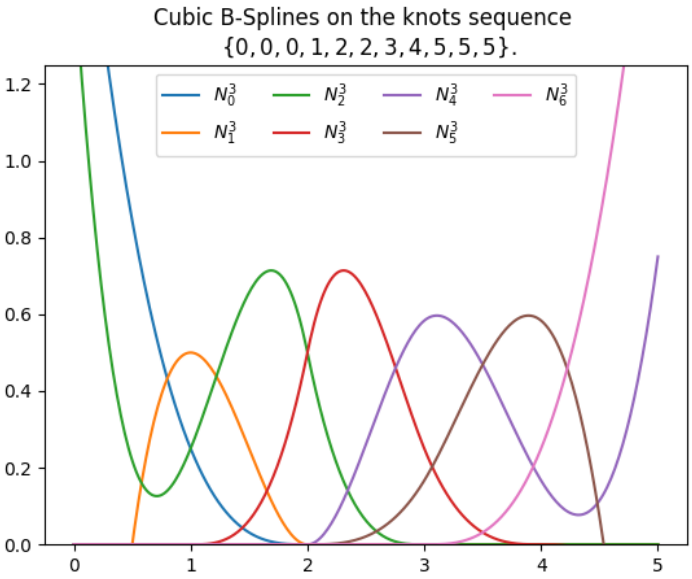

Figure 13: Cubic B-Splines generated using the knots sequence $\{0, 0, 0, 1, 2, 2, 3, 4, 5, 5, 5\}$.

Fig. 14, we show examples of clamped uniform knots. Fig. 15, we show examples of clamped non-uniform knots, while figures Fig. 16 and Fig. 17 are examples of unclamped knots sequences for uniform and non-uniform cases, respectively.

The special case of clamped sequences, where the first and the last

knots are repeated $p+1$ times exactly is known as **open knot vector**.

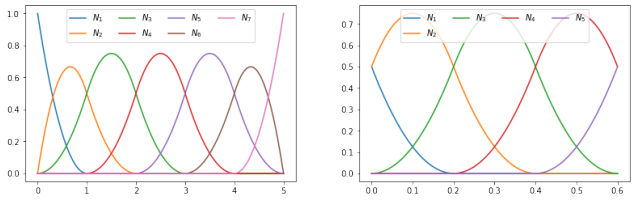

Figure 14: **Clamped uniform knots** (left) quadratic B-Splines using $T = \{0,0,0,1,2,3,4,5,5,5\}$, (right) quadratic B-Splines using $T = \{-0.2,-0.2,0.0,0.2,0.4,0.6,0.8,0.8\}$.

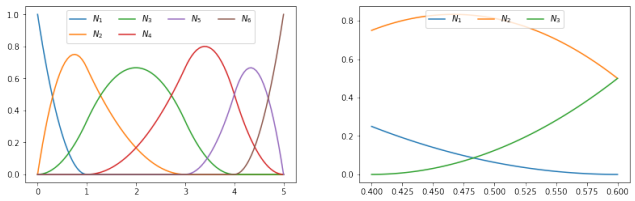

Figure 15: **Clamped non-uniform knots** (left) quadratic B-Splines using $T = \{0,0,0,1,3,4,5,5,5\}$, (right) quadratic B-Splines using $T = \{-0.2,-0.2,0.4,0.6,0.8,0.8\}$.

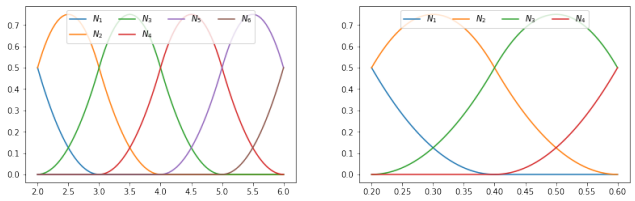

Figure 16: **Unclamped uniform knots** (left) quadratic B-Splines using $T = \{0,1,2,3,4,5,6,7,8\}$, (right) quadratic B-Splines using $T = \{-0.2,0.0,0.2,0.4,0.6,0.8,1.0\}$.

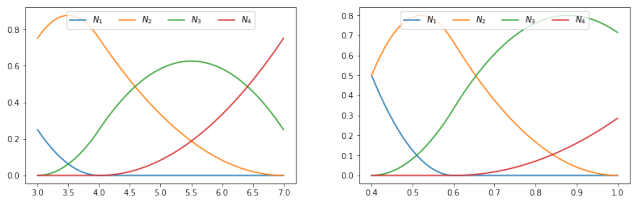

Figure 17: **Unclamped non-uniform knots** (left) quadratic B-Splines using $T = \{0,0,3,4,7,8,9\}$, (right) quadratic B-Splines using $T = \{-0.2,0.2,0.4,0.6,1.0,2.0,2.5\}$.

Examples

Before stating some B-Splines properties, let us take a look to some examples.

Example 1. Let $T = \{0,1,2\}$ and $p = 1$.

We first compute the B-Splines of degrees 0

$$N_0^0 = \begin{cases} 1, & 0 \leq t < 1 \\ 0, & \text{otherwise} \end{cases}$$

$$N_1^0 = \begin{cases} 1, & 1 \leq t < 2 \\ 0, & \text{otherwise} \end{cases}$$

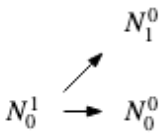

Figure 18: Evaluation diagram for examples 1, 2 and 3.

The B-Splines of degree 1 is

$$N_0^1 = \frac{t-0}{1-0}N_0^0 + \frac{2-t}{2-1}N_1^0$$

which yields

$$N_0^1 = \begin{cases} t, & 0 \leq t < 1 \\ 2-t, & 1 \leq t < 2 \\ 0, & \text{otherwise} \end{cases}$$

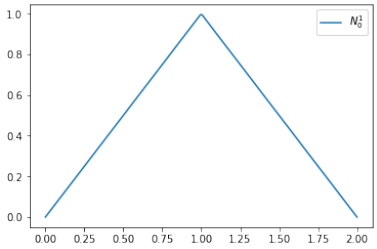

Figure 19: Linear B-Spline associated to the knot sequence $T = \{0, 1, 2\}$.

Example 2. Let $T = \{0, 0, 1\}$ and $p = 1$.
We first compute the B-Splines of degrees 0

$$N_0^0 = 0, \quad \forall t \in \mathbb{R}$$

$$N_1^0 = \begin{cases} 1, & 0 \leq t < 1 \\ 0, & \text{otherwise} \end{cases}$$

The B-Splines of degree 1 is

$$N_0^1 = \frac{t-0}{0-0}N_0^0 + \frac{1-t}{1-0}N_1^0$$

which yields

$$N_0^1 = \begin{cases} 1-t, & 0 \leq t < 1 \\ 0, & \text{otherwise} \end{cases}$$

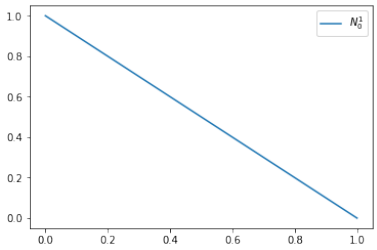

Figure 20: Linear B-Spline associated to the knot sequence $T = \{0, 0, 1\}$.

Example 3. Let $T = \{0, 1, 1\}$ and $p = 1$.
We first compute the B-Splines of degrees 0

$$N_0^0 = \begin{cases} 1, & 0 \leq t < 1 \\ 0, & \text{otherwise} \end{cases}$$

$$N_1^0 = 0, \quad \forall t \in \mathbb{R}$$

The B-Splines of degree 1 is

$$N_0^1 = \frac{t-0}{1-0}N_1^0 + \frac{1-t}{1-1}N_2^0$$

which yields

$$N_0^1 = \begin{cases} t, & 0 \leq t < 1 \\ 0, & \text{otherwise} \end{cases}$$

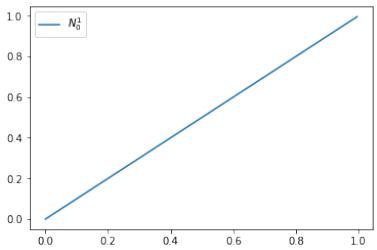

Figure 21: Linear B-Spline associated to the knot sequence $T = \{0, 1, 1\}$.

Example 4. Let $T = \{0, 0, 1, 1\}$ and $p = 1$.

In the examples 2 and 3 we computed the linear B-Splines associated to the knots sequences $\{0, 0, 1\}$ and $\{0, 1, 1\}$. Then we get immediatly that the knots sequens $\{0, 0, 1, 1\}$ will exactly generate the same B-Splines, *i.e.*

$$N_0^1 = \begin{cases} 1 - t, & 0 \leq t < 1 \\ 0, & \text{otherwise} \end{cases}$$

$$N_1^1 = \begin{cases} t, & 0 \leq t < 1 \\ 0, & \text{otherwise} \end{cases}$$

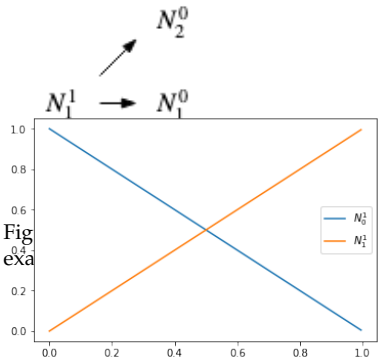

Figure 23: Linear B-Splines associated to the knots sequence $T = \{0, 0, 1, 1\}$.

Example 5. Let $T = \{0, 0, 1, 2\}$ and $p = 1$.

In the examples 2 and 1 we computed the linear B-Splines associated to the knots sequences $\{0, 0, 1\}$ and $\{0, 1, 2\}$. Then we get immediatly that the knots sequens $\{0, 0, 1, 2\}$ will exactly generate the same B-Splines, *i.e.*

$$N_0^1 = \begin{cases} 1 - t, & 0 \leq t < 1 \\ 0, & \text{otherwise} \end{cases}$$

$$N_1^1 = \begin{cases} t, & 0 \leq t < 1 \\ 2 - t, & 1 \leq t < 2 \\ 0, & \text{otherwise} \end{cases}$$

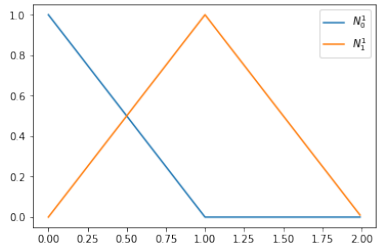

Figure 24: Linear B-Splines associated to the knot sequence $T = \{0, 0, 1, 2\}$.

Example 6. Let $T = \{0, 0, 1, 1\}$ and $p = 2$.

The linear B-Splines were computed in the previous example. Then for degree 2, we get

$$N_0^2 = \frac{t-0}{1-0} N_0^1 + \frac{1-t}{1-0} N_1^1$$

which leads to

$$N_0^2 = \begin{cases} 2(1-t)t, & 0 \leq t < 1 \\ 0, & \text{otherwise} \end{cases}$$

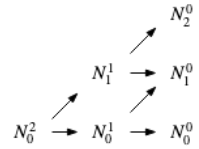

Figure 25: Evaluation diagram for examples 6 and 7.

Example 7. Let $T = \{0, 0, 1, 2\}$ and $p = 2$.

The linear B-Splines were computed in the examples 2 and 1. Then for degree 2, we get

$$N_0^2 = \frac{t-0}{1-0} N_0^1 + \frac{2-t}{2-0} N_1^1$$

which yields

$$N_0^2 = \begin{cases} 2t - \frac{3}{2}t^2, & 0 \leq t < 1 \\ \frac{1}{2}(2-t)^2, & 1 \leq t < 2 \\ 0, & \text{otherwise} \end{cases}$$

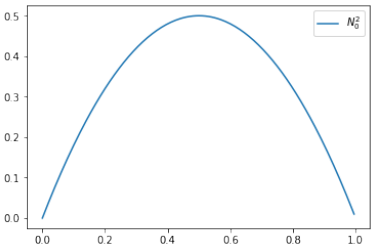

Figure 26: Quadratic B-Splines associated to the knots sequence $T = \{0, 0, 1, 1\}$.

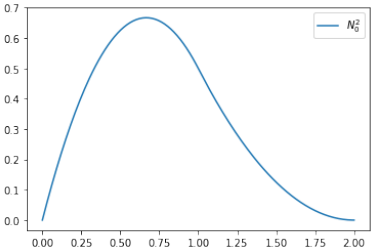

Figure 27: Quadratic B-Splines associated to the knots sequence $T = \{0, 0, 1, 2\}$.

Example 8. Let $T = \{0, 0, 1, 2, 3, 3\}$ and $p = 1$.

We first compute the B-Splines of degrees 0

$$N_0^0 = 0, \quad \forall t \in \mathbb{R}$$

$$N_1^0 = \begin{cases} 1, & 0 \leq t < 1 \\ 0, & \text{otherwise} \end{cases}$$

$$N_2^0 = \begin{cases} 1, & 1 \leq t < 2 \\ 0, & \text{otherwise} \end{cases}$$

$$N_3^0 = \begin{cases} 1, & 2 \leq t < 3 \\ 0, & \text{otherwise} \end{cases}$$

$$N_4^0 = 0, \quad \forall t \in \mathbb{R}$$

The B-Splines of degree 1 are

$$N_0^1 = \frac{t-0}{0-0} N_0^0 + \frac{1-t}{1-0} N_1^0$$

$$N_1^1 = \frac{t-0}{1-0} N_1^0 + \frac{2-t}{2-1} N_2^0$$

$$N_2^1 = \frac{t-1}{2-1} N_2^0 + \frac{3-t}{3-2} N_3^0$$

$$N_3^1 = \frac{t-2}{3-2} N_3^0 + \frac{3-t}{3-3} N_4^0$$

which gives

$$N_0^1 = \begin{cases} 1-t, & 0 \leq t < 1 \\ 0, & \text{otherwise} \end{cases}$$
$$N_1^1 = \begin{cases} t, & 0 \leq t < 1 \\ 2-t, & 1 \leq t < 2 \\ 0, & \text{otherwise} \end{cases}$$
$$N_2^1 = \begin{cases} t-1, & 1 \leq t < 2 \\ 3-t, & 2 \leq t < 3 \\ 0, & \text{otherwise} \end{cases}$$
$$N_3^1 = \begin{cases} t-2, & 2 \leq t < 3 \\ 0, & \text{otherwise} \end{cases}$$

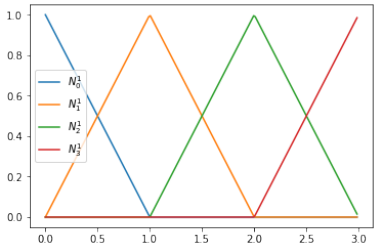

Figure 28: Linear B-Splines associated to the knots sequence $T = \{0,0,1,2,3,3\}$.

Example 9. Let $T = \{0,0,0,1,1,1\}$ and $p = 2$.

We first compute the B-Splines of degrees 0

$$N_0^0 = N_1^0 = 0, \quad \forall t \in \mathbb{R}$$
$$N_2^0 = \begin{cases} 1, & 0 \leq t < 1 \\ 0, & \text{otherwise} \end{cases}$$
$$N_3^0 = N_4^0 = 0, \quad \forall t \in \mathbb{R}$$

The B-Splines of degree 1 are

$$N_0^1 = \frac{t-0}{0-0}N_0^0 + \frac{0-t}{0-0}N_1^0$$
$$N_1^1 = \frac{t-0}{0-0}N_1^0 + \frac{1-t}{1-0}N_2^0$$
$$N_2^1 = \frac{t-0}{1-0}N_2^0 + \frac{1-t}{1-1}N_3^0$$
$$N_3^1 = \frac{t-1}{1-1}N_3^0 + \frac{1-t}{1-1}N_4^0$$

which leads to

$$N_0^1 = 0, \quad \forall t \in \mathbb{R}$$
$$N_1^1 = \begin{cases} 1-t, & 0 \leq t < 1 \\ 0, & \text{otherwise} \end{cases}$$
$$N_2^1 = \begin{cases} t, & 0 \leq t < 1 \\ 0, & \text{otherwise} \end{cases}$$
$$N_3^1 = 0, \quad \forall t \in \mathbb{R}$$

The B-Splines of degree 2 are

$$N_0^2 = \frac{t-0}{0-0}N_0^1 + \frac{1-t}{1-0}N_1^1$$
$$N_1^2 = \frac{t-0}{1-0}N_1^1 + \frac{1-t}{1-0}N_2^1$$
$$N_2^2 = \frac{t-0}{1-0}N_2^1 + \frac{1-t}{1-1}N_3^1$$

which leads to

$$N_0^2 = \begin{cases} (1-t)^2, & 0 \leq t < 1 \\ 0, & \text{otherwise} \end{cases}$$
$$N_1^2 = \begin{cases} 2t(1-t), & 0 \leq t < 1 \\ 0, & \text{otherwise} \end{cases}$$
$$N_2^2 = \begin{cases} t^2, & 0 \leq t < 1 \\ 0, & \text{otherwise} \end{cases}$$

In this case, we recover the Bernstein polynomials of degree 2.

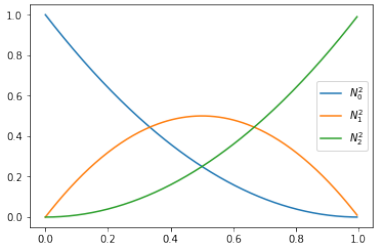

Figure 29: Linear B-Splines associated to the knots sequence $T = \{0,0,0,1,1,1\}$.

Exercise 6 *Compute the B-Splines generated by the knots sequences:*

- $T = \{0,0,0,1,2,2,3,4,5,5,5\}$ *with* $p = 2$
- $T = \{0,1,2,2,3,4,5,5,6\}$ *with* $p = 2$

B-Splines properties

B-Splines have many interesting properties that are listed below. In general, most of the proofs are done by induction on the B-Spline degree.

Proposition 1 *B-splines are piecewise polynomial of degree p*

Proof. We proceed by induction. When $p = 0$, B-Splines are either the 0 or the characteristic functions, which are constant polynomials. For $p = 1$, the Cox-DeBoor formula shows that the generated B-Splines are piecewise linear functions, because of the weights that multply the constant functions (B-Splines of degree $p = 0$).
Now assume that B-Splines of degree $p-1$ are piecewise polynomials of degree $p-1$. Again using the Cox-DeBoor formula, we see that the degree will be increased by 1 because of the linear weights, on each sub-interval. This completes the proof. ∎

Remark 6 *The B-splines functions associated to open knots sequences without internal knots, i.e. the length of the knots sequence is exactly* $2p+2$*, are the Bernstein polynomials of degreep.*

Proposition 2 (compact support) $N_j^p(t) = 0$ *for all* $t \notin [t_j, t_{j+p+1})$.

Proof. By taking a look at the triangular diagram 11 for the evaluation of the jth B-Spline of degree p. We see that N_j^p depends only on the B-Splines $\{N_j^0, N_{j+1}^0, \cdots, N_{j+p}^0\}$. The laters are exactly the characteristic functions on the intervals $[t_i, t_{i+1}), \forall i \in \{j, j+1, \cdots, j+p\}$. Therefor, $N_j^p(t) = 0$, for all $t \notin [t_j, t_{j+p+1})$. ∎

Proposition 3 *If* $t \in [t_j, t_{j+1})$, *then only the B-splines* $\{N_{j-p}^p, \cdots, N_j^p\}$ *are non vanishing at* t.

Proof. Using the last proposition, the support of N_i^p is defined as $\text{supp}\left(N_i^p\right) = [t_i, t_{i+p+1})$ for every $i \in \{j-p, \cdots, j\}$. Therefor, on the interval $[t_j, t_{j+1}) = \bigcap_{j-p \le i \le j} \text{supp}\left(N_i^p\right)$, only the B-Splines $\{N_{j-p}^p, \cdots, N_j^p\}$ are non-zeros. ∎

Proposition 4 (non-negativity) $N_j^p(t) \ge 0, \quad \forall t \in [t_j, t_{j+p+1})$

Proof. This can be proved by induction. It is true for $p = 0$, since all B-Splines are either 0 or the characteristic function. Assume the property holds for $p-1$, using the Cox-DeBoor formula we have:

$$N_j^p = \frac{x - t_j}{t_{j+p} - t_j} N_j^{p-1} + \frac{t_{j+p+1} - x}{t_{j+p+1} - t_{j+1}} N_{j+1}^{p-1}$$

since, $t \in [t_j, t_{j+p+1})$, we have $\frac{x-t_j}{t_{j+p}-t_j} \ge 0$ and $\frac{t_{j+p+1}-x}{t_{j+p+1}-t_{j+1}} \ge 0$ whenever $t_{j+p} > t_j$ and $t_{j+p+1} > t_{j+1}$, otherwise these terms are identicaly equal to 0, by convention.

On the other hand, $N_j^{p-1} \ge 0$ and $N_{j+1}^{p-1} \ge 0$. Therefor there linear combination is also positive. ∎

Proposition 5 (Partition of unity) $\sum N_i^p(t) = 1, \forall t \in \mathbb{R}$

Remark 7 *The previous sum* $\sum N_i^p(t)$ *has a meaning since for every* $t \in \mathbb{R}$, *only* $p+1$ *B-Splines are non-vanishing.*

Proof. We prove this result by induction again. For $p = 0$, the property is true. Now let us assume it is true for $p-1$.

Let j denotes the span of t. We know that $\sum N_i^p(t) = \sum_{i=j-p}^{j} N_i^p(t)$. Now, using the Cox-DeBoor formula, we have

$$\sum_{i=j-p}^{j} N_i^p(t) = \sum_{i=j-p}^{j} \left(\frac{t - t_i}{t_{i+p} - t_i} N_i^{p-1}(t) + \frac{t_{i+p+1} - t}{t_{i+p+1} - t_{i+1}} N_{i+1}^{p-1}(t) \right)$$

by changing the summation index in the second part, we get

$$\sum_{i=j-p}^{j} N_i^p(t) = \sum_{i=j-p}^{j} \frac{t - t_i}{t_{i+p} - t_i} N_i^{p-1}(t) + \sum_{i=j-p+1}^{j+1} \frac{t_{i+p} - t}{t_{i+p} - t_i} N_i^{p-1}(t)$$

On the other hand, we know that the only B-Splines of degree $p-1$ that are non-vanishing on the interval $[t_j, t_{j+1})$ are $\{N_{j-p+1}^{p-1}, \cdots, N_j^{p-1}\}$, meaning that $N_{j-p}^{p-1} = N_{j+1}^{p-1} = 0$. Therefor,

$$\sum_{i=j-p}^{j} N_i^p(t) = \sum_{i=j-p+1}^{j} \left(\frac{t - t_i}{t_{i+p} - t_i} + \frac{t_{i+p} - t}{t_{i+p} - t_i} \right) N_i^{p-1}(t)$$

hence,

$$\sum_{i=j-p}^{j} N_i^p(t) = \sum_{i=j-p+1}^{j} N_i^{p-1}(t)$$

Finaly, we use the induction assumtion to complete the proof. ■

Remark 8 *For the sake of simplicity, we shall avoid using summation indices on linear expansion of B-Splines.*

Lemma 1

$$\sum a_j N_j^p = \sum \left(\frac{t_{j+p} - t}{t_{j+p} - t_j} a_{j-1} + \frac{t - t_j}{t_{j+p} - t_j} a_j \right) N_j^{p-1} \tag{16}$$

Proof. Using the Cox-DeBoor formula, we have

$$\sum a_j N_j^p = \sum \left(a_j \frac{t - t_j}{t_{j+p} - t_j} N_j^{p-1} + a_j \frac{t_{j+p+1} - t}{t_{j+p+1} - t_{j+1}} N_{j+1}^{p-1} \right)$$

By changing the summation index in the second part of the right hand side, we get

$$\sum a_j N_j^p = \sum a_j \frac{t - t_j}{t_{j+p} - t_j} N_j^{p-1} + \sum a_{j-1} \frac{t_{j+p} - t}{t_{j+p} - t_j} N_j^{p-1}$$

which yields

$$\sum a_j N_j^p = \sum \left(a_j \frac{t - t_j}{t_{j+p} - t_j} + a_{j-1} \frac{t_{j+p} - t}{t_{j+p} - t_j} \right) N_j^{p-1}$$

■

Proposition 6 (Marsden's idenity)

$$(x - y)^p = \sum_j \rho_j^p(y) N_j^p(x) \tag{17}$$

where

$$\rho_j^p(y) = \prod_{i=j+1}^{j+p} (t_i - y) \tag{18}$$

Proof. Seting $a_j := \rho_j^p(y)$ in the lemma 1, we get

$$\sum \rho_j^p(y) N_j^p(x) = \sum \left(\frac{t_{j+p} - x}{t_{j+p} - t_j} \rho_{j-1}^p(y) + \frac{x - t_j}{t_{j+p} - t_j} \rho_j^p(y) \right) N_j^{p-1}(x)$$

on the other hand, by introducing $\alpha_j^{p-1} = \prod_{i=j+1}^{j+p-1} (t_i - y)$, we have

$$\begin{aligned} \frac{t_{j+p} - x}{t_{j+p} - t_j} \rho_{j-1}^p(y) + \frac{x - t_j}{t_{j+p} - t_j} \rho_j^p(y) &= \alpha_j^{p-1} \left(\frac{t_{j+p} - x}{t_{j+p} - t_j} (t_j - y) + \frac{x - t_j}{t_{j+p} - t_j} (t_{j+p} - y) \right) \\ &= (x - y) \rho_j^{p-1}(y) \end{aligned}$$

Therefor,

$$\sum \rho_j^p(y) N_j^p(x) = (x - y) \sum \rho_j^{p-1}(y) N_j^{p-1}(x)$$

By repeating the same computation $p - 1$ times (one can also use an induction for this), we get the desired result. ∎

Thanks to Marsden's identity and the proposition 3, we now are able to prove the local linear independence of the B-Splines basis functions.

Proposition 7 (Local linear independence) *On each interval $[t_j, t_{j+1})$, the B-Splines are lineary independent.*

Proof. On the interval $[t_j, t_{j+1})$, there are only $p + 1$ non-vanishing B-Splines. On the other hand, these B-Splines reproduce polynomials, thanks to the Marsden's identity. Hence, $\{N_{j-p}^p, \cdots, N_j^p\}$ are a basis for polynomials of degree at most p, and are therefor, lineary independent. ∎

Remark 9 *We will see in the Approximation theory part, that the B-Splines family has also a global linear independence property.*

Derivatives of B-Splines

The derivative of B-Splines can be computed reccursivly by deriving the formula 15, which gives

Proposition 8

$$N_j^{p\prime} = \frac{p}{t_{j+p} - t_j} N_j^{p-1} - \frac{p}{t_{j+p+1} - t_{j+1}} N_{j+1}^{p-1} \tag{19}$$

Proof. We prove this by induction on p.

For $p = 1$, N_j^{p-1} and N_{j+1}^{p-1} are either 0 or 1, then $N_j^{p\prime}$ is either $\frac{1}{t_{j+1} - t_j}$ or $-\frac{1}{t_{j+2} - t_{j+1}}$.

Now assume that 19, is true for $p-1$, where $p > 1$. Deriving the Cox-DeBoor formula leads to

$$N_j^{p\prime} = \frac{1}{t_{j+p} - t_j} N_j^{p-1} + \frac{t - t_j}{t_{j+p} - t_j} N_j^{p-1\prime} - \frac{1}{t_{j+p+1} - t_{j+1}} N_{j+1}^{p-1} + \frac{t_{j+p+1} - t}{t_{j+p+1} - t_{j+1}} N_{j+1}^{p-1\prime}$$

Using the induction assumption on $N_j^{p-1\prime}$ and $N_{j+1}^{p-1\prime}$ and subtituting in the last equation yields

$$\begin{aligned}
N_j^{p\prime} &= \frac{1}{t_{j+p} - t_j} N_j^{p-1} - \frac{1}{t_{j+p+1} - t_{j+1}} N_{j+1}^{p-1} \\
&+ \frac{t - t_j}{t_{j+p} - t_j} \left(\frac{p-1}{t_{j+p-1} - t_j} N_j^{p-2} - \frac{p-1}{t_{j+p} - t_{j+1}} N_{j+1}^{p-2} \right) \\
&+ \frac{t_{j+p+1} - t}{t_{j+p+1} - t_{j+1}} \left(\frac{p-1}{t_{j+p} - t_{j+1}} N_{j+1}^{p-2} - \frac{p-1}{t_{j+p+1} - t_{j+2}} N_{j+2}^{p-2} \right) \\
&= \frac{1}{t_{j+p} - t_j} N_j^{p-1} - \frac{1}{t_{j+p+1} - t_{j+1}} N_{j+1}^{p-1} \\
&+ \frac{p-1}{t_{j+p} - t_j} \frac{t - t_j}{t_{j+p-1} - t_j} N_j^{p-2} \\
&+ \frac{p-1}{t_{j+p} - t_{j+1}} \left(\frac{t_{j+p+1} - t}{t_{j+p+1} - t_{j+1}} - \frac{t - t_j}{t_{j+p} - t_j} \right) N_{j+1}^{p-2} \\
&- \frac{p-1}{t_{j+p+1} - t_{j+1}} \frac{t_{j+p+1} - t}{t_{j+p+1} - t_{j+2}} N_{j+2}^{p-2}
\end{aligned}$$

Since,

$$\frac{t_{j+p+1} - t}{t_{j+p+1} - t_{j+1}} - \frac{t - t_j}{t_{j+p} - t_j} = \frac{t_{j+p} - t}{t_{j+p} - t_j} - \frac{t - t_{j+1}}{t_{j+p+1} - t_{j+1}}$$

we get

$$\begin{aligned}
N_j^{p\prime} &= \frac{1}{t_{j+p} - t_j} N_j^{p-1} - \frac{1}{t_{j+p+1} - t_{j+1}} N_{j+1}^{p-1} \\
&+ \frac{p-1}{t_{j+p} - t_j} \left(\frac{t - t_j}{t_{j+p-1} - t_j} N_j^{p-2} + \frac{t_{j+p} - t}{t_{j+p} - t_j} N_{j+1}^{p-2} \right) \\
&- \frac{p-1}{t_{j+p+1} - t_{j+1}} \left(\frac{t - t_{j+1}}{t_{j+p} - t_{j+1}} N_{j+1}^{p-2} + \frac{t_{j+p+1} - t}{t_{j+p+1} - t_{j+2}} N_{j+2}^{p-2} \right)
\end{aligned}$$

By applying the Cox-DeBoor formula for N_j^{p-1} and N_{j+1}^{p-1} we get the desired result. ■

Exercise 7 *Show that the r-th derivative of N_j^p is given by*

$$N_j^{p(r)} = \frac{p}{t_{j+p} - t_j} N_j^{p-1(r-1)} - \frac{p}{t_{j+p+1} - t_{j+1}} N_{j+1}^{p-1(r-1)}$$

Cardinal B-Splines

Contents

Cardinal B-Splines

Cardinal B-Splines play an important role in the approximation theory (multi-resolution approximation, ...). In the sequel, we shall give a definition of the Cardinal B-Spline using the convolution operator. Then, we will present some of the most important properties, at least needed when using uniform B-Splines in a Finite Elements method.

Definition 3 *A cardinal B-spline of zero degree, denoted by ϕ_0, is the characteristic function over the interval $[0,1)$, i.e.,*

$$\phi_0(t) := \begin{cases} 1, & t \in [0,1) \\ 0, & \textit{otherwise} \end{cases} \tag{20}$$

A cardinal B-Spline of degree p, $p \in \mathbb{N}$, denoted by ϕ_p, is defined by convolution as

$$\phi_p(t) = \left(\phi_{p-1} * \phi_0\right)(t) = \int_{\mathbb{R}} \phi_{p-1}(t-s)\phi_0(s)\, ds \tag{21}$$

Example 1: When $p = 1$, it is easy to show that

$$\phi_1(t) := \begin{cases} t, & t \in [0,1) \\ 2-t, & t \in [1,2) \\ 0, & \text{otherwise} \end{cases} \tag{22}$$

When $p = 2$, it is easy to show that

$$\phi_2(t) := \begin{cases} \frac{1}{2}x^2, & t \in [0,1) \\ \frac{1}{2} + (x-1) - (x-1)^2, & t \in [1,2) \\ \frac{1}{2} - (x-2) + \frac{1}{2}(x-2)^2, & t \in [2,3) \\ 0, & \text{otherwise} \end{cases} \tag{23}$$

In figure (Fig. 30), we plot the Cardinal B-Splines of degrees $1, 2, 3$ and 4.

Remark 10 *The colored area under the graph of ϕ_2 represents the average $\int_{x-1}^{x} \phi_2(t)dt$ which is the value $\phi_3(x)$.*

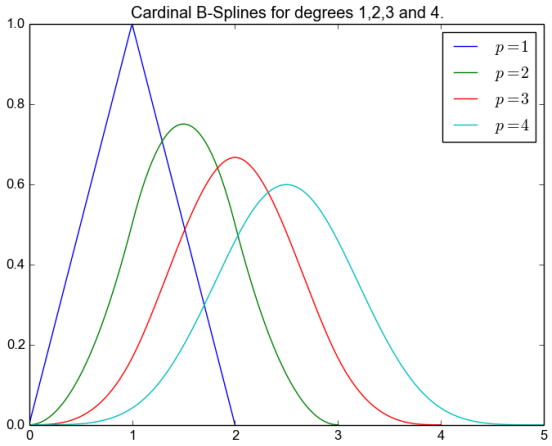

Figure 30: Cardinal B-Splines of degrees $1, 2, 3$ and 4

Cardinal B-Splines properties

Let ϕ_p be a cardinal B-Spline of degree p, $p \in \mathbb{N}$. The following properties can be proved by induction on the B-Spline degree p.

Theorem 8 (Minimal support) *the support of ϕ_p is $[0, p+1]$*

Theorem 9 (Positivity) $\phi_p(s) \geq 0, \forall s \in [0, p+1]$

Theorem 10 $\phi_p \in \mathcal{C}^{p-1}$

Theorem 11 *ϕ_p is a piecewise-polynomial of degree p at each interval $[i, i+1], \forall i \in \{0, 1, \ldots, p\}$*

The sequence $\{0, 1, 2, \ldots, p\}$ is known as the *breaks* of the cardinal B-Spline of degree p.

Theorem 12 $\forall t \in [0, p+1]$ *and* $p \geq 1$, *we have*

$$\dot{\phi}_p(t) = \phi_{p-1}(t) - \phi_{p-1}(t-1) \tag{24}$$

Theorem 13 (Symmetry) *ϕ_p is symmetric on the interval $[0, p+1]$, i.e.*

$$\phi_p(t) = \phi_p(p+1-t), \quad \forall t \in [0, p+1] \tag{25}$$

The following theorem was proved in 1972 by both Cox and Deboor separatly.

Theorem 14 (Cox-Deboor) $\forall t \in [0, p+1]$ *and* $p \geq 1$, *we have*

$$\phi_p(t) = \frac{t}{p}\phi_{p-1}(t) + \frac{p+1-t}{p}\phi_{p-1}(t-1) \tag{26}$$

Proof. Let $\phi_i^p(t) := \phi_p(t-i), \forall t \in [0, p+1]$. We will proof the result by induction. Since both sides vanish at $t = 0$, we will use the equivalence to the formula for the derivative 12.

$$\phi_0^{p-1} - \phi_1^{p-1} = \frac{1}{p}\left(\phi_0^{p-1} - \phi_1^{p-1}\right) + \left[\frac{t}{p}\left(\phi_0^{p-2} - \phi_1^{p-2}\right) + \frac{p+1-t}{p}\left(\phi_1^{p-2} - \phi_2^{p-2}\right)\right] \tag{27}$$

The last term of the previous relation, can be written as

$$\frac{p-1}{p}\left[\left(\frac{t}{p-1}\phi_0^{p-2} + \frac{p-t}{p-1}\phi_1^{p-2}\right) - \left(\frac{t-1}{p-1}\phi_1^{p-2} + \frac{p-(t-1)}{p-1}\phi_2^{p-2}\right)\right] \tag{28}$$

Now, if we assume that the recursion is valid up to $p-1$, then the last terms is equal to

$$\frac{p-1}{p}\left(\phi_0^{p-1} - \phi_1^{p-1}\right) \tag{29}$$

■

For any Cardinal B-Spline of degree p, we denote by $\alpha_i^p = \left(\alpha_{0,i}^p, \alpha_{1,i}^p, \ldots, \alpha_{p,i}^p\right)$ the sequence of its mononial coefficients on $[i, i+1]$

$$\phi_p(t) = \alpha_{0,i}^p + \alpha_{1,i}^p t^2 + \ldots + \alpha_{p,i}^p t^p, \quad \forall t \in [i, i+1] \tag{30}$$

When $i, j \notin [0, p]$, we set $\alpha_{i,j}^p$

Theorem 15 (Taylor Coefficients)

$$\alpha_{l,k}^p = \frac{k}{p}\alpha_{l,k}^{p-1} + \frac{1}{p}\alpha_{l-1,k}^{p-1} + \frac{p+1-k}{p}\alpha_{l,k-1}^{p-1} - \frac{1}{p}\alpha_{l-1,k-1}^{p-1} \tag{31}$$

Proof. Using the Cox-Deboor theorem (14), if $x = i + t$ where $t \in [0, 1]$, we have

$$\frac{x}{p}\phi^{p-1}(x) = \left(\frac{k}{p} + \frac{t}{p}\right)\left(\alpha_{0,i-1}^{p-1} + \alpha_{1,i-1}^{p-1}t^2 + \ldots + \alpha_{p,i-1}^{p-1}t^p\right)$$
$$\frac{p+1-x}{p}\phi^{p-1}(x-1) = \left(\frac{p+1-k}{p} - \frac{t}{p}\right)\left(\alpha_{0,i-1}^{p-1} + \alpha_{1,i-1}^{p-1}t^2 + \ldots + \alpha_{p,i-1}^{p-1}t^p\right)$$

Adding the last expressions together, we get the the expected relation for $\alpha_{p,i}^p$. ■

Corollary 1 (Cardinal B-Splines evaluation using pp-form) *Thanks to the theorem (15), we can compute analyticaly the Taylor coefficients for low B-Splines order (Tables 1, 2 and 3).*

Theorem 16 (Inner product)

$$\int_{\mathbb{R}} \phi_p^{(r)}(t)\phi_q^{(s)}(t+k)\,dt = (-1)^r\phi_{p+q+1}^{(r+s)}(p+1+k) = (-1)^s\phi_{p+q+1}^{(r+s)}(q+1-k) \tag{32}$$

Interval	Taylor coefficients	
$[0,1]$	$0 \quad 1$	$\alpha_{0,1}$
$[1,2]$	$1 \quad -1$	$\alpha_{1,1}$

Table 1: The linear Cardinal B-Spline Taylor coefficients.

Interval	Taylor coefficients			
$[0,1]$	0	0	$\frac{1}{2}$	$\alpha_{0,2}$
$[1,2]$	$\frac{1}{2}$	1	-1	$\alpha_{1,2}$
$[2,3]$	$\frac{1}{2}$	-1	$\frac{1}{2}$	$\alpha_{2,2}$

Table 2: The quadratic Cardinal B-Spline Taylor coefficients.

Interval	Taylor coefficients				
$[0,1]$	0	0	0	$\frac{1}{6}$	$\alpha_{0,3}$
$[1,2]$	$\frac{1}{6}$	$\frac{1}{2}$	$\frac{1}{2}$	$-\frac{1}{2}$	$\alpha_{1,3}$
$[2,3]$	$\frac{2}{3}$	0	-1	$\frac{1}{2}$	$\alpha_{2,3}$
$[3,4]$	$\frac{1}{6}$	$-\frac{1}{2}$	$\frac{1}{2}$	$-\frac{1}{6}$	$\alpha_{1,3}$

Table 3: The cubic Cardinal B-Spline Taylor coefficients.

Cardinal B-Spline series

Scaled and translated Cardinal B-Splines

From now on, $h > 0$ will denote the mesh step. $h\mathbb{Z}$ is the uniform grid of width h. The scaled and translated Cardinal B-Spline of degree p is defined by

$$\phi_{i,h,p}(x) := \phi_p\left(\frac{x}{h} - i\right) \tag{33}$$

The support of $\phi_{i,h,p}$ is $[i, i+p+1]h$. We introduce the sequence $(t_i)_{i\in\mathbb{Z}}$, where $t_i = ih$, $\forall i \in \mathbb{Z}$. The following result is another version of the Cox-Deboor theorem (14).

Theorem 17 (Cox-Deboor) *$\forall t \in \mathbb{R}$ and $p \geq 1$, we have*

$$\phi_{i,h,p}(t) = \frac{t - t_i}{t_{i+p} - t_i}\phi_{i,h,p-1}(t) + \frac{t_{i+p+1} - t}{t_{i+p+1} - t_{i+1}}\phi_{i+1,h,p-1}(t) \tag{34}$$

with $\phi_{i,h,p}(t) = 0$, $\forall t \notin [t_i, t_{i+p+1}]$.

Proof. Using the definition of the scaled and translated Cardinal B-Spline and the theorem (14), we have

$$\phi_{i,h,p}(t) = \frac{t - ih}{hp}\phi_{i,h,p-1}(t) + \frac{h(p+1+i) - t}{hp}\phi_{i+1,h,p-1}(t) \tag{35}$$

The result is straightforward, using the fact that $t_{i+p} - t_i = t_{i+p+1} - t_{i+1} = hp$. ∎

Cardinal Splines

Definition 4 (Cardinal Spline) *A Cardinal Spline, or cardinal B-Spline serie, of degree p on the grid $h\mathbb{Z}$ is the linear combination*

$$\sum_{k\in\mathbb{Z}} c_k \phi_{k,h,p} \tag{36}$$

In figure (Fig. 31), we plot all non-vanishing Cardinal B-Splines on the interval $[2, 3]$. In figure (Fig. 32), we plot a Cardinal B-Spline serie.

Proposition 9 (Marsden's identity)

$$\forall x, t \in \mathbb{R}, (x-t)^p = \sum_{k\in\mathbb{Z}} m_{k,h,p}(t)\phi_{k,h,p}(x) \tag{37}$$

where $m_{k,h,p}(t) = h^p \Pi_{i=1}^{p}\left(k + i - \frac{t}{h}\right)$

Proof. ∎

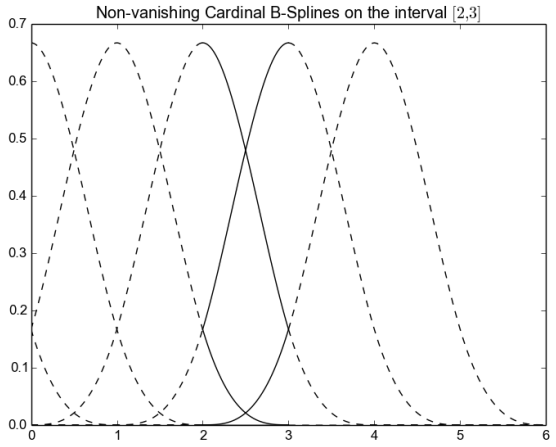

Figure 31: Non-vanishing Cardinal B-Splines on the interval $[2, 3]$

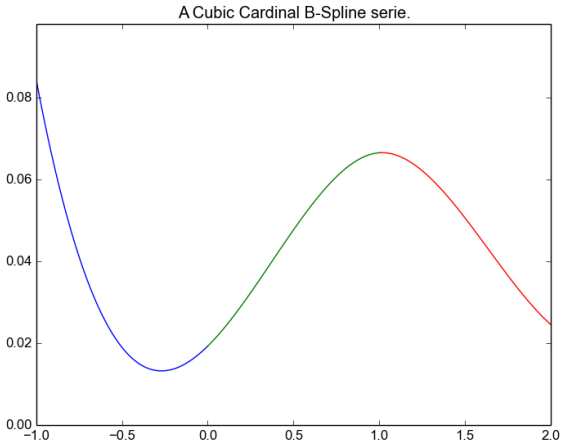

Figure 32: Example of a cubic Cardinal B-Spline serie.

Proposition 10 (Partition of unity)

$$1 = \sum_{k \in \mathbb{Z}} \phi_{k,h,p}(t), \quad \forall t \in \mathbb{R} \tag{38}$$

Proposition 11 (Linear independence) *For any element $[i, i+1]h$, the Cardinal B-Splines $\left(\phi_{k,h,p}\right)_{i-p \leq k \leq i}$ are linearly independent.*

Proposition 12 (Representation of Polynomials)

Proof. ■

B-Splines curves

Contents

B-Splines curves

Let $(\mathbf{P}_i)_{0\leqslant i\leqslant n} \in \mathbb{R}^d$ be a sequence of control points. Following the same approach as for Bézier curves, we define B-Splines curves as

Definition 5 (B-Spline curve) *The B-spline curve in $\mathbb{R}^d$ associated to $T = (t_i)_{0\leqslant i\leqslant n+p+1}$ and $(\mathbf{P}_i)_{0\leqslant i\leqslant n}$ is defined by :*

$$\mathcal{C}(t) = \sum_{i=0}^{n} N_i^p(t)\boldsymbol{P}_i$$

Remark 11 *The use of open knot vector leads to an **interpolating curve** at the endpoints.*

Examples

Example 1. We consider quadratic B-Spline curve on the knot vector $T = \{0,0,0,1,1,1\}$. This leads to a quadratic Bézier curve.

Example 2. We consider cubic B-Spline curve on the knot vector $T = \{0,0,0,0,1,1,1,1\}$. This leads to a cubic Bézier curve.

Example 3. We consider quadratic B-Spline curve on the knot vector $T = \{0,0,0,\frac{1}{4},\frac{1}{2},\frac{3}{4},1,1,1\}$.

We remark that

- the curve starts at $\mathbf{P}_0$ and ends at $\mathbf{P}_5$,
- the curve does not pass through the points $\{\mathbf{P}_i,\ 1 \leq i \leq 4\}$,
- the tangent directions to the curves at its extremeties are parallel to $\mathbf{P}_1 - \mathbf{P}_0$ and $\mathbf{P}_5 - \mathbf{P}_4$,
- the curve is localy $\mathcal{C}^2$ and only $\mathcal{C}^1$ at the knots $\{\frac{1}{4},\frac{1}{2},\frac{3}{4}\}$.

Example 4. We consider quadratic B-Spline curve on the knot vector $T = \{0,0,0,\frac{1}{4},\mathbf{\frac{1}{2}},\mathbf{\frac{1}{2}},\frac{3}{4},1,1,1\}$, where the knot $\frac{1}{2}$ has a multiplicity of 2.

We remark that

- adding a new knot increases the number of control points by 1,
- the curve starts at $\mathbf{P}_0$ and ends at $\mathbf{P}_6$ and passes through the point $\mathbf{P}_3$,
- the curve does not pass through the points $\{\mathbf{P}_i,\ 1 \leq i \leq 5,\ i \neq 3\}$,
- the tangent directions to the curves at its extremeties are parallel to $\mathbf{P}_1 - \mathbf{P}_0$ and $\mathbf{P}_6 - \mathbf{P}_5$,
- the tangent directions to the curves at $\mathbf{P}_3$ are parallel to $\mathbf{P}_3 - \mathbf{P}_2$ and $\mathbf{P}_4 - \mathbf{P}_3$,
- the curve is localy $\mathcal{C}^2$ inside each subinterval, $\mathcal{C}^1$ at the knots $\{\frac{1}{4},\frac{3}{4}\}$ and only $\mathcal{C}^0$ at $\frac{1}{2}$, where there is a *cusp*.

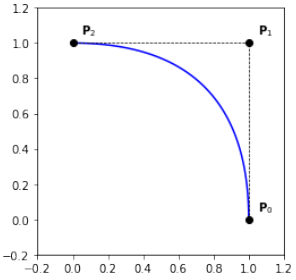

Figure 33: Quadratic B-Spline curve using the knot vector $T = \{0,0,0,1,1,1\}$

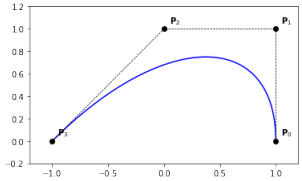

Figure 34: Cubic B-Spline curve using the knot vector $T = \{0,0,0,0,1,1,1,1\}$

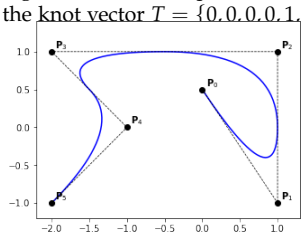

Figure 35: Quadratic B-Spline curve using the knot vector $T = \{0,0,0,\frac{1}{4},\frac{1}{2},\frac{3}{4},1,1,1\}$

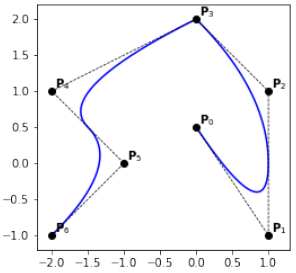

Figure 36: Quadratic B-Spline curve using the knot vector $T = \{0,0,0,\frac{1}{4},\frac{1}{2},\frac{1}{2},\frac{3}{4},1,1,1\}$ with a cusp.

Example 5. We consider quadratic B-Spline curve on the knot vector $T = \{0, 0, 0, \frac{1}{4}, \frac{1}{2}, \frac{1}{2}, \frac{3}{4}, 1, 1, 1\}$, where the knot $\frac{1}{2}$ has a multiplicity of 2.

We remark that although the knot $\frac{1}{2}$ has a multiplicity of 2, the curve is visualy smooth. In fact, it still has the same properties as in the previous example, except that the curve is more than just $\mathcal{C}^0$ at the double knot $\frac{1}{2}$, but not $\mathcal{C}^1$. To be more specific, it has a regularity of $\mathcal{G}^1$ at the knot $\frac{1}{2}$.

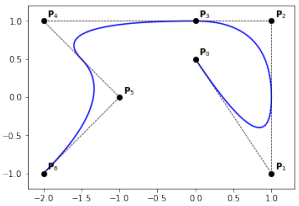

Figure 37: Quadratic B-Spline curve using the knot vector $T = \{0, 0, 0, \frac{1}{4}, \frac{1}{2}, \frac{1}{2}, \frac{3}{4}, 1, 1, 1\}$ without a cusp.

Example 6. In this example, we show the impact of increasing the degree *vs* increasing the number of internal knots.

Given a control polygon defined by the points $\{\mathbf{P}_i,\ 0 \leq i \leq 6$, we use first a Bézier representation of degree 6 (Fig. 38) and a quadratic B-Spline curve (Fig. 39) to approach the broken lines defined by the control polygon. As we can see, the use of more knots gives a better approximation. We shall give a proof for this result in the futur.

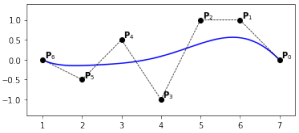

Figure 38: B-Spline curve of degree 6 using the knot vector $T = \{0, 0, 0, 0, 0, 0, 0, 1, 1, 1, 1, 1, 1, 1\}$

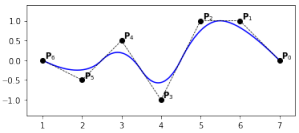

Figure 39: Quadratic B-Spline curve using the knot vector $T = \{0, 0, 0, 0.2, 0.4, 0.6, 0.8, 1, 1, 1\}$

Properties of B-Splines curves

We have the following properties for a *B-spline* curve:

- If $n = p$, then $\mathcal{C}$ is a B'ezier-curve,
- $\mathcal{C}$ is a piecewise polynomial curve,
- The curve interpolates its extremas if the associated multiplicity of the first and the last knot are maximum (*i.e.* equal to $p + 1$),
- Invariance with respect to affine transformations,
- B-Spline curves are affinely invariant; *i.e.* the image curve $\Phi(\sum_{i=0}^{n} \mathbf{P}_i N_i^p)$ of a B-Spline curve, by an affine mapping Φ, is the B-Spline curve having $(\Phi(\mathbf{P}_i))_{0 \leq i \leq n}$ as control points and the same knot vector,
- strong convex-hull property: if $t_j \leq t \leq t_{j+1}$, then $\mathcal{C}(t)$ is inside the convex-hull associated to the control points $\mathbf{P}_{j-p}, \cdots, \mathbf{P}_j$,
- local modification : moving $\mathbf{P}_j$ affects $\mathcal{C}(t)$, only in the interval $[t_j, t_{j+p+1}]$,
- the control polygon is a linear approximation of the curve. We will see later that the control polygon converges to the curve under knot insertion and degree elevation (with different *speeds*).
- *Variation diminishing*: no plane intersects the curve more than the control polygon.

Derivtive of a B-spline curve

Using the derivative formula for *B-spline*, we can compute the derivative of a B-Spline curve:

$$\begin{aligned}
\mathcal{C}'(t) &= \sum_{i=0}^{n} \left(N_i^{p\prime}(t)\mathbf{P}_i \right) \\
&= \sum_{i=0}^{n} \left(\frac{p}{t_{i+p} - t_i} N_i^{p-1}(t)\mathbf{P}_i - \frac{p}{t_{i+1+p} - t_{i+1}} N_{i+1}^{p-1}(t)\mathbf{P}_i \right) \\
&= \sum_{i=0}^{n} \frac{p}{t_{i+p} - t_i} N_i^{p-1}(t)\mathbf{P}_i - \sum_{i=1}^{n+1} \frac{p}{t_{i+p} - t_i} N_i^{p-1}(t)\mathbf{P}_{i-1} \\
&= \sum_{i} N_i^{p-1}(t) \frac{p}{t_{i+p} - t_i} \left(\mathbf{P}_i - \mathbf{P}_{i-1} \right) \\
&= \sum_{i} N_i^{p-1}(t) \frac{p}{t_{i+p} - t_i} \nabla \mathbf{P}_i
\end{aligned}$$

where we introduced the **first backward difference** operator $\nabla \mathbf{P}_i := \mathbf{P}_i - \mathbf{P}_{i-1}$.

Examples

Example 1. we consider a quadratic B-Spline curve with the knot vector $T = \{000\ \frac{2}{5}\ \frac{3}{5}\ 111\}$. We have $\mathcal{C}(t) = \sum_{i=0}^{4} N_i^{2\prime}(t)\mathbf{P}_i$, then

$$\mathcal{C}'(t) = \sum_{i} N_i^1(t)\mathbf{Q}_i$$

where

$$\mathbf{Q}_0 = 5\{\mathbf{P}_2 - \mathbf{P}_1\} \quad \mathbf{Q}_1 = \frac{10}{3}\{\mathbf{P}_3 - \mathbf{P}_2\}$$

$$\mathbf{Q}_2 = \frac{10}{3}\{\mathbf{P}_4 - \mathbf{P}_3\} \quad \mathbf{Q}_3 = 5\{\mathbf{P}_5 - \mathbf{P}_4\}$$

the *B-splines* $\{N_i^1,\ 0 \leq i \leq 3\}$ are associated to the knot vector $T^* = \{00\ \frac{2}{5}\ \frac{3}{5}\ 11\}$.

Rational B-Splines (NURBS) curves

Let $\omega = (\omega_i)_{0 \leqslant i \leqslant n}$ be a sequence of non-negative reals. The *NURBS* functions are defined by a projective transformation:

Definition 6 (NURBS function) *The i-th NURBS of order k, associated to the knot vector T and the weights ω, is defined by*

$$R_i^p = \frac{\omega_i N_i^p}{\sum_j \omega_j N_j^p} \tag{39}$$

Remark 12 *Notice that when the weights are equal to* 1 *the NURBS are B-splines.*

Remark 13 *NURBS functions inherit most of B-splines properties. Remark that in the interior of a knot span, all derivatives exist, and are rational functions with non vanishing denominator.*

Definition 7 (NURBS curve) *The NURBS curve of degree p associated to the knot vector T, the control points $(\boldsymbol{P}_i)_{0\leqslant i\leqslant n}$ and the weights ω, is defined by*

$$\mathcal{C}(t) = \sum_{i=0}^{n} R_i^p(t)\boldsymbol{P}_i \tag{40}$$

Remark 14 (NURBS using perspective mapping) *Notice that a NURBS curve in $\mathbb{R}^d$ can be described as a NURBS curve in $\mathbb{R}^{d+1}$ using the control points:*

$$\boldsymbol{P}_i^{\omega} = (\omega_i \boldsymbol{P}_i, \omega_i) \tag{41}$$

This remark is used for the evaluation and also to extend most of the B-Splines fundamental geometric operations to NURBS curves.

Remark 15 *NURBS functions allow us to model, exactly, much more domains than B-splines. In fact, all conics can be exactly represented with NURBS.*

Modeling conics using NURBS

In this section, we will show how to construct an arc of conic, using rational *B-splines*. Let us consider the following knot vector : $T = \{000\ 111\}$, the generated *B-splines* are Bernstein polynomials. The general form of a rational Bézier curve of degree 2 is:

$$\mathcal{C}(t) = \frac{\omega_0 N_0^2(t)\mathbf{P}_0 + \omega_1 N_1^2(t)\mathbf{P}_1 + \omega_2 N_2^2(t)\mathbf{P}_2}{\omega_0 N_0^2(t) + \omega_1 N_1^2(t) + \omega_2 N_2^2(t)} \tag{42}$$

Remark 16 *Because of the multiplicity of the knots* 0 *and* 1*, the curve $\mathcal{C}$ is linking the control point $\mathbf{P}_0$ to $\mathbf{P}_2$.*

Let us consider the case $\omega_1 = \omega_3 = 1$, in which case the curve will have the following form:

$$\mathcal{C}(t) = \frac{N_0^2(t)\mathbf{P}_0 + \omega N_1^2(t)\mathbf{P}_1 + N_2^2(t)\mathbf{P}_2}{N_0^2(t) + \omega N_1^2(t) + N_2^2(t)} \tag{43}$$

Depending on the value of ω the resulting Bézier arc is either a line, ellipse, parabolic or hyperbolic arcs (Tab. 4).

$\omega = 0$	line
$0 < \omega < 1$	ellipse arc
$\omega = 1$	parabolic arc
$\omega > 1$	hyperbolic arc

Table 4: Modeling conics using *NURBS*. Possible values of ω and the corresponding conic arc.

Examples

Example 1. (Quarter circle) A quarter circle can be described by a quadratic Bézier arc with the control points (Tab. 5).

In figure Fig. 40, we plot the resulting NURBS curve and its control polygon.

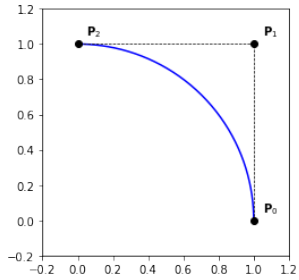

Figure 40: Quarter circle using a quadratic Bézier curve.

	$\mathbf{P}_i$	ω_i
0	$(1,0)$	1
1	$(1,1)$	$\frac{1}{\sqrt{2}}$
2	$(0,1)$	1

Table 5: Control points and their associated weights to model a quarter circle quadratic Bézier arc.

Example 2. (Circular arc 120) A circular arc of length 120 can be described with a quadratic Bézier curve, using the control points given in Tab. 6.

In figure Fig. 41, we plot the resulting NURBS curve and its control polygon.

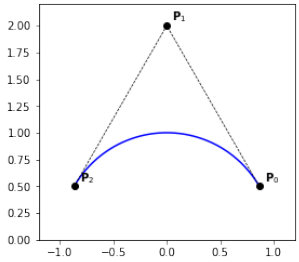

Figure 41: A circular arc of length 120 using a quadratic Bézier curve.

	$\mathbf{P}_i$	ω_i
0	$(\cos(\frac{\pi}{6}), \frac{1}{2})$	1
1	$(0,2)$	$\frac{1}{2}$
2	$(-\cos(\frac{\pi}{6}), \frac{1}{2})$	1

Table 6: Control points and their associated weights to model a circular arc of length 120.

Example 3. (half circle) In this example we show how to construct half of a circle using a cubic Bézier arc. The control points are given in the Tab. 7.

In figure Fig. 42, we plot the resulting NURBS curve and its control polygon.

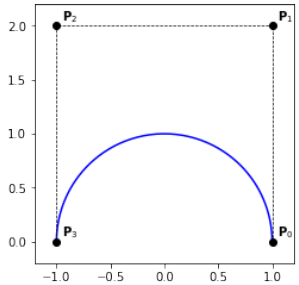

Figure 42: Half circle as a cubic Bézier curve.

	$\mathbf{P}_i$	ω_i
0	$(1,0)$	1
1	$(1,2)$	$\frac{1}{3}$
2	$(-1,2)$	$\frac{1}{3}$
3	$(-1,0)$	1

Table 7: Control points and their associated weights to model a half circle using a cubic Bézier arc.

Example 4. (Circle as four arcs) One can draw a circle using four quadratic Bézier arcs, 9 control points (Tab. 8) and the knot sequence $T = \{000, \frac{1}{4}, \frac{1}{4}, \frac{1}{2}, \frac{1}{2}, \frac{3}{4}, \frac{3}{4}, 111\}$.

In figure Fig. 43, we plot the resulting NURBS curve and its control polygon.

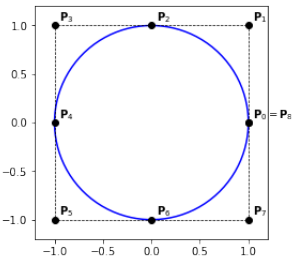

Figure 43: Circle as four Bézier curves described by a B-Spline curve using the knot vector $T = \{0,0,0,\frac{1}{4},\frac{1}{4},\frac{1}{2},\frac{1}{2},\frac{3}{4},\frac{3}{4},1,1,1\}$

	$\mathbf{P}_i$	ω_i
0	$(1,0)$	1
1	$(1,1)$	$\frac{1}{\sqrt{2}}$
2	$(0,1)$	1
3	$(-1,1)$	$\frac{1}{\sqrt{2}}$
4	$(-1,0)$	1
5	$(-1,-1)$	$\frac{1}{\sqrt{2}}$
6	$(0,-1)$	1
7	$(1,-1)$	$\frac{1}{\sqrt{2}}$
8	$(1,0)$	1

Table 8: Control points and their associated weights to model a circle using 4 quadratic Bézier arcs.

Example 5. (Circle as three arcs) One can draw a circle using three quadratic Bézier arcs of length 120, 7 control points (Tab. 9) and the knot sequence $T = \{000, \frac{1}{3}\frac{1}{3}, \frac{2}{3}, \frac{2}{3}, 111\}$.

In figure Fig. 44, we plot the resulting NURBS curve and its control polygon.

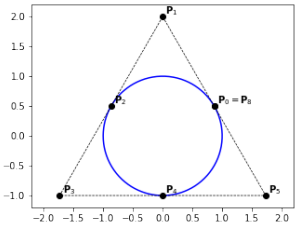

Figure 44: Circle as three Bézier curves described by a B-Spline curve using the knot vector $T = \{000, \frac{1}{3}\frac{1}{3}, \frac{2}{3}, \frac{2}{3}, 111\}$

	$\mathbf{P}_i$	ω_i
0	$(\cos(\frac{\pi}{6}), \frac{1}{2})$	1
1	$(0,2)$	$\frac{1}{2}$
2	$(-\cos(\frac{\pi}{6}), \frac{1}{2})$	1
3	$(-2\cos(\frac{\pi}{6}), -1)$	$\frac{1}{2}$
4	$(0,-1)$	1
5	$(2\cos(\frac{\pi}{6}), -1)$	$\frac{1}{2}$
6	$(\cos(\frac{\pi}{6}), \frac{1}{2})$	1

Table 9: Control points and their associated weights to model a circle using 3 quadratic Bézier arcs of length 120.

Fundamental geometric operations

When designing complex CAD models we usually start from simple geometries then manipulate them using different algorithms that are now well established. For example, one may need to have more control on a curve, by adding new control points. This can be done in two different ways:

- insert new knots
- elevate the polynomial degree

In general, one way need to use both approaches.

Remark 17 *Notice that these two operations keep the B-Spline curve unchanged.*

In the sequel, we will give two algorithms for knot insertion and degree elevation. In fact, there are many algorithms that implement these operations, but we shall only consider one for each operation.

Knot insertion

Assuming an initial B-Spline curve defined by:

- its degree p
- knot vector $T = (t_i)_{0 \leqslant i \leqslant n+p+1}$
- control points $(\mathbf{P}_i)_{0 \leqslant i \leqslant n}$

We are interested in the new B-Spline curve as the result of the insertion of the knot t, m times (with a span j, i.e. $t_j \leqslant t < t_{j+1}$).
After such operation, the degree is remain unchanged, while the knot vector is enriched by t, m times. The aim is then to compute the new control points $(\mathbf{Q}_i)_{0 \leqslant i \leqslant n+m}$

For this purpose we use the DeBoor algorithm:

$$n := n + m \tag{44}$$
$$p := p \tag{45}$$
$$T := \{t_0, .., t_j, \underbrace{t, ..., t}_{m}, t_{j+1}, .., t_{n+k}\} \tag{46}$$
$$\mathbf{Q}_i := \mathbf{Q}_i^m \tag{47}$$

where,

$$\mathbf{Q}_i^0 = \mathbf{P}_i \tag{48}$$
$$\mathbf{Q}_i^r = \alpha_i^r \mathbf{Q}_i^{r-1} + (1 - \alpha_i^r)\mathbf{Q}_{i-1}^{r-1} \tag{49}$$

with,

$$\alpha_i^r = \begin{cases} 1 & i \leqslant j-p+r-1 \\ \frac{t-t_i}{t_{i+p-r+1}-t_i} & j-p+r \leqslant i \leqslant j-m \\ 0 & j-m+1 \leqslant i \end{cases} \tag{50}$$

Examples

Example 1. We consider a cubic B-Spline curve on the knot vector $T = \{0,0,0,0,1,1,1,1\}$.

In this example, we first insert the knot $\frac{1}{2}$ with a multiplicity of 1. The result is given in Fig. 45.
In figures 46 and 47, we chose a multplicity of 2 and 3 for the new knot. As a result, we notice

- whenever we insert a new knot, a new control point appears,
- the curve is unchanged after knot insertion,
- $\mathbf{Q}_1 \in [\mathbf{P}_0\mathbf{P}_1]$ and $\mathbf{Q}_3 \in [\mathbf{P}_2\mathbf{P}_3]$.
- in Fig. 47, the curve pass through the point $\mathbf{Q}_3$, which corresponds to the knot $\frac{1}{2}$ with a multiplicity of 3. In this case, we subdivided the initial Bézier curve into two Bézier curves.

Example 2. We consider again a cubic B-Spline curve on the knot vector $T = \{0,0,0,0,1,1,1,1\}$.

In this example, we show the impact of inserting knots on the control polygon. As we see in figures 48 and 49, the control polygon converges to the initial curve. We shall prove this result in the Approximation theory part.

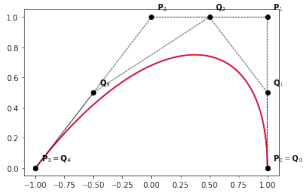

Figure 45: A cubic Bézier curve and the new B-Spline curve after inserting the knot $\frac{1}{2}$ with a multiplicity of 1.

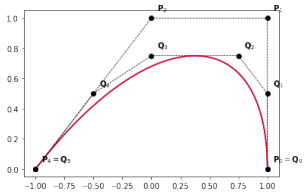

Figure 46: A cubic Bézier curve and the new B-Spline curve after inserting the knot $\frac{1}{2}$ with a multiplicity of 2.

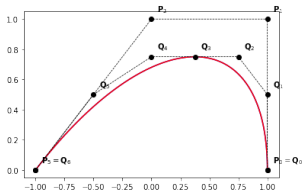

Figure 47: A cubic Bézier curve and the new B-Spline curve after inserting the knot $\frac{1}{2}$ with a multiplicity of 3.

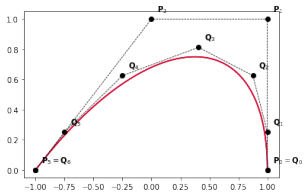

Figure 48: A cubic Bézier curve and the new B-Spline curve after inserting the knots $\{\frac{1}{4}, \frac{1}{2}, \frac{3}{4}\}$.

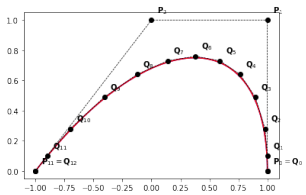

Figure 49: A cubic Bézier curve and the new B-Spline curve after inserting the knots $\{\frac{i}{10},\ i \in \{1,2,\cdots,9\}\}$.

Degree elevation

In the sequel, we shall restrict our study to the case of open knot vectors. There are also many algorithms for degree elevation of a B-Spline curve. In the sequel, we will be using the one developped by Huand, Hu and Martin [1].
Since some knots may be duplicated, we shall assume that the break-points are denoted by $\{t_i^\star,\ 0 \leq i \leq s\}$, in which case the knot vector has the following form

$$T = \{\underbrace{t_0^\star, ..., t_0^\star}_{m_0}, \underbrace{t_1^\star, ..., t_1^\star}_{m_1}, \dots, \underbrace{t_{s-1}^\star, ..., t_{s-1}^\star}_{m_{s-1}}, \underbrace{t_s^\star, ..., t_s^\star}_{m_s}, \} \tag{51}$$

Elevating the degree by m will lead to the new description (the curve does not change):

$$n := n + sm \tag{52}$$

$$p := p + m \tag{53}$$

$$T := \{\underbrace{t_0^\star, ..., t_0^\star}_{m_0+m}, \underbrace{t_1^\star, ..., t_1^\star}_{m_1+m}, \dots, \underbrace{t_{s-1}^\star, ..., t_{s-1}^\star}_{m_{s-1}+m}, \underbrace{t_s^\star, ..., t_s^\star}_{m_s+m}, \} \tag{54}$$

$$\mathbf{Q}_i := \widetilde{\mathbf{Q}}_i^0 \tag{55}$$

where the control points $\widetilde{\mathbf{Q}}_i^0$ are given by the following algorithm,

1. we define

$$\beta_i = \sum_{l=1}^{i} m_l \quad \forall 1 \leqslant i \leqslant s-1 \tag{56}$$

$$\alpha_i = \prod_{l=1}^{i} \frac{p-l}{p+m-l} \quad \forall 1 \leqslant i \leqslant p-1 \tag{57}$$

and set

$$\widetilde{\mathbf{P}}_i^0 = \widetilde{\mathbf{P}}_i \tag{58}$$

2. compute the (scaled) differential coefficients $\widetilde{\mathbf{P}}_i^l$, for $l > 0$ as

$$\widetilde{\mathbf{P}}_i^l = \begin{cases} \frac{\widetilde{\mathbf{P}}_{i+1}^{l-1} - \widetilde{\mathbf{P}}_i^{l-1}}{t_{i+p} - t_{i+l}} & ,\ t_{i+p} > t_{i+l} \\ 0 & ,\ t_{i+p} = t_{i+l} \end{cases} \tag{59}$$

3. compute for all $j \in \{0, \cdots, p\}$

$$\widetilde{\mathbf{P}}_0^j \tag{60}$$

4. compute for all $l \in \{1, \cdots, s-1\}$ and $i \in \{p+1-m_l, \cdots, p\}$

$$\widetilde{\mathbf{P}}_{\beta_l}^i \tag{61}$$

5. compute for all $j \in \{0, \ldots, p\}$

$$\widetilde{\mathbf{Q}}_0^j = \prod_{l=1}^{j} \frac{p+1-l}{p+1+m-l} \widetilde{\mathbf{P}}_0^j \tag{62}$$

6. compute for all $l \in \{1, \ldots, s-1\}$ and $i \in \{p+1-m_l, \ldots, p\}$

$$\widetilde{\mathbf{Q}}_{\beta_l+ml}^j = \prod_{l=1}^{j} \frac{p+1-l}{p+1+m-l} \widetilde{\mathbf{P}}_{\beta_l}^j \tag{63}$$

7. compute for all $l \in \{1, \ldots, s-1\}$ and $i \in \{1, \ldots, m\}$

$$\widetilde{\mathbf{Q}}_{\beta_l+ml+i}^p = \widetilde{\mathbf{Q}}_{\beta_l+ml}^{(p)} \tag{64}$$

8. compute $\widetilde{\mathbf{Q}}_i^0$

Examples

Example 1. In this example we consider a cubic B-Spline curve with the following knot vector $T = \{0, 0, 0, 0, \frac{1}{2}, \frac{1}{2}, 1, 1, 1, 1\}$.

In Fig. 50, we plot the curve before and after raising the B-Spline degree by 1.

We notice that

- in opposition to the knot insertion, elevating the degree by 1 adds two control points rather than 1.
- the curve is unchanged after degree elevation,
- $\mathbf{Q}_1 \in [\mathbf{P}_0\mathbf{P}_1]$ and $\mathbf{Q}_6 \in [\mathbf{P}_4\mathbf{P}_5]$.

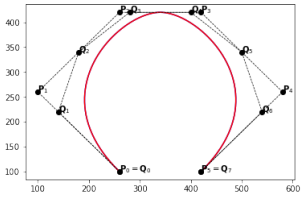

Figure 50: A cubic B-Spline curve before and after raising the polynomial degree by 1.

Example 2. In this example we show the convergence of the control polygon under degree elevation. In figures 51, 52 and 53, we plot the control polygon after raising the degree by 2, 4 and 8 respectively.

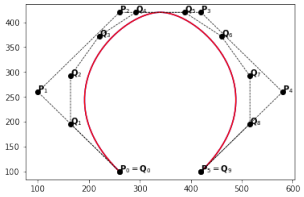

Figure 51: A cubic B-Spline curve before and after raising the polynomial degree by 2.

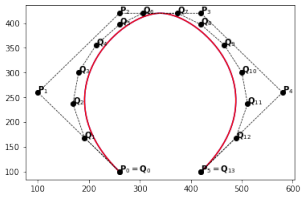

Figure 52: A cubic B-Spline curve before and after raising the polynomial degree by 4.

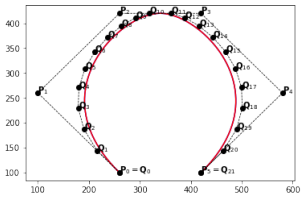

Figure 53: A cubic B-Spline curve before and after raising the polynomial degree by 8.

Part II

Approximation theory for B-Splines

Divided differences

Contents

Lagrange interpolation

Let us consider the interpolation problem for a function f on a given set of (distinct) points $\{x_0, \cdots, x_n\}$. It is well known that the Lagrange interpolating polynomial of degree n writes

$$p(x; x_0, \ldots, x_n) = \sum_{i=0}^{n} f(x_i) L_i(x), \quad \text{where } L_i(x) = \prod_{\substack{j=0 \\ j \neq i}}^{n} \frac{x - x_j}{x_i - x_j}, \quad i = 0, \ldots, n \tag{65}$$

The evaluation of the Lagrange interpolator can be done with different methods. The standard one is known as **Aitken method**. Assume we want to interpolate a function f on the points $\{x_0, \cdots, x_3\}$. We start by computing:

$$\begin{aligned}
p(x; x_0, x_1) &= \frac{1}{x_1 - x_0} \begin{vmatrix} f(x_0) & x_0 - x \\ f(x_1) & x_1 - x \end{vmatrix} \\
p(x; x_0, x_2) &= \frac{1}{x_2 - x_0} \begin{vmatrix} f(x_0) & x_0 - x \\ f(x_2) & x_2 - x \end{vmatrix} \\
p(x; x_0, x_3) &= \frac{1}{x_3 - x_0} \begin{vmatrix} f(x_0) & x_0 - x \\ f(x_3) & x_3 - x \end{vmatrix} \\
p(x; x_0, x_1, x_3) &= \frac{1}{x_3 - x_1} \begin{vmatrix} p(x; x_0, x_1) & x_1 - x \\ p(x; x_0, x_3) & x_3 - x \end{vmatrix} \\
p(x; x_0, x_1, x_2) &= \frac{1}{x_2 - x_1} \begin{vmatrix} p(x; x_0, x_1) & x_1 - x \\ p(x; x_0, x_2) & x_2 - x \end{vmatrix}
\end{aligned}$$

Then the value of the interpolation polynomial of degree 3 at x is given by

$$p(x; x_0, x_1, x_2, x_3) = \frac{1}{x_3 - x_2} \begin{vmatrix} p(x; x_0, x_1, x_2) & x_2 - x \\ p(x; x_0, x_1, x_3) & x_3 - x \end{vmatrix}$$

The complexity of the Aitken method is $O(n^2)$ which is expensive, since we know that the Horner algorithm is only about $O(n)$.

Newton form and Neville's algorithm

Another interesting form is the so called **Newtonian form** of p and writes

$$p(x) = \sum_{i=0}^{n} a_i \prod_{j=0}^{i-1} (x - x_j) \tag{66}$$

Let us explain how to use the form 66 to have a fast evaluation of the interpolant polynomial at a given point x.
First, we define the polynomial $p_{j,k}$ as the interpolant polynomials of degree k at the sites $\{x_j, x_{j+1}, \cdots, x_{j+k}\}$, *i.e.* $p_{j,k}(x_i) = f(x_i)$ for $i \in \{j, j+1, \cdots, j+k\}$. Where we assume the sites to be ordered and distincts. Therefor, these polynomials exist and are unique.
In the linear case, we have

$$p_{0,1}(x) = f(x_0) + (x - x_0)\frac{f(x_1) - f(x_0)}{x_1 - x_0} = a_0 + (x - x_0)a_1 \tag{67}$$

for some coefficients a_0 and a_1. In this case, we have

$$a_0 = f(x_0) \tag{68}$$

and

$$a_1 = \frac{f(x_1) - f(x_0)}{x_1 - x_0} \tag{69}$$

a_1 is called the **first order divided difference** of $\mathcal{X} := \{f(x_0), \cdots, f(x_n)\}$.
In the quadratic case, we can write

$$p_{0,2}(x) = p_{0,1}(x) + (x - x_0)(x - x_1)a_2 \tag{70}$$

where

$$a_2 = \frac{f(x_2) - p_{0,1}(x_2)}{(x_2 - x_0)(x_2 - x_1)} \tag{71}$$

a_2 is called the **second order divided difference** of $\mathcal{X}$. We notice that, we can write, for a given coefficient a,

$$p_{j,k}(x) = p_{j,k-1}(x) + (x - x_i)\dots(x - x_{i+k-1})a$$

The coefficient a is the k**-th order divided difference** of $\mathcal{X}$ and will be denoted $[x_i, \cdots, x_{i+k}]f$.
Since,

$$p_{j,k}(x) = \frac{x_{j+k} - x}{x_{j+k} - x_j}p_{j-1,k-1}(x) + \frac{x - x_j}{x_{j+k} - x_j}p_{j,k-1}(x), \quad j \in \{0, \dots, p-k\}$$

we get the following result, by comparing the coefficients of the monomial x^k,

$$[x_j, \dots, x_{j+k}]f := \frac{1}{x_{j+k} - x_j}\Big([x_{j+1}, \dots, x_{j+k}]f - [x_j, \dots, x_{j+k-1}]f\Big) \tag{72}$$

The Neville's algorithm is then given as follows

1. set $[x_j]f := f(x_j)$, for all $j \in \{0, \dots, p\}$,
2. use 72 to compute $[x_j, \dots, x_{j+k}]f$, for all $j \in \{0, \dots, p-k\}$ and $k \in \{1, \dots, p\}$

Horner algorithm

We give here a modified version for the Horner algorithm based on the Newtonian form.

1. set $q := a_p$
2. for every $k \in \{p-1, p-2, \cdots, 0\}$, we update q using $q := a_k + (x - x_k)q$
3. the evaluation of the polynom at x is then given by $p_{0,p}(x) := q$

A quick study of the complexity leads to p multiplications and $2p$ additions and substractions.

Hermite interpolation

In the Hermite interpolation, not only the values of a function are given, but also some of its successive derivatives. Given the set of interpolations points $X := \{x_0, \cdots, x_n\}$, we construct the set of distinct points $X^\star := \{x_0^\star, \cdots, x_s^\star\}$, for which we associate a multiplicity $m_j > 0$ with $\sum_{j=0}^{s} m_j = n + 1$. Let $c_{j,l}$ be given constants. The Hermite interpolation problems is

Definition 8 (Hermite interpolation) *Find a polynomial $H_n \in \Pi_n$ such that*

$$H_n^{(l)}(x_j^\star) = c_{j,l} \quad 0 \leq l \leq m_j - 1 \quad \textit{and} \quad 0 \leq j \leq s \tag{73}$$

It is easy to prove that there exist a unique polynomial H_n that solves the Hermite interpolation problem.
In the sequel, we shall define the set of constraints by reordering the coefficients $c_{j,l}$ such that $\left(d_j\right)_{j=0}^{n} := \{c_{j,l}, 0 \leq j \leq s, 0 \leq l \leq m_j - 1\}$. Now we can state the general theorem for the Newton's method:

Theorem 18 (Newton's method) *There exist unique constants $a_0, \cdots, a_n$ for which the polynomials*

$$\begin{cases} P_0(x) = a_0 \\ P_1(x) = a_0 + a_1(x - x_0) \\ P_2(x) = a_0 + a_1(x - x_0) + a_2(x - x_0)(x - x_1) \\ \cdots \\ P_n(x) = a_0 + a_1(x - x_0) + \ldots + a_n \prod_{j=0}^{n-1} \left(x - x_j\right) \end{cases} \tag{74}$$

are solutions of the Hermite interpolation problems for the sets of points $\{x_0\}, \{x_0, x_1\}, \ldots, \{x_0, \cdots, x_n\}$ and given data $\left(d_j\right)_{j=0}^{n}$.

Remark 18 *The Hermite interpolation is a generalization of both Lagrange interpolation and the Taylor interpolation. Recall that Taylor interpolant of a smooth function $f \in C^n([a,b])$ is defined by*

$$T_n(x) := f(x_0) + f'(x_0)(x - x_0) + \ldots + f^{(n)}(x_0)\frac{(x - x_0)^n}{n!} \tag{75}$$

These are the two extreme cases of Hermite interpolation where for the Lagrange interpolation the interpolation points are all distinct, while for Taylor interpolation there all equal.

Divided differences

Definition 9 (Divided Differences (G. Kowalewski 1932)) *For a set of points (not necessarily ordered) $X := \{x_0, \cdots, x_n\}$, and a function f, we define the n-th divided difference of f by*

$$[x_0, \cdots, x_n]f := a_n \tag{76}$$

where a_n is the coefficient of x^n of the polynomial which interpolates f at $x_0, \cdots, x_n$ as shown in the Newtonian form 66.

Now let's go back to the divided differences operator. After giving additional examples, we shall present some properties.

Examples

Example 1. $[x_0]f = f(x_0)$

Example 2. $[x_0, x_1]f = \frac{f(x_0)-f(x_1)}{x_0-x_1}$ if $x_0 \neq x_1$

Example 3. $[x_0, x_0]f = f'(x_0)$

Because of the symmetry of the Newton form we have

Proposition 13 *$[x_0, \cdots, x_n]f$ is symmetric in $x_0, \cdots, x_n$.*

From the Newton form, we also deduce

Proposition 14 *$[x_0, \cdots, x_n]f$ is constant if f is a polynomial of degree $\leq n$, and zero for a polynomial of degree $< n$.*

Use the Taylor polynomial we have

Proposition 15 $[x_0, \cdots, x_0]f = \frac{1}{n!}f^{(n)}(x_0)$.

Proposition 16 *$[x_0, \cdots, x_n]f$ is a linear combinaition of the derivatives $f^{(l)}(x_i)$, $0 \leq l \leq m_i - 1$, where m_i is the multiplicity of the point x_i in the set X.*

Proposition 17 *if* $f \in \mathcal{C}^n([a,b])$, $a \leq x_i \leq b, \quad 0 \leq i \leq n$, *then :*

$$[x_0, \cdots, x_n]f = \frac{1}{n!} f^{(n)}(\xi), \quad \text{for some } \xi \in [a,b]$$

Proposition 18 $[x_0, \cdots, x_n]f$ *is continuous at the sites in* X, *if the derivatives of* f *of proper orders are continuous at the considered site.*

Proposition 19 *if* $x_0 \neq x_n$, *we have*

$$[x_0, \cdots, x_n]f = \frac{1}{x_n - x_0}\{[x_1, \cdots, x_n]f - [x_0, \cdots, x_{n-1}]f\} \tag{77}$$

Proposition 20 (Leibniz's Formula)

$$[x_0, \cdots, x_n](fg) = \sum_{i=0}^{n} [x_0, \cdots, x_i](f)\ [x_i, \cdots, x_n](g)$$

Proposition 21 *If* $f^{(n-1)}$ *is absolutely continuous, and if not all* x_i *coincide, we have*

$$[x_0, \cdots, x_n]f = \int_0^1 dt_1 \int_0^{t_1} dt_2 \cdots \int_0^{t_{n-1}} f^{(n)}(x_0 + h_1 t_1 + h_2 t_2 + \cdots + h_n t_n) dt_n$$

where we denote $h_i = x_{i+1} - x_i, \ \ i \in \{0, \cdots, n-1\}$.

Corollary 2

$$|[x_0, \cdots, x_n]f| \leq \frac{1}{n!} \|f^{(n)}\|_\infty$$

This shows, that the functional $f \ \rightarrow \ [x_0, \cdots, x_n]f$ *is continuous on* $\mathcal{C}^n[a,b]$.

Proposition 22 *If all* x_i *are distinct, then*

$$[x_0, \cdots, x_n]f = \int_a^b f^{(n)}(t)[x_0, \cdots, x_n]\left(\frac{(\cdot - t)_+^{n-1}}{(n-1)!}\right) dt$$

This gives a representation of the functional $[x_0, \cdots, x_n]$ *in term of the Peano kernel.*

Schoenberg space of Spline functions

Contents

Basic Splines

In the previous chapters, we introduced the B-Splines through the Cox-DeBoor formula. In this section, we shall give a more specific definition, using the Divided Differences operator.

Definition 10 (M-Spline) *Let $X = \{x_0, \cdots, x_{p+1}\}$ a non-decreasing sequence of $p+2$ points such that $x_0 \neq x_{p+1}$. The M-Spline will be defined in term of the following Divided-Difference :*

$$M(x) = M(x; X) := M(x; x_0, \cdots, x_{p+1}) = (p+1)[x_0, \cdots, x_{p+1}](\cdot - x)_+^p \tag{78}$$

The points forming the set X, are called *knots*, and X is said to be a *knot vector*.

Proposition 23 $M(x) = 0, \forall x \notin [x_0, x_{p+1}]$

Proposition 24 $M(x) > 0, \forall x \in (x_0, x_{p+1})$

Proposition 25 $\frac{M}{n!}$ *is the Peano kernel of the divided-difference at the set* $X = \{x_0, \cdots, x_{p+1}\}$. *Then, for any* $f \in W_1^{p+1}$, *we have,*

$$[x_0, \cdots, x_{p+1}]f = \int_{-\infty}^{+\infty} f^{(p+1)}(t)M(t)dt$$

Proposition 26 $\int_{-\infty}^{+\infty} M(t)dt = 1$

Proposition 27 *If* $p \geq 1$, *we have the recurrence formula,*

$$M(x; x_0, \cdots, x_{p+1}) = \frac{p+1}{p}\left(\frac{x - x_0}{x_{p+1} - x_0}M(x; x_0, \cdots, x_p) + \frac{x_{p+1} - x}{x_{p+1} - x_0}M(x; x_1, \cdots, x_{p+1})\right) \tag{79}$$

The B-Splines are then defined in terms of M-Splines as

$$N(x; x_0, \cdots, x_{p+1}) = \frac{x_{p+1} - x_0}{p+1}M(x; x_0, \cdots, x_{p+1}) \tag{80}$$

In this case we recover the Cox-DeBoor formula

$$N(x; x_0, \cdots, x_{p+1}) = \frac{x - x_0}{x_p - x_0}N(x; x_0, \cdots, x_p) + \frac{x_{p+1} - x}{x_{p+1} - x_1}N(x; x_1, \cdots, x_{p+1}) \tag{81}$$

In fact, one can see the property 26 of the M-Splines as a normalization of the basic splines, such that the integral is one. Another normalization is to have the patition unity, which is given by the B-Splines.

Smoothness of a B-Spline

Proposition 28 *Suppose that $x^\star \in X := \{x_0, \ldots, x_{p+1}\}$ occurs m times in the knot sequence in X. If $1 \leq m \leq p+1$, then $N^{(r)}$ is continuous at $x^\star$ for all $r \in \{0, \ldots, p-m\}$, while N^{p-m+1} is discontinuous at $x^\star$.*

Proof. TODO ■

Spline functions

Splines are piecewise polynomials defined on the real line. We shall require that on each compact interval, they consist of a small number of non-vanishing polynomial pieces.
Let $T^\star = \{t_i^\star,\ 0 \leqslant i \leqslant s\}$ be a finite strictly increasing sequence of points of $\mathbb{R}$. A function S on $\mathbb{R}$ is a **spline** of **degree** $p, p \geqslant 0$ with the breakpoints $T^\star$ if on each interval $(t_i^\star, t_{i+1}^\star)$, it is a **polynomial of degree** $\leqslant p$. At every breakpoint $t_i^\star$, S and its derivatives (which are also splines) are defined by continuity whenever it is possible. For example, splines of order one are step functions, those of order two are broken lines.
At every breakpoint $t_i^\star$, a spline S shall have a **smoothness** r_i, which is defined as the following:

- $r_i := -1$ if S is discontinuous at $t_i^\star$, otherwise,
- r_i is such that $S^{(j)}$ is well defined and continuous at $t_i^\star$ for all $0 \leq j \leq r_i$ and $1 \leq i \leq s-1$.

Remark 19 *We will not consider the case of discontinuous splines at internal breakpoints. Meaning that $r_i \geq 0$.*

Remark 20 *$k_i := p - r_i$ is called the **defect** and is the number of degrees of freedom of S at $t_i^\star$*

In the sequel, we shall consider the case of the interval $I = [a, b]$, where $a := t_0^\star$ and $b = t_s^\star$.

Definition 11 (Schoenberg space) *Given a set of breakpoints $T^\star$ as defined previously and a sequence of integers $\mathbf{r} := \{r_i,\ 1 \leqslant i \leqslant s-1\}$. The space of functions which consists of all splines S of degree $\leqslant p$ with breakpoints contained in $T^\star$ and of smoothness $\geqslant r_i$ at $t_i^\star$ is called **Schoenberg space**, which we denote $\mathcal{S}_p^{\mathbf{r}}(T^\star)$.*

An example of a spline function is the *truncated power*, if $i > 0$ and $\tau \in T^\star$,

$$(x-\tau)_+^i := \begin{cases} (x-\tau)^i, & x \geq 0 \\ 0, & x < \tau \end{cases} \tag{82}$$

Exercise 19 *Show that the truncated powers* $\left(x - t_i^\star\right)_+^j \in \mathcal{S}_p^r(T^\star)$ *, for all* $j \in \{r_i, \cdots, p\}$.

Using the truncated powers, one can construct a basis for the Schoenberg space. However, this basis will not have the compact support property. We shall see in the next sections, that the B-Splines form a basis for the Schoenberg space. There are different methods to prove this fact, the one that we will follow is based on the DeBoor-Fix quasi-interpolation approach.

Dual functionals

In this section, we are interested in the construction of dual functionals $(\lambda_i)_{0\leq i\leq n}$ for a family of B-Splines $\left(N_j^p\right)_{0\leq j\leq n}$ such that

$$\lambda_i(N_j^p) = \delta_{ij}, \quad \forall i,j \in \{0,\dots,n\} \tag{83}$$

We recall the Mardsen's identity 17:

$$(x-y)^p = \sum_j \psi_{j,p}(y) N_j^p(x)$$

where

$$\psi_{j,p}(y) = \prod_{i=j+1}^{j+p} (t_i - y) \tag{84}$$

Proposition 29 (representation of polynomials) *Let $g \in \Pi_p$, then*

$$g(x) = \sum_{j=0}^{n} \mu_j^p(g) N_j^p(x) \tag{85}$$

where

$$\mu_j^p(g) = \frac{1}{p!} \sum_{r=0}^{p} (-1)^{p-r} \psi_{j,p}^{(r)}(\tau_j) g^{(p-r)}(\tau_j) \tag{86}$$

for some $\tau_j \in [a,b]$.

Proof. Let $g \in \Pi_p$ and $\tau_j \in [a,b]$. Using the Taylor expansion (or Taylor form of the polynomial) we get

$$g(x) = \sum_{r=0}^{p} \frac{1}{(p-r)!} (x-\tau_j)^{p-r} g^{(p-r)}(\tau_j) \tag{87}$$

but using the Mardsen identity for $y = \tau_j$, we have

$$(x-\tau_j)^{p-r} = \sum_{j=0}^{n} (-1)^{p-r} \frac{(p-r)!}{p!} \psi_{j,p}^{(r)}(\tau_j) N_j^p(x)$$

by subtituting this expression in Eq. 87, we get

$$g(x) = \sum_{r=0}^{p} \frac{1}{(p-r)!} \sum_{j=0}^{n} (-1)^{p-r} \frac{(p-r)!}{p!} \psi_{j,p}^{(r)}(\tau_j) N_j^p(x) g^{(p-r)}(\tau_j)$$

which leads to

$$g(x) = \sum_{j=0}^{n} \frac{1}{p!} \sum_{r=0}^{p} (-1)^{p-r} \psi_{j,p}^{(r)}(\tau_j) g^{(p-r)}(\tau_j) N_j^p(x)$$

■

Next, we give a general representation of any spline function in terms of B-Splines.

Proposition 30 (representation of splines) *Let $g \in \mathcal{S}_p(T)$, then*

$$g(x) = \sum_{j=0}^{n} \lambda_j^p(g) N_j^p(x) \tag{88}$$

where

$$\lambda_j^p(g) = \frac{1}{p!} \begin{cases} \sum_{r=0}^{p} (-1)^{p-r} \psi_{j,p}^{(r)}(\tau_j) D_+^{p-r} g(\tau_j) & , \tau_j = t_j \\ \sum_{r=0}^{p} (-1)^{p-r} \psi_{j,p}^{(r)}(\tau_j) g^{(p-r)}(\tau_j) & , t_j < \tau_j < t_{j+p+1} \\ \sum_{r=0}^{p} (-1)^{p-r} \psi_{j,p}^{(r)}(\tau_j) D_-^{p-r} g(\tau_j) & , \tau_j = t_{j+p+1} \end{cases} \tag{89}$$

Proof. Let $\tau_j \in [t_j, t_{j+p+1}]$. We also denote by m_j the integer such that $\tau_j \in I_j := [t_{m_j}, t_{m_j+1}]$. There are three cases to consider: either τ_j is inside the interval I_j or is equal to one of its bounds. For the moment, let us consider the case where $t_{m_j} < \tau_j < t_{m_j} + 1$.
Since $s|_{I_j} \in \Pi_p$, we use the representation of polynomials to get

$$s|_{I_j} = \sum_{i=m_j-p}^{m_j} \mu_i^p(s|_{I_j}) N_i^p$$

on the other hand, since $j \leq m_j \leq j + p$, we have $m_j - p \leq j \leq m_j$ and using the local independence of B-Splines on I_j, we get

$$\lambda_j^p(s) = \mu_j^p(s|_{I_j})$$

The other cases are treated in the same way by replacing the derivatives on τ_j by the right (left) derivatives if $\tau_j = t_j$ (or $\tau_j = t_{j+p+1}$). ■

Remark 21 *If we denote by μ_j the multiplicity of τ_j in $\{t_{j+1}, \cdots, t_{j+p}\}$, then $\psi_{j,p}^{(r)}(\tau_j) = 0$ for all $r \leq \mu_j - 1$. Therefor, the summation index in 89 starts from μ_j rather than 0.*

Let T be a knot sequence associated to a set of breakpoints $T^\star$ for which each internal knot has a multiplicity m_i. From Prop 28, we know that a B-Spline N_j has $p - m_i$ continuous derivatives at a breakpoint $t_i^\star$ with a multiplicity m_i, which lies in the support of N_j.

Proposition 31 (B-Splines as a basis for Schoenberg space) *TODO*

Proof. TODO ■

Spline Approximation

Contents

Introduction

The aim of this chapter is to construct a spline approximation of a function f, in terms of B-Splines as

$$\mathcal{L}f(x) = \sum_{j=0}^{n} \lambda_i(f) N_j^p(x) \tag{90}$$

Depending on the nature of the functionals λ_i the approximation will be global (interpolation and least square approximation) or local (quasi-interpolation).

Examples

Piecewise linear interpolation

We consider in this example, a set of increasing points (which will represent our grid points) $x_0 < x_1 < \cdots < x_m$. We also denote $a = x_0$ and $b = x_m$. We first construct a knot vector from the grid points, by duplicating the first and the last points

$$T_1 := \{x_0, x_0, x_1, \ldots, x_{m-1}, x_m, x_m\}$$

We consider the set of linear B-Splines associated to T_1, denoted by $\left(N_j^1\right)_{j=0}^m$.

Proposition 32 *Let $f \in \mathcal{C}[a,b]$. The spline defined as*

$$I_1 f(x) = \sum_{j=0}^{m} f(x_j) N_j^1(x) \tag{91}$$

satisfies the interpolation condition, i.e.

$$I_1 f(x_i) = f(x_i) \quad \forall i \in \{0, \ldots, m\}$$

Exercise 20 *Prove the previous proposition.*

Variation diminishing spline approximation

In the sequel, we present an approximation that preserves the bounds, monotonicity and convexity. In addition, it reproduces all linear piecewise polynomials.

Definition 12 (Variation diminishing approximation) *Let $f \in \mathcal{C}[a,b]$ and p a positive integer. Moreover, we consider a $p+1$-regular knot sequence $T = \{t_0, \cdots, t_{n+p+1}\}$, with $t_p = a$ and $t_{n+1} = b$. We also define the knot averages, also known as the Greville points,*

$$t_j^\star = \frac{1}{p}\left(t_{j+1} + \ldots + t_{j+p}\right) \tag{92}$$

The Variation diminishing spline approximation of degree p to f, on the knot sequence T, is defined as

$$Vf(x) = \sum_{j=0}^{n} f(t_j^\star) N_j^p(x) \tag{93}$$

Remark 22 *The first knot t_0 and the last one t_{n+p+1} do not appear in the definition of the Greville points.*

Remark 23 *If all internal knots occur less than $p+1$, i.e. the Schoenberg space $\mathcal{S}_p(T) \subset \mathcal{C}[a,b]$, then*

$$t_0^\star < t_1^\star < \ldots < t_n^\star$$

Preserving the bounds

Lemma 2 *If $g = \sum_{j=0}^{n} c_j N_j^p$ is an element of the Schoenberg space $\mathcal{S}_p(T)$, then*

$$\min_{0 \le j \le n} c_j \le g \le \max_{0 \le j \le n} c_j$$

Proof. Since the B-Splines are positive, we have

$$\min_{0 \le j \le n} c_j \left(\sum_{j=0}^{n} N_j^p \right) \le g \le \max_{0 \le j \le n} c_j \left(\sum_{j=0}^{n} N_j^p \right)$$

we conclude by using the fact that the B-Splines forms a partition of unity. ∎

Proposition 33 *Let $f \in \mathcal{C}[a,b]$ such that $m \le \|f\|_\infty \le$ for some real numbers m and M. Then*

$$m \le \|Vf\|_\infty \le \tag{94}$$

Proof. Since $Vf(x) = \sum_{j=0}^{n} f(t_j^\star) N_j^p(x)$ and for all $0 \le j \le n$ we have $m \le f(t_j^\star) \le M$. We conclude by using the previous lemma. ∎

Preserving the monotonicity

Lemma 3 *If $g = \sum_{j=0}^{n} c_j N_j^p$ is an element of the Schoenberg space $\mathcal{S}_p(T)$, then*

1. *if $\forall j \; 0 \le j \le n-1$, $c_j \le c_{j+1}$ then g is increasing*
2. *if $\forall j \; 0 \le j \le n-1$, $c_j \ge c_{j+1}$ then g is decreasing*

Proof. We shall assume $p \geq 1$, since the case $p = 0$ is straightforward. We shall also give the proof only for the first point, the second case is treated in a similar way. Let $x \in [a, b]$, we have

$$g'(x) = \sum_j \nabla c_j N_j^{p-1}(x)$$

with $\nabla c_j := \frac{c}{t_{j+p} - t_j} \left(c_j - c_{j-1}\right)$.
But since $\nabla c_j \geq 0$, then $g'(x) \geq 0$. Therefor g is increasing. ■

Proposition 34 *If $f \in \mathcal{C}[a, b]$ is increasing (decreasing) then Vf is increasing (decreasing).*

Proof. We use the fact that the coefficients in the Variation diminishing approximation are the evaluation of the function f at the Greville points. The order of these coefficients will be given by the monotonicity of the function f. Then we use the previous lemma to conclude. ■

Preserving the convexity

Lemma 4 *If $g = \sum_{j=0}^{n} c_j N_j^p$ is an element of the Schoenberg space $\mathcal{S}_p(T)$, then g is convex if*

$$\nabla c_j \leq \nabla c_{j+1} \quad \forall 0 \leq j \leq n-1$$

Proof. We shall consider two cases

1. g is differentiable everywhere.
   Then we know that

   $$g'(x) = \sum_j \nabla c_j N_j^{p-1}(x)$$

   But since $\nabla c_j \leq \nabla c_{j+1} \quad \forall 0 \leq j \leq n-1$, and using the lemma 3, we get that g' is an increasing function, which means that g is convex.

2. Now assume there exists only one point z where g is not differentiable and let $x_0 < x_1 <_2$ be three points in $[a, b]$. We shall prove that

   $$\frac{g(x_1) - g(x_0)}{x_1 - x_0} \leq \frac{g(x_2) - g(x_1)}{x_2 - x_1}$$

   The case where $z \notin (x_0, x_2)$ is covered by the previous point. The interesting cases are the one for which $z \in [x_0, x_2]$. Assume for the moment that $x_0 < z < x_1$. Then using the fact that

   $$\frac{g(x_1) - g(x_0)}{x_1 - x_0} = \frac{g(z) - g(x_0)}{z - x_0} \frac{z - x_0}{x_1 - x_0} + \frac{g(x_1) - g(z)}{x_1 - z} \frac{x_1 - z}{x_1 - x_0}$$

we get

$$\frac{g(x_1) - g(x_0)}{x_1 - x_0} \leq \frac{g(x_1) - g(z)}{x_1 - z}$$

but since g is convex on the right of z, we have also

$$\frac{g(x_1) - g(z)}{x_1 - z} \leq \frac{g(x_2) - g(x_1)}{x_2 - x_1}$$

then

$$\frac{g(x_1) - g(x_0)}{x_1 - x_0} \leq \frac{g(x_1) - g(z)}{x_1 - z} \leq \frac{g(x_2) - g(x_1)}{x_2 - x_1}$$

Now if $z = x_1$, we use the mean value theorem and the fact that f' is increasing at the interior of each sub-interval.
The other cases and the one with several discontinuities is treated in a similar way.

■

Proposition 35 *If $f \in \mathcal{C}[a, b]$ is convex then Vf is convex.*

Proof. If f is convex then we have

$$\frac{f(t_j^\star) - f(t_{j-1}^\star)}{t_j^\star - t_{j-1}^\star} \leq \frac{f(t_{j+1}^\star) - f(t_j^\star)}{t_{j+1}^\star - t_j^\star}$$

$$\nabla c_j \leq \nabla c_{j+1} \quad \forall 0 \leq j \leq n-1$$

where $c_j = f(t_j^\star)$. We conclude by using the previous lemma. ■

Quasi-Interpolation

In this section, we give a general procedure to construct quasi-interpolant for B-Splines and we provide some examples.

General recipe for quasi-interpolants

In the sequel, we shall give a general procedure to construct local approximation on a Schoenberg space. Let $f \in \mathcal{C}[a,b]$. We will denote the quasi-interpolant by $\mathcal{Q}$ and assume that

$$\mathcal{Q}f = \sum_{j=0}^{n} \lambda_i(f) N_j^p \tag{95}$$

1. We consider a span index j,
2. We assume that there exist μ and ν such that the interval $I := [t_\mu, t_\nu] \subset [a,b]$ and the interior of $I \bigcap [t_j, t_{j+p+1}]$ is not empty.
3. We choose a local approximation method P^I and determine an approximation $P^I f$ to f on I such that

$$P^I f = \sum_{i=\mu-p}^{\nu-1} b_i N_i^p \tag{96}$$

4. We set the coefficient $\lambda_j f$ in Eq. 95 to b_j

The last point makes sense only if $\mu - p \leq j \leq \nu - 1$, which is true since it is equivalent to having $j+1 \leq \nu$ and $\nu \leq j+p$. But this is simply a consequence of the second point.
It is important to notice that the global representation of polynomials and splines are just a consequence of the local case. The following lemma states this idea.

Lemma 5 *If $\mathcal{Q}$ is constructed using the previous procedure, then for an integer $l \leq p$, if P^I reproduces the polynomial space $\Pi_l(I)$ the quasi-interpolant $\mathcal{Q}$ reproduces also all polynomials of degree l on $[a,b]$, i.e.*

$$P^I g = g \quad \forall g \in \Pi_l(I) \quad \Rightarrow \mathcal{Q}g = g \quad \forall g \in \Pi_l \tag{97}$$

Moreover, if P^I reproduces the splines on I then it reproduces the splines on $[a,b]$, i.e.

$$P^I g = g \quad \forall g \in \mathcal{S}_p(T, I) \quad \Rightarrow \mathcal{Q}g = g \quad \forall g \in \mathcal{S}_p(T) \tag{98}$$

Proof. TODO ■

Examples

In the following examples, we assume that all interior knots are distincts.

Piecewise linear interpolation

In this case, we can define $I := [t_j, t_{j+1}]$ and

$$P^I f = f(t_j)N_{j-1}^1 + f(t_{j+1})N_j^1$$

which gives the global approximation

$$\mathcal{Q}f = \sum_j f(t_j)N_j^1 \tag{99}$$

3-point quadratic quasi-interpolation

We consider $I := [t_{j+1}, t_{j+2}]$ and the local spline space $\mathcal{S}_2(T, I) :=$ span $\left(N_i^2, j-1 \leq i \leq j+1\right)$.
On I we take three points

$$\begin{cases} x_0^j = t_{j+1} \\ x_1^j = \frac{t_{j+1}+t_{j+2}}{2} \\ x_2^j = t_{j+2} \end{cases}$$

The local approximation is defined as

$$P^I f = \sum_{i=j-1}^{j+1} b_i N_i^2 \tag{100}$$

In order to find the coefficients b_i, we need to solve the linear system

$$P^I f(x_k^j) = f(x_k^j), \quad k \in \{0, 1, 2\} \tag{101}$$

In the next section, we shall show how to compute these coefficients. For the moment, we will give the global approximation in terms of the functionals λ_j

$$\lambda_j f = \begin{cases} f(t_0) & , j = 0 \\ -\frac{1}{2}f(x_0^j) + 2f(x_1^j) - \frac{1}{2}f(x_2^j) & , 1 \leq j \leq n-1 \\ f(t_{n+1}) & , j = n \end{cases} \tag{102}$$

5-point cubic quasi-interpolation

We consider $I := [t_{j+1}, t_{j+3}]$ and the local spline space $\mathcal{S}_3(T, I) :=$ span $\left(N_i^3, j-2 \leq i \leq j+2\right)$.
On I we take five points

$$\begin{cases} x_0^j = t_{j+1} \\ x_1^j = \frac{t_{j+1}+t_{j+2}}{2} \\ x_2^j = t_{j+2} \\ x_3^j = \frac{t_{j+2}+t_{j+3}}{2} \\ x_4^j = t_{j+3} \end{cases}$$

The local approximation is defined as

$$P^I f = \sum_{i=j-2}^{j+2} b_i N_i^3 \tag{103}$$

In order to find the coefficients b_i, we need to solve the linear system

$$P^I f(x_k^j) = f(x_k^j), \quad k \in \{0,1,2,3,4\} \tag{104}$$

The global approximation in terms of the functionals λ_j

$$\lambda_j f = \begin{cases} f(t_3) & , j = 0 \\ -\frac{1}{18}\left(-5f(x_0^j) + 40f(x_1^j) - 24f(x_2^j) + 8f(x_3^j) - f(x_4^j)\right) & , j = 1 \\ -\frac{1}{6}\left(f(x_0^j) - 8f(x_1^j) + 20f(x_2^j) - 8f(x_3^j) + f(x_4^j)\right) & , 2 \leq j \leq n-2 \\ -\frac{1}{18}\left(-f(x_0^j) + 8f(x_1^j) - 24f(x_2^j) + 40f(x_3^j) - 5f(x_4^j)\right) & , j = n-1 \\ f(t_{n+1}) & , j = n \end{cases} \tag{105}$$

Computing the coefficients functionals

In the sequel, we shall explain how to compute the coefficients λ_j through the example of the 3-point quadratic quasi-interpolant. We will be looking for λ_j in the general form

$$\lambda_j : f \mapsto \omega_0 f(x_0^j) + \omega_1 f(x_1^j) + \omega_2 f(x_2^j)$$

By taking f to be one of the B-Splines $\{N_{j-1}^2, N_j^2, N_{j+1}^2\}$ we get the linear system

$$\begin{cases} \lambda_j N_{j-1}^2 = \omega_0 N_{j-1}^2(x_0^j) + \omega_1 N_{j-1}^2(x_1^j) + \omega_2 N_{j-1}^2(x_2^j) \\ \lambda_j N_j^2 = \omega_0 N_j^2(x_0^j) + \omega_1 N_j^2(x_1^j) + \omega_2 N_j^2(x_2^j) \\ \lambda_j N_{j+1}^2 = \omega_0 N_{j+1}^2(x_0^j) + \omega_1 N_{j+1}^2(x_1^j) + \omega_2 N_{j+1}^2(x_2^j) \end{cases} \tag{106}$$

On the other hand, by construction we have $\lambda_j N_i^2 = \delta_{ij}$. Therefor, the left hand side of our system is known. Now what remains is to have numerical values for the B-Splines evaluation on $\{x_0^j, x_1^j, x_2^j\}$. Since $I = [t_{j+1}, t_{j+2}]$ only the knots t_{j+1} and t_{j+2} are *seen* by the space of quadratic polynomials on I. We can then extend theses knots with any knots we want to get a set of B-Splines that can be easily evaluated (let's say analyticaly). The simplest way is to consider the Bernstein polynomials, meaning we take the knot sequence $\{t_{j+1}, t_{j+1}, t_{j+1}, t_{j+2}, t_{j+2}, t_{j+2}\}$. In this case, we get the linear system

$$\begin{cases} \omega_0 B_0^2(0) + \omega_1 B_0^2(\frac{1}{2}) + \omega_2 B_0^2(1) = 0 \\ \omega_0 B_1^2(0) + \omega_1 B_1^2(\frac{1}{2}) + \omega_2 B_1^2(1) = 1 \\ \omega_0 B_2^2(0) + \omega_1 B_2^2(\frac{1}{2}) + \omega_2 B_2^2(1) = 0 \end{cases} \tag{107}$$

which gives

$$\begin{cases} 0 &= \omega_0 &+ \frac{1}{4}\omega_1 & & \\ 1 &= & \frac{1}{2}\omega_1 & & \\ 0 &= & \frac{1}{4}\omega_1 &+ \omega_2 \end{cases} \tag{108}$$

Therefor

$$\begin{cases} \omega_0 &= -\frac{1}{2} \\ \omega_1 &= 2 \\ \omega_2 &= -\frac{1}{2} \end{cases} \tag{109}$$

Global approximation

Interpolation

Given the set of interpolations points $X := \{x_0, \cdots, x_n\}$ and data $Y := \{y_0, \cdots, y_n\}$, we aim to find a spline s such that $y_i = s(x_i)$. The Spline interpolation problems is

Definition 13 (Spline interpolation) *Find a spline* $s := \sum_{j=0}^{n} c_j N_j^p \in \mathcal{S}_p(T)$ *such that*

$$s(x_i) = y_i \qquad 0 \leq i \leq n \tag{110}$$

In a matrix form, the Spline interpolation problem writes

$$Mc = y \tag{111}$$

where c is the unkown vector of the spline coefficients,

$$c = \begin{pmatrix} c_0 \\ c_1 \\ \vdots \\ c_n \end{pmatrix}$$

M is the **collocation matrix** given by

$$M = \begin{pmatrix} N_0^p(x_0) & \dots & N_n^p(x_0) \\ N_0^p(x_1) & \dots & N_n^p(x_1) \\ \vdots & \dots & \vdots \\ N_0^p(x_n) & \dots & N_n^p(x_n) \end{pmatrix} \tag{112}$$

while y is the given data

$$y = \begin{pmatrix} y_0 \\ y_1 \\ \vdots \\ y_n \end{pmatrix}$$

Notice that when interpolating a function f, the given data will be $y_i := f(x_i)$.
In general the linear system given by the Eq. 111 is not always solvable. The following result by Whitney-Schoenberg gives a necessary and sufficient condition to ensure that the interpolation problem has a unique solution.

Theorem 21 *The collocation matrix is nonsingular if and only if the diagonal elements are positive, i.e.*

$$N_i^p(x_i) > 0 \quad \forall i \in \{0, \dots, n\} \tag{113}$$

This condition is also equivalent to

$$t_i < x_i < t_{i+p+1} \quad \forall i \in \{0, \dots, n\} \tag{114}$$

Exercise 22 *Show that the Greville points fullfill the Whitney-Schoenberg condition Eq. 113.*

Histopolation

Another interesting way to approximate a function, is to preserve the integrals between given points, rather than the value of the function on these points. Given the set of interpolations points $X := \{x_0, \cdots, x_{n+1}\}$ and a continuous function f, the histopolation problem writes

Definition 14 (Spline histopolation) *Find a spline* $s := \sum_{j=0}^{n} c_j N_j^p \in \mathcal{S}_p(T)$ *such that*

$$\int_{x_i}^{x_{i+1}} s \, dx = \int_{x_i}^{x_{i+1}} f \, dx \qquad 0 \leq i \leq n \tag{115}$$

In a matrix form, the Spline histopolation problem writes

$$Mc = y \tag{116}$$

where c is the unkown vector of the spline coefficients,

$$c = \begin{pmatrix} c_0 \\ c_1 \\ \vdots \\ c_n \end{pmatrix}$$

M is the **histopolation matrix** given by

$$M = \begin{pmatrix} \int_{x_0}^{x_1} N_0^p \, dx & \dots & \int_{x_0}^{x_1} N_n^p \, dx \\ \int_{x_1}^{x_2} N_0^p \, dx & \dots & \int_{x_1}^{x_2} N_n^p \, dx \\ \vdots & \dots & \vdots \\ \int_{x_n}^{x_{n+1}} N_0^p \, dx & \dots & \int_{x_n}^{x_{n+1}} N_n^p \, dx \end{pmatrix} \tag{117}$$

while y is the given data

$$y = \begin{pmatrix} \int_{x_0}^{x_1} f \, dx \\ \int_{x_1}^{x_2} f \, dx \\ \vdots \\ \int_{x_n}^{x_{n+1}} f \, dx \end{pmatrix}$$

Theorem 23 *The histopolation matrix is nonsingular if and only if*

$$t_i < x_i < t_{i+p+1} \quad \forall i \in \{0, \dots, n\} \tag{118}$$

Proof. TODO ∎

Histopolation using M-Splines

Rather than using the B-Splines for the histopolation problem, one can use the M-Splines. In this case, the histopolation matrix given in Eq. 117 can be computed easily using the following result.

Proposition 36 *For every $0 \leq i \leq n$ and $0 \leq j \leq n$, we have*

$$\int_{x_i}^{x_{i+1}} M_j^p(t)\, dt = \sum_{k=0}^{j-1} \left(N_k^p(x_i) - N_k^p(x_{i+1}) \right) \tag{119}$$

Proof. Integrating the relation $\frac{d}{dt} N_k^p(t) = M_k^p(t) - M_{k+1}^p(t)$ on the interval $[x_i, x_{i+1}]$, we have

$$N_k^p(x_{i+1}) - N_k^p(x_i) = \int_{x_i}^{x_{i+1}} \left(M_k^p(t) - M_{k+1}^p(t) \right)\, dt$$

summing the last equation for $k = 0$ to $k = j - 1$, we get

$$\begin{aligned} \sum_{k=0}^{j-1} \left(N_k^p(x_{i+1}) - N_k^p(x_i) \right) &= \int_{x_i}^{x_{i+1}} \sum_{k=0}^{j-1} \left(M_k^p(t) - M_{k+1}^p(t) \right)\, dt \\ &= \int_{x_i}^{x_{i+1}} \left(M_0^p(t) - M_j^p(t) \right)\, dt \end{aligned}$$

hence,

$$\int_{x_i}^{x_{i+1}} M_j^p(t)\, dt = \sum_{k=0}^{j-1} \left(N_k^p(x_i) - N_k^p(x_{i+1}) \right)$$

∎

Remark 24 *The last result gives an optimized implementation for the assembly of the histopolation matrix, since the right hand side term can be computed by accumulating the summation for each j.*

Least-square approximation

In the sequel, we consider a set of points $X := \{x_0, \cdots, x_m\}$ where $m \geq n$ and given data $Y := \{y_0, \cdots, y_m\}$. The least square problem writes

Definition 15 (Spline least-square approximation) *Find a spline $s := \sum_{j=0}^{n} c_j N_j^p \in \mathcal{S}_p(T)$ such that*

$$\min_{g \in \mathcal{S}_p(T)} \sum_{i=0}^{m} (g(x_i) - y_i)^2 \tag{120}$$

where $(w_i)_{i=0}^m$ is a set of positive weights.

Lemma 6 *The problem 120 is equivalent to the linear least square problem*

$$\min_{c \in \mathbb{R}^n} \|Mc - b\|^2 \tag{121}$$

where $M_{ij} = \sqrt{w_i} N_j^p(x_i)$ *and* $b_i = \sqrt{w_i} y_i$.

Proof. TODO ■

Lemma 7 *The matrix* $M^T M$ *is symmetric and nonsingular.*

Proof. TODO ■

Proposition 37 *The problem 121 has a solution given by*

$$M^T M c = M^T b \tag{122}$$

The solution is unique if M has linearly independent columns.

Proof. TODO ■

Theorem 24 *The problem 121 has a unique solution if and only if we can find a sub-sequence* $(x_{i_l})_{l=0}^n$ *such that*

$$N_l^p(x_{i_l}) \neq 0 \quad \forall l \in \{0, \dots, n\} \tag{123}$$

Proof. TODO ■

Approximation with Quasi-Interpolation

In this section, we are interested in local linear methods to construct an approximation of a given function f. This means that each functional λ_i will be a linear functional that depends only on the values of f on the support of N_i^p.

In the sequel, we will assume that $f \in \mathcal{C}^{-1}[a,b]$ and we consider a knot vector such that $t_p = a$ and $t_{n=1} = b$. We first start by giving some definitions.

Definition 16 *Let $S \subset [a,b]$ be a nonempty set. A linear functional $\lambda : \mathcal{C}^{-1}[a,b] \mapsto \mathbb{R}$ is said to be **supported** on S if*

$$\lambda(f) = 0, \quad \forall f \in \mathcal{C}^{-1}[a,b] \quad \text{such that } f|_S = 0 \tag{124}$$

Definition 17 *The quasi-interpolant $\mathcal{Q}$ is called a **local quasi-interpolants** if*

1. *each λ_i is supported on the interval I_i, where*

$$I_i := [t_i, t_{i+p+1}] \bigcap [a,b] \tag{125}$$

2. *the quasi-interpolant $\mathcal{Q}$ reproduces Π_l, for some $l \in [0,p]$, i.e.*

$$\mathcal{Q}f(x) = f(x), \quad \forall x \in [a,b] \text{ and } \forall f \in \Pi_l \tag{126}$$

Definition 18 *A local quasi-interpolant $\mathcal{Q}$ is **bounded** in a L_q-norm, with $1 \leq q \leq \infty$, if there is a constant $C_{\mathcal{Q}}$ such that for each λ_i we have*

$$\forall f \in \mathcal{C}^{-1}[a,b], \quad |\lambda_i f| \leq C_{\mathcal{Q}} h_i^{-\frac{1}{q}} \|f\|_{L_q(I_i)} \tag{127}$$

with $h_i = \max_{l \in D_i} t_{l+1} - t_l$, with $D_i := [\max(i, p+1)], \min(i+p, n)]$.

Lemma 8 *Suppose that $f \in L_q([t_p, t_{n+1}])$ for some q, with $1 \leq q \leq \infty$ and there exists a set of strictly increasing integers $\{m_{i_1}, \cdots, m_{i_2}\}$, with $t_p \leq t_{m_{i_1}}$ and $t_{m_{i_2}+r} \leq t_{n+1}$ for some positive integer r and integers i_1 and i_2. Then*

$$\left(\sum_{j=i_1}^{i_2} \|f\|^q_{L_q([t_{m_j}, t_{m_j+r}])} \right)^{\frac{1}{q}} \leq r^{\frac{1}{q}} \|f\|_{L_q([t_p, t_{n+1}])} \tag{128}$$

Proof. TODO ∎

Theorem 25 (Local estimation) *Let $\mathcal{Q}$ be a bounded local quasi-interpolant in an L_q-norm, with $1 \leq q \leq \infty$. Let l and p be integers with $0 \leq l \leq p$. Suppose $t_m < t_{m+1}$ for some $p \leq m \leq n$ and let $f \in W_q^{l+1}(J_m)$ with*

$$J_m := [t_{m-p}, t_{m+p+1}] \bigcap [a,b]$$

Then

$$\|f - \mathcal{Q}f\|_{L_q([t_m,t_{m+1}])} \leq \frac{(2p+1)^{l+1}}{l!}\,(1 + C_{\mathcal{Q}})\,h_m^{l+1}\|f^{(l+1)}\|_{L_q(J_m)} \quad (129)$$

where $h_m = \max_{m-p\leq i\leq m+p,[t_i,t_{i+1}]\subset J_m} t_{i+1} - t_i$

Proof. We recall that for $l \geq 0$, f is a continuous function. Let $x \in [t_m, t_{m+1})$. Using lemma 2 and the fact that $\mathcal{Q}$ is bounded in L_q-norm, we have

$$|\mathcal{Q}f(x)| \leq \max_{m-p\leq j\leq m} |\lambda_j f| \leq \max_{m-p\leq j\leq m} C_{\mathcal{Q}} h_j^{-\frac{1}{q}} \|f\|_{L_q(I_j)}$$

But $t_{m+1} - t_m \leq \max_{m-p\leq j\leq m} h_j$ and $J_m = \bigcup_{m-p\leq j\leq m} I_j$, we get

$$\|\mathcal{Q}f\|_{L_q([t_m,t_{m+1}])} \leq C_{\mathcal{Q}}\|f\|_{L_q(J_m)} \quad (130)$$

Now let g be any polynomial of degree l, *i.e.* $g \in \Pi_l$. Since $\mathcal{Q}$ reproduces all polynomials of degree l, we have

$$\|f - \mathcal{Q}f\|_{L_q([t_m,t_{m+1}])} \leq \|f - g\|_{L_q([t_m,t_{m+1}])} + \|\mathcal{Q}(g - f)\|_{L_q([t_m,t_{m+1}])}$$

But since $[t_m, t_{m+1}] \subset J_m$, using Eq. 130 we get

$$\|f - \mathcal{Q}f\|_{L_q([t_m,t_{m+1}])}(1 + C_{\mathcal{Q}})\|f - g\|_{L_q(J_m)}$$

Now let us choose g to be the Taylor polynomial of degree l with $\tau = \max(t_{m-p}, a)$. Byt taking $r = 0$ in refTODO we get

$$\|f - g\|_{L_q(J_m)} \leq \frac{(2p+1)^{l+1}}{l!} h_m^{l+1}\|f^{(l+1)}\|_{L_q(J_m)} \quad (131)$$

Therefor

$$\|f - \mathcal{Q}f\|_{L_q([t_m,t_{m+1}])}(1 + C_{\mathcal{Q}})\frac{(2p+1)^{l+1}}{l!} h_m^{l+1}\|f^{(l+1)}\|_{L_q(J_m)}$$

■

Theorem 26 (Global estimation) *Let $\mathcal{Q}$ be a bounded local quasi-interpolant in an L_q-norm, with $1 \leq q \leq \infty$. Let l and p be integers with $0 \leq l \leq p$. For all $f \in W_q^{l+1}([a, b])$ we have*

$$\|f - \mathcal{Q}f\|_{L_q([a,b])} \leq \frac{(2p+1)^{l+1+\frac{1}{q}}}{l!}\,(1 + C_{\mathcal{Q}})\,h^{l+1}\|f^{(l+1)}\|_{L_q([a,b])} \quad (132)$$

where $h = \max_{p\leq i\leq n} t_{i+1} - t_i$

Proof. Use the local estimation theorem and the lemma 8 gives the desired result. ■

Quasi-interpolation and reproduction of polynomials

In order to use the previous results, one still needs to show that a quasi-interpolant reproduces polynomials of a given degree l. In the sequel, we shall give conditions to find the degree l.

Proposition 38 *We consider a set of $n+1$ basis functions for Π_l, given by*

$$\{\phi_{j,0}, \dots, \phi_{j,l}\}, \quad j \in \{0, \dots, n\}, \quad 0 \leq l \leq p \tag{133}$$

and we consider their B-Splines representations as

$$\phi_{i,j} = \sum_{k=0}^{n} c_{ijk} N_k^p \tag{134}$$

A linear quasi-interpolant $\mathcal{Q}$ reproduces Π_l if the corresponding linear functionals satisfy

$$\lambda_j(\phi_{ij}) = c_{jij}, \quad j \in \{0, \dots, n\}, \quad i \in \{0, \cdots, l\} \tag{135}$$

Proof. TODO ■

The next proposition gives a sufficient condition for a quasi-interpolant to reporoduce the Schoenberg space.

Proposition 39 *The linear quasi-interpolant $\mathcal{Q}$ reproduces the whole spline space if*

1. *$\mathcal{Q}$ reproduces Π_l*
2. *each linear functional λ_j is supported on one knot interval*

$$[t_{m_j}^+, t_{m_j+1}^-] \subset [t_j, t_{j+p+1}] \tag{136}$$

Proof. TODO ■

Examples

Variation diminishing approximation

Proposition 40 *For every function $f \in W_\infty^2([a,b])$ we have*

$$\|f - Vf\|_{L_\infty([a,b])} \leq 2(2p+1)^2 h^2 \|f''\|_{L_\infty([a,b])} \tag{137}$$

Exercise 27 *Prove the last proposition.*
(Hint: use the global estimation theorem with the L_∞-norm.)

3-points quadratic quasi-interpolation

Proposition 41 *For every function $f \in W_\infty^3([a,b])$ we have*

$$\|f - \mathcal{Q}_2 f\|_{L_\infty([a,b])} \leq 250 h^3 \|f^{(3)}\|_{L_\infty([a,b])} \tag{138}$$

Proof. TODO ■

Approximation power of Splines

The following result gives the approximation power on the Schoenberg space. After stating this important result, we shall give the proof through different steps.

Proposition 42 (Approximation Error) *Let $f \in W_q^{l+1}([a,b])$ with $1 \leq q \leq \infty$ and $0 \leq l \leq p$. Then there exists a spline $s_p \in \mathcal{S}_p(T)$ such that*

$$\|D^{(r)}(f - s_p)\|_{L_q([a,b])} \leq Kh^{l+1-r}\|f^{(l+1)}\|_{L_q([a,b])}, \quad 0 \leq r \leq l \tag{139}$$

where $h := \max_{p \leq j \leq n}$ and K is a constant depending only on p.

Remark 25 *The constant K grows exponentially with p, but can be removed in some cases.*

Part III

IGA Finite Elements method

Functional Analysis

Contents

Notations and Preliminaries

In the course of the lecture we shall work with the Sobolev spaces $H^m(\Omega)$, $H(\mathrm{div},\Omega)$ and $H(\mathrm{div},\Omega)$ and recall here there basic properties without proof. For a more detailed presentation with proofs we refer to Section 2.1. of [2].

- we use blodface notation for spaces of vector functions. For instance in $3D$, $\boldsymbol{H}^1(\Omega)$ denotes the space $\left(H^1(\Omega)\right)^3$.
- for an operator $d \in \{\boldsymbol{\nabla}, \nabla\times, \nabla\cdot\}$, we denote the kernel space $\mathcal{N}(d)$ while the range will be $\mathcal{R}(d)$.

We shall need the following Sobolev spaces, given first without boundary conditions,

$$H^1(\Omega) = \left\{\varphi \in L^2(\Omega),\ \nabla\varphi \in \boldsymbol{L}^2(\Omega)\right\} \tag{140}$$

$$\boldsymbol{H}^1(\Omega) = \left\{\boldsymbol{\Psi} \in L^2(\Omega),\ \nabla\boldsymbol{\Psi} \in \boldsymbol{L}^2(\Omega)\right\} \tag{141}$$

$$\boldsymbol{H}(\mathrm{curl},\Omega) = \left\{\boldsymbol{\Psi} \in L^2(\Omega),\ \nabla\times\boldsymbol{\Psi} \in \boldsymbol{L}^2(\Omega)\right\} \tag{142}$$

$$\boldsymbol{H}(\mathrm{div},\Omega) = \left\{\boldsymbol{\Psi} \in L^2(\Omega),\ \nabla\cdot\boldsymbol{\Psi} \in L^2(\Omega)\right\} \tag{143}$$

and using the correspondant boundary conditions,

$$H^1_0(\Omega) = \left\{\varphi \in H^1(\Omega),\ \varphi = 0 \text{ on } \partial\Omega\right\} \tag{144}$$

$$\boldsymbol{H}^1_0(\Omega) = \left\{\boldsymbol{\Psi} \in \boldsymbol{H}^1(\Omega),\ \boldsymbol{\Psi} = 0 \text{ on } \partial\Omega\right\} \tag{145}$$

$$\boldsymbol{H}_0(\mathrm{curl},\Omega) = \{\boldsymbol{\Psi} \in \boldsymbol{H}(\mathrm{curl},\Omega),\ \boldsymbol{\Psi}\times\boldsymbol{n} = 0 \text{ on } \partial\Omega\} \tag{146}$$

$$\boldsymbol{H}_0(\mathrm{div},\Omega) = \{\boldsymbol{\Psi} \in \boldsymbol{H}(\mathrm{div},\Omega),\ \boldsymbol{\Psi}\cdot\boldsymbol{n} = 0 \text{ on } \partial\Omega\} \tag{147}$$

$$L^2_0(\Omega) = \left\{\varphi \in L^2(\Omega);\ \int_\Omega \varphi = 0\right\} \tag{148}$$

Sobolev spaces

We shall denote by $\mathcal{D}(\Omega)$ the space of distribution.

The Sobolev space $W^{s,m}$

We start by recalling the definition of Sobolev spaces:

Definition 19 *Let s and m be two integers with $s \geq 0$ and $1 \leq m \leq \infty$. The Sobolev space $W^{s,m}(\Omega)$ is defined as*

$$W^{s,m}(\Omega) = \{u \in \mathcal{D}'(\Omega),\ D^\alpha u \in L^m(\Omega), |\alpha| \leq s\} \tag{149}$$

The space $W^{s,m}(\Omega)$ can be equipped with norm

$$\|u\|_{W^{s,m}(\Omega)} := \sum_{|\alpha|\leq s} \|D^\alpha u\|_{L^p(\Omega)} \tag{150}$$

The Sobolev space H^m

For any integer $m \geq 1$, one can define

$$H^m(\Omega) = W^{m,2}(\Omega) := \{v \in L^2(\Omega) \mid D^\alpha v \in L^2(\Omega),\ |\alpha| \leq m\} \quad (151)$$

$H^m(\Omega)$ is a Hilbert space equipped with the scalar product

$$(u, v)_{m,\Omega} := \sum_{|\alpha| \leq m} \int_\Omega D^\alpha u D^\alpha v \quad (152)$$

the associated norm will be denoted $\| \cdot \|_{s,\Omega}$.

The most classical second order operator is the Laplace operator, which reads in an arbitrary dimension d (generally $d = 1, 2$ or 3),

$$\Delta u = \sum_{i=1}^{d} \frac{\partial^2 u}{\partial x_d^2}.$$

The classical Green formula for the Laplace operator reads: for $u \in H^1(\Omega)$ and $v \in H^1(\Omega)$

$$-\int_\Omega \Delta u\, v \, \mathrm{d}x = \int_\Omega \nabla u \cdot \nabla v \, dx - \int_{\partial\Omega} \frac{\partial u}{\partial n} v \, \mathrm{d}\sigma. \quad (153)$$

For essential boundary conditions related with this Green formula we shall define the space

$$H_0^1(\Omega) = \{v \in H^1(\Omega) \mid v_{|\partial\Omega} = 0\}.$$

Another classical operator which comes from elasticity is the bilaplacian operator $\Delta^2 = \Delta\Delta$, which is a fourth order operator. The Green formula needed for variational formulations of PDEs based on the bilaplacian reads

$$\int_\Omega \Delta^2 u\, v \, \mathrm{d}\mathbf{x} = \int_\Omega u\, \Delta^2 v \, \mathrm{d}\mathbf{x} + \int_{\partial\Omega} \left(u \frac{\partial \Delta v}{\partial n} - v \frac{\partial \Delta u}{\partial n} + \Delta u \frac{\partial v}{\partial n} - \Delta v \frac{\partial u}{\partial n} \right) \mathrm{d}\sigma \quad (154)$$

$$H_0^2(\Omega) = \{v \in H^1(\Omega) \mid v_{|\partial\Omega} = 0,\ \frac{\partial v}{\partial n}|_{\partial\Omega} = 0\}.$$

Inequalities

Lemma 9 (Poincaré) *Let $1 \leq p \leq \infty$ and Ω be a bounded open set. Then, there exists a constant $C = C(p, \Omega)$, such that*

$$\forall v \in W_0^{1,p}(\Omega), \quad C\|v\|_{L^p(\Omega)} \leq \|\nabla v\|_{L^p(\Omega)} \quad (155)$$

The Sobolev space $H(curl, \Omega)$

The Sobolev space $H(div, \Omega)$

DeRham sequences

For any function $u \in H^1(\Omega)$ we have $\nabla \times \boldsymbol{\nabla} u = 0$. On the other hand, we have for any function $\boldsymbol{u} \in \boldsymbol{H}(\text{curl}, \Omega)$, $\nabla \cdot \nabla \times \boldsymbol{u} = 0$. We just have shown that $\boldsymbol{\nabla}(H^1(\Omega)) \subset \mathcal{N}(\nabla\times)$ and $\nabla \times (\boldsymbol{H}(\text{curl}, \Omega)) \subset \mathcal{N}(\nabla\cdot)$. This is summarized in the following diagram, known as DeRham sequence, without boundary conditions in this case,

$$\mathbb{R} \hookrightarrow H^1(\Omega) \xrightarrow{\boldsymbol{\nabla}} \boldsymbol{H}(\text{curl}, \Omega) \xrightarrow{\nabla\times} \boldsymbol{H}(\text{div}, \Omega) \xrightarrow{\nabla\cdot} L^2(\Omega) \longrightarrow 0 \tag{156}$$

and using the correspondant boundary conditions,

$$H_0^1(\Omega) \xrightarrow{\boldsymbol{\nabla}} \boldsymbol{H}_0(\text{curl}, \Omega) \xrightarrow{\nabla\times} \boldsymbol{H}_0(\text{div}, \Omega) \xrightarrow{\nabla\cdot} L_0^2(\Omega) \longrightarrow 0 \tag{157}$$

In fact, DeRham complexes are sequences of spaces V_i and operators d_i such that $\mathrm{d}_{i+1} \circ \mathrm{d}_i = 0$. It leads to a sepcific algebraic structure that has been subject to active research in Analysis and Algebraic Geometry.

Galerkin methods

Contents

Abstract framework

We consider a and L to be continuous bilinear and linear forms, respectively, on a Hilbert space V. We want to find a computable approximation for the solution $u \in V$ of the variational problem

$$a(u,v) = \langle L, v \rangle, \quad \forall v \in V \tag{158}$$

where $\langle \cdot, \cdot \rangle$ denotes the duality product between V' and V.

The idea of Galerkin approximation, is to find the solution in a family of subspaces of finite dimension, then prove that the constructed solutions converge to the solution of the variational problem Eq. (158). There are two major strategies, the first one is based on the coercivity and the other one on the *inf-sup* conditions. While the coercivity is easy to use, unfortunately, most of problems in CFD do not fullfill it.

Definition 20 (V-ellipcity or Coercivity) *a is said to be coercive, if there exists a constant $\alpha > 0$ such that*

$$a(v,v) \geq \alpha \|v\|_V^2, \quad \forall v \in V \tag{159}$$

Definition 21 (*inf-sup* conditions) *a is said to statisfy the inf-sup conditions, if there exists a constant $\alpha > 0$ such that*

1.

$$\sup_{v \in V} \frac{a(u,v)}{\|v\|_V} \geq \alpha \|u\|_V, \quad \forall u \in V \tag{160}$$

2.

$$\sup_{u \in V} \frac{a(u,v)}{\|u\|_V} \geq \alpha \|v\|_V, \quad \forall v \in V \tag{161}$$

Remark 26 *Notice that when a satisfies the inf-sup conditions and it is symmetric, then both conditions are the same. In general, the two conditions can be written as*

$$\inf_{u \in V} \sup_{v \in V} \frac{a(u,v)}{\|u\|_V \|v\|_V} > 0$$

and

$$\inf_{v \in V} \sup_{u \in V} \frac{a(u,v)}{\|u\|_V \|v\|_V} > 0$$

Finally, let us notice that the coercivity implies the *inf-sup* conditions.

Lemma 10 *If a is coercive then it satisfies the inf-sup conditions.*

Proof. We have

$$\sup_{v \in V} \frac{a(u,v)}{\|v\|_V} \geq \frac{a(u,u)}{\|u\|_V}$$

then we conclude using the coercivity of a. ∎

Galerkin Approximation

We consider a family of finite dimensional subspaces of V, denoted by $(V_h)_{h>0}$. The Galerkin approximation $u_h \in V_h$ is defined as the solution of the varional problem Eq. (158) by restricting the test functions on V_h, *i.e.*

$$a(u_h, v) = \langle L, v \rangle, \quad \forall v \in V_h \tag{162}$$

It is important to notice that while coercivity is inherited on subspaces, the *inf-sup* conditions are not. It is therefor important to have an additional *inf-sup* condition on the subspace, known as **stability condition**.

Convergence under coercivity

We recall Cea's lemma, which states that the Galerkin approximation is bounded by the best approximation of u from the subspace.

Lemma 11 (Cea) *If a is a continuous and coercive bilinear form, then*

$$\|u - u_h\|_V \leq \frac{M}{\alpha} \inf_{v \in V_h} \|u - v\|_V \tag{163}$$

Proof. Since both u and u_h are solutions to the variational problem (158) respectively on V and V_h, we have

$$a(u - u_h, v) = 0, \quad \forall v \in V_h$$

therefor, for $v \in V_h$, we have

$$a(u - u_h, u - v) = a(u - u_h, u - u_h) + a(u - u_h, u_h - v) = a(u - u_h, u - u_h)$$

Using the coercivity, we have

$$\alpha \|u - u_h\|_V \leq a(u - u_h, u - u_h) = a(u - u_h, u - v)$$

finaly, the continuity of a gives

$$a(u - u_h, u - v) \leq M \|u - u_h\|_V \|u - v\|_V$$

by combining the two previous inequalities we get the desired result. ■

Theorem 28 *If a is a continuous and coercive bilinear form and the subspaces V_h are such that*

$$\lim_{h \to 0} d(u, V_h) = 0 \tag{164}$$

with $d(u, V_h) := \inf_{v \in V_h} \|u - v\|_V$. Then

$$\lim_{h \to 0} u_h = u$$

Proof. Follows immedialty from Cea's lemma. ■

Convergence under inf-sup conditions

As mentioned before, the *inf-sup* conditions are not inherited on the subspaces V_h. In general, we must prove that there exists $\beta > 0$, such that the *inf-sup* holds on V_h, *i.e.*

$$\sup_{v \in V_h} \frac{a(u,v)}{\|v\|_V} \geq \beta \|u\|_V, \quad \forall u \in V_h \tag{165}$$

Idealy, β should be independent of N, in order to get the convergence.

Exercise 29 *Prove that the second part of the inf-sup conditions is a consequence of the inequality* (165).

As in the coercive case, we first state a result that compares the Galerkin approximation with the distance to the space of approximation. This result is a generalization of Cea's lemma, and is due to Babuska.

Lemma 12 (Babuska) *If a is a continuous bilinear form and satisfies the inf-sup+stability conditions, then*

$$\|u - u_h\|_V \leq \left(1 + \frac{M}{\beta}\right) \inf_{v \in V_h} \|u - v\|_V \tag{166}$$

Proof. Let $v \in V_h$. since $v - u_h \in V_h$, the stability condition gives

$$\sup_{\phi \in V_h} \frac{a(v - u_h, \phi)}{\|\phi\|_V} \geq \beta \|v - u_h\|_V$$

but $a(u - u_h, v) = 0$, meaning $a(v - u_h, \phi) = a(v - u, \phi)$ for all $\phi \in V_h$. Now using the continuity of a we get

$$M\|v - u\|_V \geq \sup_{\phi \in V_h} \frac{a(v - u, \phi)}{\|\phi\|_V} \geq \beta \|v - u_h\|_V$$

we conclude the proof by using the triangle inequality

$$\|u - u_h\|_V \leq \|u - v\|_V + \|v - u_h\|_V \leq \|u - v\|_V + \frac{M}{\beta}\|v - u\|_V$$

■

Theorem 30 *If a is a continuous bilinear form and satisfies the inf-sup+stability conditions. If the subspaces V_h are such that condition* (164) *holds, then*

$$\lim_{h \to 0} u_h = u$$

Proof. Follows immedialty from Babuska's lemma. ■

Remark 27 *Under the additional stability condition, we have $\|u_h\|_V \leq \frac{1}{\beta}\|L\|_{V'}$, which is valid uniformuly in N if β is independent of N.*

The three basic aspects of the Finite Elements method

Let $\Omega \subset \mathbb{R}^d$, with $d \geq 1$, be a bounded domain.

In order to apply the Galerkin method, we face, by definition the problem of constructing the family of finite dimensional subspaces $V_h \subset V$, such that V is $H^1(\Omega)$, $H_0^1(\Omega)$, $H^2(\Omega)$, $H(\text{curl}, \Omega)$, ... As stating by P. Ciarlet, the Finite Elements Method is in its simplest form, a specific process of constructing the family $(V_h)_{h \geq 0}$. This construction is characterized by three basic aspects and are described below.

First basic aspect: Triangulation

A triangulation $\mathcal{T}_h$ is estabilshed over $\bar{\Omega}$, *i.e.* $\bar{\Omega}$ is subdivided into a finite number of subsets K, called **finite elements**, such that

1. $\bar{\Omega} = \bigcup_{K \in \mathcal{T}_h} K$
2. for all $K \in \mathcal{T}_h$, K is closed and its interior is not empty
3. for all $K_1 \neq K_2 \in \mathcal{T}_h$ we have $\mathring{K}_1 \bigcap \mathring{K}_2 = \emptyset$
4. for all $K \in \mathcal{T}_h$, ∂K is Lipschitz-continuous

Second basic aspect: power approximation

On every $K \in \mathcal{T}_h$, a space of functions P_K is constructed. P_K should contain polynomials or functions which are close to polynomials.

- this is the key to all convergence results
- it is also important for having simple and fast computations of the coefficients of the resulting linear system

Third basic aspect: basis functions

There exists at least one **canonical basis** in the space V_h whose corresponding basis functions have a *local support* property, are as small as possible and can be easily described. This aspect leads to sparsity in the resulting matrix.

Examples

Scalar linear elliptic equations of second order

For $\Omega \subset \mathbb{R}^d$, we consider the following problem

$$\left\{ \begin{array}{rl} -\sum\limits_{1\leq i,j\leq d} \partial_{x_i}\left(a_{ij}\partial_{x_j}u\right) & = f, \quad \Omega \\ u & = 0, \quad \partial\Omega \end{array} \right. \tag{167}$$

where the coefficients functions $a_{ij} : \Omega \to \mathbb{R}$ are bounded and there exists $\gamma > 0$ (ellipticity condition) such that

$$\gamma|y|^2 \leq \sum_{1\leq i,j\leq d} a_{ij}(x)y_iy_j, \quad \forall x \in \Omega,\ \forall y \in \mathbb{R}^d \tag{168}$$

Before writing the variational formulation associated to (167), we need to define the space of function V which is in this case given by $V := H_0^1(\Omega)$ where

$$H_0^1(\Omega) = \{u \in H^1(\Omega),\ u = 0 \text{ on } \partial\Omega\} \tag{169}$$

and

$$H^1(\Omega) = \{u \in L^2(\Omega),\ \nabla u \in (L^2(\Omega))^d\} \tag{170}$$

$H_0^1(\Omega)$ is a Hilbert space under the norm $\|\cdot\|_{H_0^1(\Omega)}$ with

$$\|u\|^2_{H_0^1(\Omega)} := \|u\|^2_{L^2(\Omega)} + \|\nabla u\|^2_{L^2(\Omega)} \tag{171}$$

the bilinear and linear forms are given by

$$a(u,v) := \sum_{1\leq i,j\leq d} \int_\Omega a_{ij}\partial_{x_j}u\partial_{x_i}v$$

and

$$\langle L, v\rangle = \int_\Omega fv\ dx$$

Using the ellipticity condition, the boundness of the coefficients and the Poincaré inequality, we show that a is coercive and continuous. Moreover, if $f \in L^2(\Omega)$ then L is countinuous.

Bilaplacian problem

TODO

***H**(curl, Ω)-elliptic problem*

TODO

***H**(div, Ω)-elliptic problem*

TODO

Saddle-point problems

In the sequel, we consider a special case of the problem (158). Consider two Hilbert spaces V and W, two continuous bilinear forms $a \in \mathcal{L}(V \times V, \mathbb{R})$ and $b \in \mathcal{L}(V \times W, \mathbb{R})$ and two continuous linear forms $l_V \in \mathcal{L}(V, \mathbb{R})$ and $l_W \in \mathcal{L}(W, \mathbb{R})$. We denote M_a and M_b the continuity constants for the bilinear forms a and b respectively. Then we define the abstract mixed variational problem as *Find* $(u, p) \in V \times W$ *such that*

$$\left\{ \begin{array}{rcccl} a(u,v) & + & b(v,p) & = & l_V(v) \quad \forall v \in V \\ & & b(u,q) & = & l_W(q) \quad \forall q \in W \end{array} \right. \tag{172}$$

Many problems arising in CFD fit into this abstract framework, such as the Stokes equation. For saddle point problems the Lax-Milgram framework cannot be applied. The alternative solution is then to use the **inf-sup** conditions, known in this case as Banach-Nečas-Babuška (BNB) theorem.
The link with the previous section is achieved by using the bilinear form $c \in \mathcal{L}(X \times X, \mathbb{R})$

$$c((u,p),(v,q)) := a(u,v) + b(v,p) + b(u,q) \tag{173}$$

and the linear form $l_X \in \mathcal{L}(X, \mathbb{R})$

$$l_X(v,q) := l_V(v) + l_W(q) \tag{174}$$

with $X := V \times W$ endowed with the norm $\|(u,p)\|_X := \|u\|_V + \|p\|_W$. Let us introduce the operators $A : V \to V'$ and $B : V \to W'$ such that

$$\langle Au, v \rangle_{V',V} := a(u,v) \quad \forall (u,v) \in V \times V \tag{175}$$

and

$$\langle Bu, p \rangle_{W',V} := b(u,p) \quad \forall (u,p) \in V \times W \tag{176}$$

Since all Hilbert spaces are reflexive Banach spaces, we have $W'' = W$. Hence we can define the following operator $B^T : W \to V'$ such that

$$\langle B^T p, u \rangle_{V',W} := b(u,p) \quad \forall (u,p) \in V \times W \tag{177}$$

Therefor, the problem (172) is equivalent to *Find* $(u, p) \in V \times W$ *such that*

$$\left\{ \begin{array}{rcccl} Au & + & B^T p & = & l_V \\ & & Bu & = & l_W \end{array} \right. \tag{178}$$

Now, let us introduce the nullspace of B

$$\text{Ker } B := \{ v \in V, \ \forall q \in W \quad b(v,q) = 0 \} \tag{179}$$

The following theorem gives shows under which conditions the saddle problem (172) has a solution.

Theorem 31 *The variational problem (172) admits a unique solution if and only if*

1) there exists $\alpha > 0$, such that

$$\begin{cases} \inf\limits_{u \in Ker\ B} \sup\limits_{v \in Ker\ B} \frac{a(u,v)}{\|u\|_V \|v\|_V} \geq \alpha \\ \forall v \in Ker\ B, \quad (\forall u \in Ker\ B,\ a(u,v) = 0) \Rightarrow (v = 0) \end{cases} \tag{180}$$

2) The Babuska-Brezzi, or inf-sup condition, is verified: there exists $\beta > 0$ such that

$$\inf_{q \in W} \sup_{v \in V} \frac{b(u,q)}{\|v\|_V \|q\|_W} \geq \beta \tag{181}$$

In addition, the following a priori estimates hold

$$\begin{cases} \|u\|_V \leq & \frac{1}{\alpha}\|l_V\|_{V'} + \frac{1}{\beta}(1 + \frac{M_a}{\alpha})\|l_W\|_{W'} \\ \|p\|_W \leq & \frac{1}{\beta}(1 + \frac{M_a}{\alpha})\|l_V\|_{V'} + \frac{M_a}{\beta^2}(1 + \frac{M_a}{\alpha})\|l_W\|_{W'} \end{cases} \tag{182}$$

A special case is when the bilinear form a is coercive. In this case, the first conditions can be replaced by a coercivity on Ker B.

Theorem 32 *Let V and W be Hilbert space. Assume a is a continuous bilinear form on $V \times V$ and that b is a continuous linear form on $V \times W$, that l_V and L_W are continuous linear forms on V and W respectively and that the following two hypotheses are verified*

1) a is coercive on $K = \{v \in V \mid b(q,v) = 0,\ \forall q \in W\}$, i.e. there exists $\alpha > 0$ such that

$$a(v,v) \geq \alpha \|v\|_V^2 \quad \forall v \in K.$$

2) The Babuska-Brezzi, or inf-sup condition, is verified: there exists $\beta > 0$ such that

$$\inf_{q \in W} \sup_{v \in V} \frac{b(v,q)}{\|q\|_W \|v\|_V} \geq \beta.$$

Then the variational problem admits a unique solution and the solution satisfies the a priori estimate

$$\begin{cases} \|u\|_V \leq & \frac{1}{\alpha}\|l_V\|_{V'} + \frac{1}{\beta}(1 + \frac{M_a}{\alpha})\|l_W\|_{W'} \\ \|p\|_W \leq & \frac{1}{\beta}(1 + \frac{M_a}{\alpha})\|l_V\|_{V'} + \frac{M_a}{\beta^2}(1 + \frac{M_a}{\alpha})\|l_W\|_{W'} \end{cases} \tag{183}$$

The inf-sup conditions plays an essential role, as it is only satisfied if the spaces V and W are compatible in some sense. This condition being satisfied at the discrete level with a constant β that does not depend on the mesh size being essential for a well behaved Finite Element method. It can be written equivalently

$$\beta \|q\|_W \leq \sup_{v \in V} \frac{b(v,q)}{\|v\|_V} \quad \forall q \in W. \tag{184}$$

And often, a simple way to verify it is, given any $q \in W$, to find a specific $v = v(q)$ depending on q such that

$$\beta \|q\|_W \leq \frac{b(v(q), q)}{\|v(q)\|_V} \leq \sup_{v \in V} \frac{b(v, q)}{\|v\|_V}$$

with a constant β independent of w.

Galerkin approximation

Let us now come to the Galerkin discretisation. The principle is simply to construct finite dimensional subspaces $W_h \subset W$ and $V_h \subset V$ and to write the variational formulation (172) replacing W by W_h and V by V_h. The variational formulations are the same as in the continuous case, like for conforming finite elements. This automatically yields the consistency of the discrete formulation. In order to get the stability property needed for convergence, we need that the coercivity constant α and the inf-sup constant β are independent of h.

Because $V_h \subset V$ the coercivity property is automatically verified in the discrete case, with a coercivity constant that is the same as in the continuous case and hence does not depend on the discretisation parameter h.

Here, however, there is an additional difficulty, linked to the inf-sup conditions, which is completely dependent on the two spaces V_h and W_h. By far not any conforming approximation of the two spaces will verify the discrete inf-sup condition with a constant β that is independent on h. Finding compatible discrete spaces for a given mixed variational formulation, has been an active area of research.

The variational problem for the Galerkin approximation is *Find* $(u_h, p_h) \in V_h \times W_h$ *such that*

$$\left\{ \begin{array}{rcccl} a(u_h, v_h) & + & b(v_h, p_h) & = & l_V(v_h) \quad \forall v_h \in V_h \\ & & b(u_h, q_h) & = & l_W(q_h) \quad \forall q_h \in W_h \end{array} \right. \tag{185}$$

Let us introduce the operator $B_h : V_h \to W_h'$ such that

$$\langle B_h u_h, p_h \rangle_{W_h', V_h} := b(u_h, p_h) \quad \forall (u_h, p_h) \in V_h \times W_h \tag{186}$$

and its nullspace

$$\text{Ker } B_h := \{ v_h \in V_h, \ \forall q_h \in W_h \quad b(v_h, q_h) = 0 \} \tag{187}$$

The following proposition states the conditions under which the Galerkin approximation of the problem (185) admits a solution

Proposition 43 *The variational problem* (185) *admits a unique solution if and only if*

1) there exists $\alpha_h > 0$, such that

$$\inf_{u_h \in Ker\ B_h} \sup_{v_h \in Ker\ B_h} \frac{a(u_h, v_h)}{\|u_h\|_V \|v_h\|_V} \geq \alpha_h \tag{188}$$

2) there exists $\beta_h > 0$ such that

$$\inf_{q_h \in W_h} \sup_{v_h \in V_h} \frac{b(u_h, q_h)}{\|v_h\|_V \|q_h\|_W} \geq \beta_h \tag{189}$$

Remark 28 *The second condition is equivalent to assuming B_h is surjective.*

Finally, we state the following lemma which is equivalent to Cea's lemma.

Lemma 13 *Under the assumptions of theorem 43, we have*

a) if Ker $B_h \subset$ Ker B,

$$\begin{cases} \|u - u_h\|_V \leq & \left(1 + \frac{M_a}{\alpha_h}\right)\left(1 + \frac{M_b}{\beta_h}\right) \inf_{v_h \in V_h} \|u - v_h\|_V \\ \|p - p_h\|_W \leq & \frac{M_a}{\beta_h}\left(1 + \frac{M_a}{\alpha_h}\right)\left(1 + \frac{M_b}{\beta_h}\right) \inf_{v_h \in V_h} \|u - v_h\|_V \\ & + \left(1 + \frac{M_b}{\beta_h}\right) \inf_{q_h \in W_h} \|p - q_h\|_W \end{cases} \tag{190}$$

b) otherwise,

$$\begin{cases} \|u - u_h\|_V \leq & \left(1 + \frac{M_a}{\alpha_h}\right)\left(1 + \frac{M_b}{\beta_h}\right) \inf_{v_h \in V_h} \|u - v_h\|_V \\ & + \frac{M_b}{\alpha_h} \inf_{q_h \in W_h} \|p - q_h\|_W \\ \|p - p_h\|_W \leq & \frac{M_a}{\beta_h}\left(1 + \frac{M_a}{\alpha_h}\right)\left(1 + \frac{M_b}{\beta_h}\right) \inf_{v_h \in V_h} \|u - v_h\|_V \\ & + \left(1 + \frac{M_b}{\beta_h} + \frac{M_a}{\alpha_h}\frac{M_b}{\beta_h}\right) \inf_{q_h \in W_h} \|p - q_h\|_W \end{cases} \tag{191}$$

Examples

Mixed formulation of the Poisson problem

Let $\Omega \subset \mathbb{R}^3$ and consider the Poisson problem

$$\begin{cases} -\Delta p = f & , \Omega \\ p = 0 & , \partial\Omega \end{cases} \tag{192}$$

Using that $\Delta p = \nabla \cdot \nabla p$, we set $\mathbf{u} = \nabla p$, then the Poisson equation (192) can be written equivalently

$$\mathbf{u} = -\nabla p, \quad \nabla \cdot \mathbf{u} = f.$$

Instead of having one unknown, we now have two, along with the above two equations. In order to get a mixed variational formulation,

we first take the dot product of the first one by $\mathbf{v}$ and integrate by parts

$$\int_\Omega \mathbf{u}\cdot\mathbf{v}\,\mathrm{d}\mathbf{x} - \int_\Omega p\,\nabla\cdot\mathbf{v}\,\mathrm{d}\mathbf{x} + \int_{\partial\Omega} p\,\mathbf{v}\cdot\mathbf{n}\,\mathrm{d}\sigma = \int_\Omega \mathbf{u}\cdot\mathbf{v}\,\mathrm{d}\mathbf{x} - \int_\Omega p\,\nabla\cdot\mathbf{v}\,\mathrm{d}\mathbf{x} = 0,$$

using $p = 0$ as a natural boundary condition. Then multiplying the second equation by q and integrating yields

$$\int_\Omega \nabla\cdot\mathbf{u}\,q\,\mathrm{d}\mathbf{x} = \int_\Omega fq\,\mathrm{d}\mathbf{x}.$$

No integration by parts is necessary here. And we thus get the following mixed variational formulation: *Find* $(\mathbf{u},p)\in H(\mathrm{div},\Omega)\times L^2(\Omega)$ *such that*

$$\left\{\begin{array}{lll} \int_\Omega \mathbf{u}\cdot\mathbf{v}\,\mathrm{d}\mathbf{x} - \int_\Omega p\,\nabla\cdot\mathbf{v}\,\mathrm{d}\mathbf{x} = 0, & \forall \mathbf{v}\in H(\mathrm{div},\Omega) \\ \int_\Omega \nabla\cdot\mathbf{u}\,q\,\mathrm{d}\mathbf{x} = \int_\Omega fq\,\mathrm{d}\mathbf{x}, & \forall q\in L^2(\Omega) \end{array}\right. \tag{193}$$

Here also, we get an alternative formulation by not integrating by parts, the mixed term in the first formulation but in the second. The first formulation simply becomes

$$\int_\Omega \mathbf{u}\cdot\mathbf{v}\,\mathrm{d}\mathbf{x} + \int_\Omega \nabla p\cdot\mathbf{v}\,\mathrm{d}\mathbf{x} = 0,$$

and the second, removing immediately the boundary term due to the essential boundary condition $q = 0$

$$\int_\Omega \nabla\cdot\mathbf{u}\,q\,\mathrm{d}\mathbf{x} = -\int_\Omega \mathbf{u}\cdot\nabla q\,\mathrm{d}\mathbf{x} = \int_\Omega fq\,\mathrm{d}\mathbf{x},$$

which leads to the variational formulation *Find* $(\mathbf{u},p)\in L^2(\Omega)^3\times H_0^1(\Omega)$ *such that*

$$\left\{\begin{array}{lll} \int_\Omega \mathbf{u}\cdot\mathbf{v}\,\mathrm{d}\mathbf{x} + \int_\Omega \nabla p\cdot\mathbf{v}\,\mathrm{d}\mathbf{x} = 0, & \forall \mathbf{v}\in L^2(\Omega)^3 \\ \int_\Omega \mathbf{u}\cdot\nabla q\,\mathrm{d}\mathbf{x} = -\int_\Omega fq\,\mathrm{d}\mathbf{x}, & \forall q\in H_0^1(\Omega) \end{array}\right. \tag{194}$$

Note that this formulation actually contains the classical variational formulation for the Poisson equation. Indeed for $q\in H_0^1(\Omega)$, $\nabla q\in L^2(\Omega)^3$ can be used as a test function in the first equation. And plugging this into the second we get

$$\int_\Omega \nabla p\cdot\nabla q\,\mathrm{d}\mathbf{x} = \int_\Omega fq\,\mathrm{d}\mathbf{x},\quad \forall q\in H_0^1(\Omega).$$

Mixed formulation of the Stokes problem

We consider now the Stokes problem for the steady-state modelling of an incompressible fluid

$$\left\{\begin{array}{rl} -\nabla^2\boldsymbol{u} + \nabla p = \boldsymbol{f} & \text{in } \Omega, \\ \nabla\cdot\boldsymbol{u} = 0 & \text{in } \Omega, \\ \boldsymbol{u} = 0 & \text{on } \partial\Omega, \end{array}\right. \tag{195}$$

For the variational formulation, we take the dot product of the first equation with v and integrate over the whole domain

$$\int_\Omega (-\Delta \mathbf{u} + \nabla p) \cdot \mathbf{v} \, \mathrm{d}\mathbf{x} = \int_\Omega \nabla \mathbf{u} : \nabla \mathbf{v} \, \mathrm{d}\mathbf{x} + \int_\Omega \nabla p \cdot \mathbf{v} \, \mathrm{d}\mathbf{x} = \int_\Omega \mathbf{f} \cdot \mathbf{v} \, \mathrm{d}\mathbf{x}$$

The integration by parts is performed component by component. We impose the essential boundary condition $\mathbf{v} = 0$ on $\partial\Omega$, and we denote by

$$\int_\Omega \nabla \mathbf{u} : \nabla \mathbf{v} \, \mathrm{d}\mathbf{x} = \sum_{i=1}^{3} \int_\Omega \nabla u_i \cdot \nabla v_i \, \mathrm{d}\mathbf{x} = \sum_{i,j=1}^{3} \int_\Omega \partial_j u_i \partial_j v_i \, \mathrm{d}\mathbf{x}.$$

We now need to deal with the constraint $\nabla \cdot \mathbf{u} = 0$. The theoretical framework for saddle point problems requires that the corresponding bilinear form is the same as the second one appearing in the first part of the variational formulation. To this aim we multiply $\nabla \cdot \mathbf{u} = 0$ by a scalar test function (which will be associated to p) and integrate on the full domain, with an integration by parts in order to get the same bilinear form as in the first equation

$$\int_\Omega \nabla \cdot \mathbf{u} \, q \, \mathrm{d}\mathbf{x} = -\int_\Omega \mathbf{u} \cdot \nabla q \, \mathrm{d}\mathbf{x} = 0,$$

using that $q = 0$ on the boundary as an essential boundary condition. We finally obtain the mixed variational formulation: *Find* $(\mathbf{u}, p) \in H_0^1(\Omega)^3 \times H_0^1(\Omega)$ *such that*

$$\begin{cases} \int_\Omega \nabla \mathbf{u} : \nabla \mathbf{v} \, \mathrm{d}\mathbf{x} & + \int_\Omega \nabla p \cdot \mathbf{v} \, \mathrm{d}\mathbf{x} & = \int_\Omega \mathbf{f} \cdot \mathbf{v} \, \mathrm{d}\mathbf{x}, & \forall \mathbf{v} \in H_0^1(\Omega)^3 \\ \int_\Omega \mathbf{u} \cdot \nabla q \, \mathrm{d}\mathbf{x} & & = 0, & \forall p \in H_0^1(\Omega) \end{cases} \tag{196}$$

Another possibility to obtained a well posed variational formulation, is to integrate by parts the $\int_\Omega \nabla p \cdot \mathbf{v} \, \mathrm{d}\mathbf{x}$ term in the first formulation:

$$\int_\Omega \nabla p \cdot \mathbf{v} \, \mathrm{d}\mathbf{x} = -\int_\Omega p \nabla \cdot \mathbf{v} \, \mathrm{d}\mathbf{x} + \int_{\partial\Omega} p \mathbf{v} \cdot \mathbf{n} \, \mathrm{d}\sigma = -\int_\Omega p \, \nabla \cdot \mathbf{v} \, \mathrm{d}\mathbf{x},$$

using here $p = 0$ as a natural boundary condition. Note that in the other variational formulation the same boundary condition was essential. In this case, for the second variational formulation, we just multiply $\nabla \cdot \mathbf{u} = 0$ by q and integrate. No integration by parts is needed in this case.

$$\int_\Omega \nabla \cdot \mathbf{u} \, q \, \mathrm{d}\mathbf{x} = 0.$$

This then leads to the following variational formulation: *Find* $(\mathbf{u}, p) \in H^1(\Omega)^3 \times L^2(\Omega)$ *such that*

$$\begin{cases} \int_\Omega \nabla \mathbf{u} : \nabla \mathbf{v} \, \mathrm{d}\mathbf{x} & - \int_\Omega p \, \nabla \cdot \mathbf{v} \, \mathrm{d}\mathbf{x} & = \int_\Omega \mathbf{f} \cdot \mathbf{v} \, \mathrm{d}\mathbf{x}, & \forall \mathbf{v} \in H^1(\Omega)^3 \\ \int_\Omega \nabla \cdot \mathbf{u} \, q \, \mathrm{d}\mathbf{x} & & = 0, & \forall q \in L^2(\Omega) \end{cases} \tag{197}$$

Isogeometric Finite Elements

Contents

Sobolev estimations under h-refinement

Approximation properties without mapping

We consider a computational domain $\hat{\Omega} := (0,1)^d$, with $d \geq 1$. Given d knot vectors for each direction $T^{(\alpha)} := \{t_0^{(\alpha)}, \cdots, t_{n_\alpha+p_\alpha+1}^{(\alpha)}\}$. For $\alpha \in \{1, \cdots, d\}$, we denote $I_i^{(\alpha)} := (t_i^{(\alpha)}, t_{i+1}^{(\alpha)})$ and by construction we have $t_{p_\alpha}^{(\alpha)} = 0$ and $t_{n_\alpha}^{(\alpha)} = 1$. We shall denote $I := (0,1)$, *i.e.* $\hat{\Omega} = I^d$. The d knot vectors will define a natural triangulation of $\hat{\Omega}$, which we denote $\mathcal{Q}_h(\hat{\Omega})$ (the subscript h will be made clear later). An element of $Q \in \mathcal{Q}_h(\hat{\Omega})$ is of the form $\bigotimes_{1\leq\alpha\leq d} I_{i_\alpha}^{(\alpha)}$, for some multi-index $\mathbf{i} := (i_1, \cdots, i_d)$. We will denote the element size of $Q \in \mathcal{Q}_h(\hat{\Omega})$ by $h_Q := \text{diam}(Q)$, moreover, we shall define $h_{Q,\alpha}$ for $1 \leq \alpha \leq d$ as the length of $I_{i_\alpha}^{(\alpha)}$, while $h := \max_{Q\in\mathcal{Q}_h(\hat{\Omega})} h_Q$ will represent the global mesh size.

We shall also assume our mesh to be **locally quasi-uniform**, meaning, there exists a constant $\theta \geq 1$ such that

$$\frac{1}{\theta} \leq \frac{h_{I_{i_\alpha}^{(\alpha)},\alpha}}{h_{I_{i_\alpha+1}^{(\alpha)},\alpha}} \leq \theta, \quad \forall\, 1 \leq \alpha \leq d \tag{198}$$

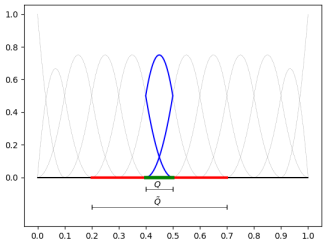

Figure 54: An element Q and its extension $\tilde{Q}$ for an open knot sequence, with quadratic B-Splines.

For every element Q we define its extension as the union of supports of non-vanishing B-Splines on Q, which we will denote by $\tilde{Q}$, (see figure **??**). Finally, the α-coordinate will be denoted by η_α for all $1 \leq \alpha \leq d$.

We recall that the Schoenberg space of degree p and associated to the knot sequence T is denoted by $\mathcal{S}_p(T)$. Another equivalent notation would be $\mathcal{S}_{\boldsymbol{\mu}}^p(T^\star)$ (or simply $\mathcal{S}_{\boldsymbol{\mu}}^p$ for the sake of simplicity), where as usual $T^\star$ denotes the set of breakpoints associated to T and $\boldsymbol{\mu}$ is a sequence of multiplicities of each breakpoint. More generaly, in higher dimensions, the Schoenberg space is defined by tensor product

$$V_h := \bigotimes_{1\leq\alpha\leq d} \mathcal{S}_{\boldsymbol{\mu}_\alpha}^{p_\alpha} \tag{199}$$

Finally, we shall denote by Π_h a quasi-interpolant on V_h.

Let us introduce the following space of functions, which will be needed to define the bent Sobolev space:

$$\mathcal{D}_T^s(I) := \{f \in L^2(I);\ D_-^k f(t_i) = D_+^k f(t_i), \quad \forall\, 0 \leq k \leq \min(s-1, \mu_i),\ \forall\, 1 \leq i \leq n-1\} \tag{200}$$

We define the **bent Sobolev space** on I as

$$\mathcal{H}^s(I) = \{f \in L^2(I),\ f|_Q \in H^s(Q),\ \forall Q \in \mathcal{Q}_h(I) \text{ and } f \in \mathcal{D}_T^s\} \tag{201}$$

The bent Sobolev spaces are endowed with the broken norm and seminorms

$$\|f\|^2_{\mathcal{H}^s(I)} := \sum_{0\leq j\leq s} |f|^2_{\mathcal{H}^j(I)} \tag{202}$$

where

$$|f|^2_{\mathcal{H}^j(I)} := \sum_{I_i\in\mathcal{Q}_h(I)} |f|^2_{H^j(I_i)} \tag{203}$$

In higher dimensions, the bent Sobolev spaces are defined by tensor product, for a multi-index $\mathbf{s} = (s_1, \cdots, s_d)$, as follows

$$\mathcal{H}^{\mathbf{s}}(\hat{\Omega}) = \bigotimes_{1\leq\alpha\leq d} \mathcal{H}^{s_\alpha}(I) \tag{204}$$

which are endowed by the tensor-product norm and seminorms.

For any sufficiently regular function $f : \hat{\Omega} \to \mathbb{R}$, we shall define the partial derivative operator of order $\mathbf{r}$ (a multi-index)

$$D^{\mathbf{r}} f := \frac{\partial^{r_1}\dots\partial^{r_d}}{\partial\eta_1^{r_1}\dots\partial\eta_d^{r_d}} f \tag{205}$$

Finally, for any union $A \subset \hat{\Omega}$ of elements of the triangulation $\mathcal{Q}_h(\hat{\Omega})$, we will define

$$\|f\|^2_{L^2_h(A)} := \sum_{Q\in\mathcal{Q}_h(\hat{\Omega}) \text{ and } Q\subset A} \|f\|^2_{L^2(Q)} \tag{206}$$

The following proposition gives a local anisotropic estimation of the best approximation.

Proposition 44 (Anisotropic estimation in 2d) *If $0 \leq \mathbf{r} \leq \mathbf{s} \leq \mathbf{p}+1$, there exists a constant $C(\mathbf{p},\theta)$ such that for all elements $Q \in \mathcal{Q}_h(\hat{\Omega})$, we have*

$$\|D^{\mathbf{r}}(f-\Pi_f)\|_{L^2(Q)} \leq C\left(h_{Q,1}^{s_1-r_1}\|D^{(s_1,r_2)}f\|_{L^2_h(\widetilde{Q})} + h_{Q,2}^{s_2-r_2}\|D^{(r_1,s_2)}f\|_{L^2_h(\widetilde{Q})}\right) \tag{207}$$

for all $f \in \mathcal{H}^{(s_1,r_2)}(\hat{\Omega}) \cap \mathcal{H}^{(r_1,s_2)}(\hat{\Omega})$.

Approximation properties with mapping

We now turn to the general case, where the domain $\Omega := \mathbf{F}(\hat{\Omega})$ with $\mathbf{F} : \mathbb{R}^d \to \mathbb{R}^d$ is a one to one map. We shall use the results from the previous section on $\hat{\Omega}$, and then assume that $\hat{\Omega} := (0,1)^d$. The α-coordinate will be denoted, in this case, by x_α for all $1 \leq \alpha \leq d$. Ω will be subdivided into elements $K := \mathbf{F}(Q)$ where $Q \in \mathcal{Q}_h(\hat{\Omega})$, hence

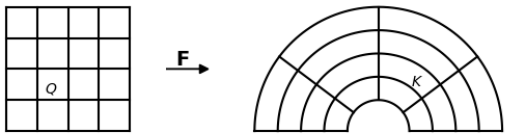

Figure 55: The triangulation $\mathcal{Q}_h(\hat{\Omega})$ in the logical domain and its image $\mathcal{Q}_h(\Omega)$, under the mapping $\mathbf{F}$. An element $Q \in \mathcal{Q}_h(\hat{\Omega})$ is mapped onto $K \in \mathcal{Q}_h(\Omega)$.

$\mathcal{Q}_h(\Omega) := \mathbf{F}(\mathcal{Q}_h(\hat{\Omega}))$. Moreover, every extension $\widetilde{K}$ of K is also of the form $\mathbf{F}(\widetilde{Q})$ with $K = \mathbf{F}(Q)$.

In order to define the bent Sobolev space, we will first introduce the following broken norms and seminorms

$$\|f\|^2_{\mathcal{H}^{\mathbf{s}}_{\mathbf{F}}(A)} := \sum_{0\leq \mathbf{j}\leq \mathbf{s}} |f|^2_{\mathcal{H}^{\mathbf{j}}_{\mathbf{F}}(A)} \tag{208}$$

where

$$|f|^2_{\mathcal{H}^{\mathbf{s}}_{\mathbf{F}}(A)} := \sum_{K\in\mathcal{Q}_h(\Omega) \text{ s.t. } K\subset A} \|D^{\mathbf{s}}_{\mathbf{F}} f\|^2_{L^2(K)} \tag{209}$$

Finally, we shall consider the *bent Sobolev space* $\mathcal{H}^{\mathbf{s}}_{\mathbf{F}}$ as the **closure** of $C^\infty(\Omega)$ with respect to the norm $\|\cdot\|_{\mathcal{H}^{\mathbf{s}}_{\mathbf{F}}}$. We can now state the approximation theorem on the bent Sobolev space, which is suitable for anistropic estimates.

Theorem 33 *If $0 \leq \mathbf{r} \leq \mathbf{s} \leq \mathbf{p}+1$, there exists a constant $C(\mathbf{p},\theta,\mathbf{F})$ such that for all elements $K \in \mathcal{Q}_h(\Omega)$, we have*

$$\|f-\Pi_h f\|_{\mathcal{H}^{\mathbf{r}}_{\mathbf{F}}(K)} \leq C\left(h^{s_1-r_1}_{K,1}\|f\|_{\mathcal{H}^{(s_1,r_2)}_{\mathbf{F}}(\widetilde{K})} + h^{s_2-r_2}_{K,2}\|f\|_{\mathcal{H}^{(r_1,s_2)}_{\mathbf{F}}(\widetilde{K})}\right) \tag{210}$$

for all $f \in \mathcal{H}^{(s_1,r_2)}(\Omega) \cap \mathcal{H}^{(r_1,s_2)}(\Omega)$.

Corollary 3 *If $0 \leq r \leq s \leq \min(\mathbf{p})+1$, there exists a constant $C(\mathbf{p},\theta,\mathbf{F})$ such that for all elements $K \in \mathcal{Q}_h(\Omega)$, we have*

$$\|f-\Pi_h f\|_{H^r(K)} \leq C h^{s-r}_K \|f\|_{H^s(\widetilde{K})} \tag{211}$$

and

$$\|f-\Pi_h f\|_{H^r(\Omega)} \leq C h^{s-r} \|f\|_{H^s(\Omega)} \tag{212}$$

for all $f \in H^s(\Omega)$.

Galerkin approximation

As in the previous section, we shall distinguish between the two cases with and without mapping.

Case without mapping

We consider a first coarse mesh, which is given in this case by one element in each direction $\hat{\Omega} = (0,1)^d$. Then we define a sequence of d knot vectors $\left(\{T_N^{(\alpha)},\ 1 \leq \alpha \leq d\}\right)_{N\geq 0}$ such that $\lim_{N\to\infty} h_N = 0$ where h_N is the diameter associated to the triangulation endowed by the knot vectors $\{T_N^{(\alpha)},\ 1 \leq \alpha \leq d\}$.

Remark 29 *Creating such a sequence of knot vectors can be done through the insertion of knots, as presented in the CAD part of this lecture.*

For every N, we have a Schoenberg space associated to the knot vectors $\{T_N^{(\alpha)},\ 1 \leq \alpha \leq d\}$, which is denoted by V_h.

Matrix form for Poisson: We consider the Poisson problem with Homogeneous Dirichlet boundary conditions, for which the variational problem writes: *Find* $u \in H_0^1(\hat{\Omega})$ *such that*

$$\int_{\hat{\Omega}} \nabla u \cdot \nabla v \ \mathrm{d}\boldsymbol{\eta} = \int_{\hat{\Omega}} f v \ \mathrm{d}\boldsymbol{\eta}, \quad \forall v \in H_0^1(\hat{\Omega}) \tag{213}$$

One can create a subspace of $H_0^1(\hat{\Omega})$ from the tensor product of Schoenberg spaces (199), by removing the first and last B-Splines, which are interpolatories (equal to 1) at the endpoints in every direction, which we will denote by V_h^0. From now on, we shall use multi-indices and introduce the tensor B-Splines functions

$$N_{\boldsymbol{i}}^{\boldsymbol{p}}(\boldsymbol{\eta}) := \prod_{1\leq\alpha\leq d} N_{i_\alpha}^{p_\alpha}(\eta_\alpha) \tag{214}$$

where $\boldsymbol{\eta} = (\eta_1, \cdots, \eta_d)$, $\boldsymbol{p} = (p_1, \cdots, p_d)$ and $\boldsymbol{i} = (i_1, \cdots, i_d)$. Using these notations, we have

$$V_h = \mathrm{span}\{N_{\boldsymbol{i}}^{\boldsymbol{p}};\ 0 \leq \boldsymbol{i} \leq \boldsymbol{n}\} \tag{215}$$

while

$$V_h^0 = \mathrm{span}\{N_{\boldsymbol{i}}^{\boldsymbol{p}};\ 1 \leq \boldsymbol{i} \leq \boldsymbol{n} - 1\} \tag{216}$$

where $\boldsymbol{n} = (n_1, \cdots, n_d)$.

The discrete variational formulation is: *Find* $u \in V_h^0$ *such that*

$$\int_{\hat{\Omega}} \nabla u \cdot \nabla v \ \mathrm{d}\boldsymbol{\eta} = \int_{\hat{\Omega}} f v \ \mathrm{d}\boldsymbol{\eta}, \quad \forall v \in V_h^0 \tag{217}$$

Let $u_h \in V_h^0$ such that $u_h = \sum_j u_j N_j^{\boldsymbol{p}}$. Then the weak formulation for the Poisson equation writes

$$\sum_j u_j \int_{\hat{\Omega}} \nabla N_j^{\boldsymbol{p}} \cdot \nabla N_i^{\boldsymbol{p}} \ \mathrm{d}\boldsymbol{\eta} = \int_{\hat{\Omega}} f N_i^{\boldsymbol{p}} \ \mathrm{d}\boldsymbol{\eta}, \quad \forall 1 \leq \boldsymbol{i} \leq \boldsymbol{n} - 1$$

In practice, in order to store these terms, we will need to have a reordering of the indices so that we map the set of multi-indices $\{1 \leq \boldsymbol{i} \leq \boldsymbol{n} - 1\}$ onto a set of 1d indices $\{1 \leq I \leq N\}$. Using this reordering, we get the following linear system

$$MU = F$$

where U denotes the coefficients $(u_J,\ 1 \leq J \leq N)$ and F is a vector consisting of the terms $\int_{\hat{\Omega}} f N_i^{\boldsymbol{p}} \ \mathrm{d}\boldsymbol{\eta}$ for $1 \leq \boldsymbol{i} \leq \boldsymbol{n} - 1$. Finally, the matrix M is called the stiffness matrix and its entries are defined as

$$M_{IJ} = \int_{\hat{\Omega}} \nabla N_j^{\boldsymbol{p}} \cdot \nabla N_i^{\boldsymbol{p}} \ \mathrm{d}\boldsymbol{\eta}$$

Exercise 34 *We assume in this exercise $d = 2$. Show that solving the associated linear system to the Poisson problem is equivalent to*

Find $X \in \mathbb{R}^{n_1 - 1} \times \mathbb{R}^{n_2 - 1}$, such that

$$S_1 X M_2 + M_1 X S_2 = F \tag{218}$$

where the vector of unknowns (and right hand side) are viewed as matrices in $X \in \mathbb{R}^{n_1 - 1} \times \mathbb{R}^{n_2 - 1}$.

Matrix form for the Bilaplacian problem: TODO

Case with mapping

In this case, the coarse mesh is given by the mapping $\mathbf{F}$ if it is discrete (constructed using B-Splines or NURBS). Let us denote $V_{\mathbf{F}}$ the Schoenberg space associated to the mapping $\mathbf{F}$. We shall denote $\{T_{\mathbf{F}}^{(\alpha)},\ 1 \leq \alpha \leq d\}$ the knot vectors associated $V_{\mathbf{F}}$, the corresponding multiplicities to the beakpoints will be denoted $\boldsymbol{\mu}_{\mathbf{F}}^{\alpha}$, for every $1 \leq \alpha \leq d$.

The family of discrete subspaces needed for the Galerkin approximation, must be created such that the breakpoints of $T_{\mathbf{F}}^{(\alpha)}$ are contained in $T_N^{(\alpha)}$, for every $1 \leq \alpha \leq d$. There are two reasons for this constraint:

1. A theoretical one, due to the definition of the bent Sobolev spaces,
2. A computational one, due to the quadrature rule that will be used on each element $Q \in \mathcal{Q}_h(\hat{\Omega})$ of the logical domain.

Figure 56: Coarse mesh in the logical and physical domain induced by a quadratic representation using two Bézier patchs for each quarter of the annulus. In the radial direction, linear splines are used.

Figure 57: Coarse mesh in the logical and physical domain induced by a cubic representation using one Bézier patch. In the radial direction, linear splines are used.

In figure 56, we show a parametrization of half of the annulus using quadratic B-Splines (NURBS) in the angular direction, with the knot vector $\{0, 0, 0, \frac{1}{2}, \frac{1}{2}, 1, 1, 1\}$. In the radial direction, we use linear B-Splines with the knot vector $\{0, 0, 1, 1\}$. This leads to a coarse mesh of two elements in the first parametric direction and one in the second direction.

In figure 57, we show a parametrization of half of the annulus using cubic B-Splines (NURBS) in the angular direction, with the knot vector $\{0, 0, 0, 0, 1, 1, 1, 1\}$. In the radial direction, we use linear B-Splines with the knot vector $\{0, 0, 1, 1\}$. This leads to a coarse mesh of one element in each parametric direction.

Given a coarse parametrization of the domain, we can use the *h-refinement* strategy which is achieved by inserting new knots in each direction.

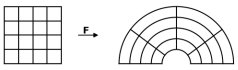

Figure 58: The mapping used in Fig. 57 after inserting 3 new knots in each direction, leading to 4 elements in each direction.

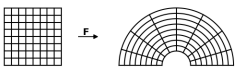

Figure 59: The mapping used in Fig. 57 after inserting 7 new knots in each direction, leading to 8 elements in each direction.

Matrix form for Poisson The discrete subspaces are defined as

$$V_h^0 = \text{span}\{N_{\boldsymbol{i}}^{\boldsymbol{p}} \circ \mathbf{F}^{-1};\ 1 \leq \boldsymbol{i} \leq \boldsymbol{n} - 1\} \tag{219}$$

where $\boldsymbol{n} = (n_1, \cdots, n_d)$.

The discrete variational formulation is: *Find* $u \in V_h^0$ *such that*

$$\int_\Omega \nabla u \cdot \nabla v \ \mathrm{d}\boldsymbol{x} = \int_\Omega f v \ \mathrm{d}\boldsymbol{x}, \quad \forall v \in V_h^0 \tag{220}$$

The next step is to map back the gradients from the physical domain to the logical one. Since for any function u we have,

$$\nabla u(\boldsymbol{x}) = (\mathcal{D}\mathbf{F})^{-T}\, \hat{\nabla} u(\mathbf{F}^{-1}(\boldsymbol{x})) \tag{221}$$

we can plug this expression in (220) which will lead to a kind of general elliptic problem on the logical domain. It is important to notice that for performance issues, we will not invert the jacobian matrix everytime, but rather computing the inverse analyticaly (or symbolicaly) in 2d and 3d.

Exact DeRham sequences

In the sequel, we shall give exact DeRham sequences based on B-Splines in $\mathbb{R}^d$ for $d = 1, 2, 3$. We assume that the domain Ω is **simply connected**. Let us first recall that in 1D, DeRham sequence is reduced to

$$H^1(\Omega) \quad \xrightarrow{\boldsymbol{\nabla}} \quad L^2(\Omega)$$

in 2d, we have two sequences

$$H^1(\Omega) \quad \xrightarrow{\boldsymbol{\nabla}} \quad \boldsymbol{H}(\text{curl}, \Omega) \xrightarrow{\nabla\times} \quad L^2(\Omega)$$

and

$$H^1(\Omega) \quad \xrightarrow{\boldsymbol{\nabla}\times} \quad \boldsymbol{H}(\mathrm{div},\Omega) \xrightarrow{\nabla\cdot} \quad L^2(\Omega)$$

while in 3d, we have the following sequence

$$H^1(\Omega) \quad \xrightarrow{\boldsymbol{\nabla}} \quad \boldsymbol{H}(\mathrm{curl},\Omega) \quad \xrightarrow{\nabla\times} \quad \boldsymbol{H}(\mathrm{div},\Omega) \quad \xrightarrow{\nabla\cdot} \quad L^2(\Omega)$$

For simplicity, we shall introduce the operator d , that corresponds to the appropriate operator ($\boldsymbol{\nabla}$, $\nabla\times$, ...) for a given space, and rewrite our diagrams as

- 1D case:

$$H^1(\Omega) \quad \xrightarrow{\mathrm{d}} \quad L^2(\Omega) \tag{222}$$

- 2D case:

$$H^1(\Omega) \quad \xrightarrow{\mathrm{d}} \quad \boldsymbol{H}(\mathrm{curl},\Omega) \xrightarrow{\mathrm{d}} \quad L^2(\Omega) \tag{223}$$

$$H^1(\Omega) \quad \xrightarrow{\mathrm{d}} \quad \boldsymbol{H}(\mathrm{div},\Omega) \xrightarrow{\mathrm{d}} \quad L^2(\Omega) \tag{224}$$

- 3D case:

$$H^1(\Omega) \quad \xrightarrow{\mathrm{d}} \quad \boldsymbol{H}(\mathrm{curl},\Omega) \quad \xrightarrow{\mathrm{d}} \quad \boldsymbol{H}(\mathrm{div},\Omega) \quad \xrightarrow{\mathrm{d}} \quad L^2(\Omega) \tag{225}$$

Exact sequence in 1D

We start by taking a subspace $V_h(\mathrm{grad},\Omega) \subset H^1(\Omega)$. In 1D, $V_h(\mathrm{grad},\Omega)$ is a Schoenberg space associated to a given knot sequence T. We know that both B-Splines and M-Splines can be used as basis for the Schoenberg space. If we take the B-Splines as the canonical basis on $V_h(\mathrm{grad},\Omega) := \mathrm{span}\{N_i^p, 0 \leq i \leq n\}$, we know that every function $u \in V_h(\mathrm{grad},\Omega)$ can be written as $u = \sum_i u_i N_i^p$. By taking its derivative, we get

$$u' = \sum_i u_i \left(N_i^p\right)' = \sum_i (-u_{i-1} + u_i) M_i^{p-1}$$

since

$$\left(N_i^p\right)' = M_i^{p-1} - M_{i+1}^{p-1}$$

Now if we introduce the space $V_h(L^2,\Omega) := \mathrm{span}\{M_i^{p-1}, 0 \leq i \leq n\}$. We just have shown that

$$\forall u \in V_h(\mathrm{grad},\Omega), \quad u' \in V_h(L^2,\Omega) \tag{226}$$

On the other hand, it is clear that the operator d is surjective (for any function $u \in V_h(L^2,\Omega)$, the function $\int_{x_0}^{x} u(t)\,dt$ is clearly in $V_h(\text{grad},\Omega)$). This is summarized in the following diagram

$$V_h(\text{grad},\Omega) \quad \xrightarrow{\text{d}} \quad V_h(L^2,\Omega) \tag{227}$$

where

$$\left\{\begin{array}{lll} V_h(\text{grad},\Omega) & = \mathcal{S}_{\boldsymbol{\mu}}^{p} & := \text{span}\{N_i^p,\ 0 \leq i \leq n\} \\ V_h(L^2,\Omega) & = \mathcal{M}_{\boldsymbol{\mu}-1}^{p-1} & := \text{span}\{M_i^{p-1},\ 0 \leq i \leq n\} \end{array}\right. \tag{228}$$

Remark 30 *Let us introduce the B-Splines coefficients vector* $\mathbf{u} := (u_i)_{1\leq i\leq n}$ *(and* $\mathbf{u}^\star$ *for the derivative), we have*

$$\mathbf{u}^\star = \mathcal{D}\mathbf{u} \tag{229}$$

where $\mathcal{D}$ *is the incidence matrix (of entries* -1 *and* $+1$*).*

Exact sequences in 2D

Let us introduce the spaces

$$\left\{\begin{array}{ll} V_h(\text{grad},\Omega) & = \mathcal{S}_{\mu_1}^{p_1} \otimes \mathcal{S}_{\mu_2}^{p_2} \\ \boldsymbol{V}_h(\text{curl},\Omega) & = \begin{pmatrix} \mathcal{M}_{\mu_1-1}^{p_1-1} \otimes \mathcal{S}_{\mu_2}^{p_2} \\ \mathcal{S}_{\mu_1}^{p_1} \otimes \mathcal{M}_{\mu_2-1}^{p_2-1} \end{pmatrix} \\ \boldsymbol{V}_h(\text{div},\Omega) & = \begin{pmatrix} \mathcal{S}_{\mu_1}^{p_1} \otimes \mathcal{M}_{\mu_2-1}^{p_2-1} \\ \mathcal{M}_{\mu_1-1}^{p_1-1} \otimes \mathcal{S}_{\mu_2}^{p_2} \end{pmatrix} \\ V_h(L^2,\Omega) & = \mathcal{M}_{\mu_1-1}^{p_1-1} \otimes \mathcal{M}_{\mu_2-1}^{p_2-1} \end{array}\right. \tag{230}$$

Lemma 14 *We have the following properties*

- $\boldsymbol{\nabla} V_h(grad,\Omega) \subset \boldsymbol{V}_h(curl,\Omega)$
- $\nabla \times \boldsymbol{V}_h(curl,\Omega) \subset V_h(L^2,\Omega)$
- $\boldsymbol{\nabla} \times V_h(grad,\Omega) \subset \boldsymbol{V}_h(curl,\Omega)$
- $\nabla \cdot \boldsymbol{V}_h(curl,\Omega) \subset V_h(L^2,\Omega)$

Proof. Can be deduced thanks to the property (226). ∎

Proposition 45 *We have the following diagrams*

$$V_h(grad,\Omega) \quad \xrightarrow{\text{d}} \quad \boldsymbol{V}_h(curl,\Omega) \xrightarrow{\text{d}} \quad V_h(L^2,\Omega) \tag{231}$$

$$V_h(grad,\Omega) \quad \xrightarrow{\text{d}} \quad \boldsymbol{V}_h(div,\Omega) \xrightarrow{\text{d}} \quad V_h(L^2,\Omega) \tag{232}$$

Proof. We shall restrict our proofto the sequence (231) and show that using the previous discrete spaces, we maintain the same relationships as in the continuous case.

Since Ω is simply connected, we know that in the continuous case, the kernel of the curl operator is equal to the range of the gradient operator, *i.e.*

$$\boldsymbol{\nabla}(H^1(\Omega)) = \mathcal{N}(\nabla\times)$$

Showing the exactness of the discrete DeRham sequence means that the last property is preserved in the discrete case. We shall then show that

$$\boldsymbol{\nabla}(V_h(\text{grad},\Omega)) = \mathcal{N}(\nabla\times) \cap \boldsymbol{V}_h(\text{curl},\Omega)$$

since fpr amm $u \in V_h(\text{grad},\Omega)$ we have $\nabla \times \boldsymbol{\nabla} u = 0$, we get

$$\boldsymbol{\nabla}(V_h(\text{grad},\Omega)) \subset \mathcal{N}(\nabla\times) \cap \boldsymbol{V}_h(\text{curl},\Omega)$$

In order to show the equality, it is enough to show that both spaces have the same dimension. But we have $\dim V_h(\text{grad},\Omega) = (n_1 + 1)(n_2 + 1)$. But since, Ω is simply connected we hae $\dim \mathcal{N}(\boldsymbol{\nabla}) = 1$ and therefor we have

$$\dim \boldsymbol{\nabla}(V_h(\text{grad},\Omega)) = (n_1+1)(n_2+1) - 1$$

On the other hand, we have

$$\begin{aligned}\dim \boldsymbol{V}_h(\text{curl},\Omega) &= \dim\left(\mathcal{N}(\nabla\times) \cap \boldsymbol{V}_h(\text{curl},\Omega)\right) + \dim\left(\mathcal{R}(\nabla\times) \cap \boldsymbol{V}_h(\text{curl},\Omega)\right)\\ &= n_1(n_2+1) + (n_1+1)n_2\end{aligned}$$

meaning

$$\dim\left(\mathcal{N}(\nabla\times) \cap \boldsymbol{V}_h(\text{curl},\Omega)\right) = 2n_1n_2 + n_1 + n_2 - \dim\left(\mathcal{R}(\nabla\times) \cap \boldsymbol{V}_h(\text{curl},\Omega)\right)$$

In order to show that

$$\dim \boldsymbol{\nabla}(V_h(\text{grad},\Omega)) = \dim\left(\mathcal{N}(\nabla\times) \cap \boldsymbol{V}_h(\text{curl},\Omega)\right)$$

it is then enough to show that

$$\dim\left(\mathcal{R}(\nabla\times) \cap \boldsymbol{V}_h(\text{curl},\Omega)\right) = n_1n_2$$

but since the operator $\nabla\times : \boldsymbol{V}_h(\text{curl},\Omega) \to V_h(L^2,\Omega)$ is surjective (proof similar to the 1d case), we deduce that $\nabla \times (\boldsymbol{V}_h(\text{curl},\Omega)) = V_h(L^2,\Omega)$. Finally, we have $\dim V_h(L^2,\Omega) = n_1n_2$ which completes the proof. ∎

Remark 31 *The discrete derivatives in 2D are given by*

$$\begin{cases} \mathbb{G} &= \begin{pmatrix} \mathcal{D} \otimes \mathbb{I} \\ \mathbb{I} \otimes \mathcal{D} \end{pmatrix} \\ \mathbb{C} &= \begin{pmatrix} \mathbb{I} \otimes \mathcal{D} \\ -\mathcal{D} \otimes \mathbb{I} \end{pmatrix} \\ \mathbb{C} &= \begin{pmatrix} -\mathbb{I} \otimes \mathcal{D} & \mathcal{D} \otimes \mathbb{I} \end{pmatrix} \\ \mathbb{D} &= \begin{pmatrix} \mathcal{D} \otimes \mathbb{I} & \mathbb{I} \otimes \mathcal{D} \end{pmatrix} \end{cases} \tag{233}$$

where we used the identity matrix $\mathbb{I}$*.*

Exact sequence in 3D

Let us introduce the spaces

$$\begin{cases} V_h(\text{grad}, \Omega) &= \mathcal{S}^{p_1}_{\mu_1} \otimes \mathcal{S}^{p_2}_{\mu_2} \otimes \mathcal{S}^{p_3}_{\mu_3} \\ \boldsymbol{V}_h(\text{curl}, \Omega) &= \begin{pmatrix} \mathcal{M}^{p_1-1}_{\mu_1-1} \otimes \mathcal{S}^{p_2}_{\mu_2} \otimes \mathcal{S}^{p_3}_{\mu_3} \\ \mathcal{S}^{p_1}_{\mu_1} \otimes \mathcal{M}^{p_2-1}_{\mu_2-1} \otimes \mathcal{S}^{p_3}_{\mu_3} \\ \mathcal{S}^{p_1}_{\mu_1} \otimes \mathcal{S}^{p_2}_{\mu_2} \otimes \mathcal{M}^{p_3-1}_{\mu_3-1} \end{pmatrix} \\ \boldsymbol{V}_h(\text{div}, \Omega) &= \begin{pmatrix} \mathcal{S}^{p_1}_{\mu_1} \otimes \mathcal{M}^{p_2-1}_{\mu_2-1} \otimes \mathcal{M}^{p_3-1}_{\mu_3-1} \\ \mathcal{M}^{p_1-1}_{\mu_1-1} \otimes \mathcal{S}^{p_2}_{\mu_2} \otimes \mathcal{M}^{p_3-1}_{\mu_3-1} \\ \mathcal{M}^{p_1-1}_{\mu_1-1} \otimes \mathcal{M}^{p_2-1}_{\mu_2-1} \otimes \mathcal{S}^{p_3}_{\mu_3} \end{pmatrix} \\ V_h(L^2, \Omega) &= \mathcal{M}^{p_1-1}_{\mu_1-1} \otimes \mathcal{M}^{p_2-1}_{\mu_2-1} \otimes \mathcal{M}^{p_3-1}_{\mu_3-1} \end{cases} \tag{234}$$

Proposition 46 *We have the following diagram*

$$V_h(grad, \Omega) \xrightarrow{\text{d}} \boldsymbol{V}_h(curl, \Omega) \xrightarrow{\text{d}} \boldsymbol{V}_h(div, \Omega) \xrightarrow{\text{d}} V_h(L^2, \Omega) \tag{235}$$

Remark 32 *The discrete derivatives in 3D are given by*

$$\begin{cases} \mathbb{G} &= \begin{pmatrix} \mathcal{D} \otimes \mathbb{I} \otimes \mathbb{I} \\ \mathbb{I} \otimes \mathcal{D} \otimes \mathbb{I} \\ \mathbb{I} \otimes \mathbb{I} \otimes \mathcal{D} \end{pmatrix} \\ \mathbb{C} &= \begin{pmatrix} 0 & -\mathbb{I} \otimes \mathbb{I} \otimes \mathcal{D} & \mathbb{I} \otimes \mathcal{D} \otimes \mathbb{I} \\ \mathbb{I} \otimes \mathbb{I} \otimes \mathcal{D} & 0 & -\mathcal{D} \otimes \mathbb{I} \otimes \mathbb{I} \\ -\mathbb{I} \otimes \mathcal{D} \otimes \mathbb{I} & \mathcal{D} \otimes \mathbb{I} \otimes \mathbb{I} & 0 \end{pmatrix} \\ \mathbb{D} &= \begin{pmatrix} \mathcal{D} \otimes \mathbb{I} \otimes \mathbb{I} & \mathbb{I} \otimes \mathcal{D} \otimes \mathbb{I} & \mathbb{I} \otimes \mathbb{I} \otimes \mathcal{D} \end{pmatrix} \end{cases} \tag{236}$$

where we used the identity matrix $\mathbb{I}$*.*

Commuting diagrams

DeRham diagrams such as (222), (223), (224) and (225) can be extended with additional operators. Among the important properties,

one can build specific projectors that make these diagrams commute. We shall start with the 1D case, then extend it by tensor product. For this purpose, we take any interpolator, denoted by I_T^p, (Fix-DeBoor for theoretical studies, or B-Splines interpolator), quasi-interpolator or least-square approximation associated to a given knot sequence T and degree p, and then we define the corresponding histopolation operator by

$$H_T^p f := D I_T^{p+1} \left(x \mapsto \int_{x_0}^{x} f \, dx \right) \tag{237}$$

1D case

We then introduce the operators

$$\begin{cases} P_h^{\text{grad}} & := I_T^p \\ P_h^{L^2} & := H_T^{p-1} \end{cases} \tag{238}$$

Proposition 47 *For any $u \in C^\infty(\Omega)$, we have*

$$\mathrm{d}\, P_h^{grad}(u) = P_h^{L^2}(\mathrm{d}\, u) \tag{239}$$

Exercise 35 *Prove the previous proposition.*

These results are summarized in the following commuting diagram

$$\begin{array}{ccc} H^s(\Omega) & \xrightarrow{\mathrm{d}} & H^{s-1}(\Omega) \\ P_h^{\text{grad}} \downarrow & & P_h^{L^2} \downarrow \\ V_h(\text{grad}, \Omega) & \xrightarrow{\mathrm{G}} & V_h(L^2, \Omega) \end{array} \tag{240}$$

2D case

We then introduce the operators

$$\begin{cases} P_h^{\text{grad}} & := I_{T_1}^{p_1} \odot I_{T_2}^{p_2} \\ P_h^{\text{curl}} & := \begin{pmatrix} H_{T_1}^{p_1-1} \odot I_{T_2}^{p_2} \\ I_{T_1}^{p_1} \odot H_{T_2}^{p_2-1} \end{pmatrix} \\ P_h^{\text{div}} & := \begin{pmatrix} I_{T_1}^{p_1} \odot H_{T_2}^{p_2-1} \\ H_{T_1}^{p_1-1} \odot I_{T_2}^{p_2} \end{pmatrix} \\ P_h^{L^2} & := H_{T_1}^{p_1-1} \odot H_{T_2}^{p_2-1} \end{cases} \tag{241}$$

where the notation $\odot$ to express the composition of operators on each coordinate, for example,

$$I_{T_1}^{p_1} \odot I_{T_2}^{p_2} f := I_{T_1}^{p_1} \left(x \mapsto I_{T_2}^{p_2} \left(y \mapsto f(x, y) \right) \right)$$

Proposition 48 *For any $u \in C^\infty(\Omega)$ and $\boldsymbol{u} \in \mathbf{C}^\infty(\Omega)$, we have*

1) for the first sequence (231)

$$\mathrm{d}\, P_h^{grad}(u) = P_h^{curl}(\mathrm{d}\, u) \tag{242}$$

$$\mathrm{d}\, P_h^{curl}(\boldsymbol{u}) = P_h^{L^2}(\mathrm{d}\, \boldsymbol{u}) \tag{243}$$

2) for the second sequence (232)

$$\mathrm{d}\, P_h^{grad}(u) = P_h^{div}(\mathrm{d}\, u) \tag{244}$$

$$\mathrm{d}\, P_h^{div}(\boldsymbol{u}) = P_h^{L^2}(\mathrm{d}\, \boldsymbol{u}) \tag{245}$$

Exercise 36 *Prove the previous proposition.*

These results are summarized in the following commuting diagrams

$$\begin{array}{ccccc} H^1(\Omega) & \xrightarrow{\boldsymbol{\nabla}} & \boldsymbol{H}(\mathrm{curl},\Omega) & \xrightarrow{\nabla\times} & L^2(\Omega) \\ \downarrow{\scriptstyle P_h^{\mathrm{grad}}} & & \downarrow{\scriptstyle P_h^{\mathrm{curl}}} & & \downarrow{\scriptstyle P_h^{L^2}} \\ V_h(\mathrm{grad},\Omega) & \xrightarrow{\mathbb{G}} & \boldsymbol{V}_h(\mathrm{curl},\Omega) & \xrightarrow{\mathbb{C}} & V_h(L^2,\Omega) \end{array} \tag{246}$$

and

$$\begin{array}{ccccc} H^1(\Omega) & \xrightarrow{\nabla\times} & \boldsymbol{H}(\mathrm{div},\Omega) & \xrightarrow{\nabla\cdot} & L^2(\Omega) \\ \downarrow{\scriptstyle P_h^{\mathrm{grad}}} & & \downarrow{\scriptstyle P_h^{\mathrm{div}}} & & \downarrow{\scriptstyle P_h^{L^2}} \\ V_h(\mathrm{grad},\Omega) & \xrightarrow{\mathbf{C}} & \boldsymbol{V}_h(\mathrm{div},\Omega) & \xrightarrow{\mathbb{D}} & V_h(L^2,\Omega) \end{array} \tag{247}$$

3D case

We then introduce the operators

$$\left\{\begin{array}{ll} P_h^{\mathrm{grad}} & := I_{T_1}^{p_1} \odot I_{T_2}^{p_2} \odot I_{T_3}^{p_3} \\ P_h^{\mathrm{curl}} & := \begin{pmatrix} H_{T_1}^{p_1-1} \odot I_{T_2}^{p_2} \odot I_{T_3}^{p_3} \\ I_{T_1}^{p_1} \odot H_{T_2}^{p_2-1} \odot I_{T_3}^{p_3} \\ I_{T_1}^{p_1} \odot I_{T_2}^{p_2} \odot H_{T_3}^{p_3-1} \end{pmatrix} \\ P_h^{\mathrm{div}} & := \begin{pmatrix} I_{T_1}^{p_1} \odot I_{T_2}^{p_2} \odot H_{T_3}^{p_3-1} \\ I_{T_1}^{p_1} \odot H_{T_2}^{p_2-1} \odot I_{T_3}^{p_3} \\ H_{T_1}^{p_1-1} \odot I_{T_2}^{p_2} \odot I_{T_3}^{p_3} \end{pmatrix} \\ P_h^{L^2} & := H_{T_1}^{p_1-1} \odot H_{T_2}^{p_2-1} \odot H_{T_3}^{p_3-1} \end{array}\right. \tag{248}$$

Proposition 49 *For any $u \in C^\infty(\Omega)$ and $\boldsymbol{u} \in \mathbf{C}^\infty(\Omega)$, we have*

$$\mathrm{d}\, P_h^{grad}(u) = P_h^{curl}(\mathrm{d}\, u) \tag{249}$$

$$\mathrm{d}\, P_h^{curl}(\boldsymbol{u}) = P_h^{div}(\mathrm{d}\, \boldsymbol{u}) \tag{250}$$

$$\mathrm{d}\, P_h^{div}(\boldsymbol{u}) = P_h^{L^2}(\mathrm{d}\, \boldsymbol{u}) \tag{251}$$

Exercise 37 *Prove the previous proposition.*

These results are summarized in the following commuting diagram

$$\begin{array}{ccccccc} H^1(\Omega) & \xrightarrow{\boldsymbol{\nabla}} & \boldsymbol{H}(\mathrm{curl},\Omega) & \xrightarrow{\nabla\times} & \boldsymbol{H}(\mathrm{div},\Omega) & \xrightarrow{\nabla\cdot} & L^2(\Omega) \\ \downarrow{\scriptstyle P_h^{\mathrm{grad}}} & & \downarrow{\scriptstyle P_h^{\mathrm{curl}}} & & \downarrow{\scriptstyle P_h^{\mathrm{div}}} & & \downarrow{\scriptstyle P_h^{L^2}} \\ V_h(\mathrm{grad},\Omega) & \xrightarrow{\mathrm{G}} & \boldsymbol{V}_h(\mathrm{curl},\Omega) & \xrightarrow{\mathrm{C}} & \boldsymbol{V}_h(\mathrm{div},\Omega) & \xrightarrow{\mathbb{D}} & V_h(L^2,\Omega) \end{array} \tag{252}$$

Pullbacks

In the case where the physical domain $\Omega := \mathcal{F}(\hat{\Omega})$ is the *image* of a *logical* domain $\hat{\Omega}$ by a smooth mapping $\mathcal{F}$ (at least $\mathcal{C}^1$), we have the following *parallel* diagrams (253)

$$\begin{array}{ccccccc} H^1(\Omega) & \xrightarrow{\boldsymbol{\nabla}} & \boldsymbol{H}(\mathrm{curl},\Omega) & \xrightarrow{\nabla\times} & \boldsymbol{H}(\mathrm{div},\Omega) & \xrightarrow{\nabla\cdot} & L^2(\Omega) \\ \uparrow{\scriptstyle \imath^0} & & \uparrow{\scriptstyle \imath^1} & & \uparrow{\scriptstyle \imath^2} & & \uparrow{\scriptstyle \imath^3} \\ H^1(\hat{\Omega}) & \xrightarrow{\boldsymbol{\nabla}} & H(\mathrm{curl},\hat{\Omega}) & \xrightarrow{\nabla\times} & H(\mathrm{div},\hat{\Omega}) & \xrightarrow{\nabla\cdot} & L^2(\hat{\Omega}) \end{array} \tag{253}$$

Where the mappings $\imath^0, \imath^1, \imath^2$ and $\imath^3$ are called *pullbacks* and are given by Eq. (254), (255), (256) and (257). with $D\mathcal{F}$ is the jacobian matrix

$$\imath^0\hat{\phi} := \quad \boldsymbol{x} \to \hat{\phi}(\mathbf{F}^{-1}(\boldsymbol{x})) \qquad \forall\, \hat{\phi} \in H^1(\hat{\Omega}) \tag{254}$$

$$\imath^1\hat{\Psi} := \quad \boldsymbol{x} \to (\mathcal{D}\mathbf{F})^{-T}\,\hat{\Psi}(\mathbf{F}^{-1}(\boldsymbol{x})) \quad \forall\, \hat{\Psi} \in H(\mathrm{curl},\hat{\Omega}) \tag{255}$$

$$\imath^2\hat{\Phi} := \quad \boldsymbol{x} \to \frac{1}{J}\mathcal{D}\mathbf{F}\hat{\Phi}(\mathbf{F}^{-1}(\boldsymbol{x})) \quad \forall\, \hat{\Phi} \in H(\mathrm{div},\hat{\Omega}) \tag{256}$$

$$\imath^3\hat{\rho} := \quad \boldsymbol{x} \to \hat{\rho}(\mathbf{F}^{-1}(\boldsymbol{x})) \qquad \forall\, \hat{\rho} \in L^2(\hat{\Omega}) \tag{257}$$

of the mapping $\mathcal{F}$. We recall that the pullbacks $\imath^0, \imath^1, \imath^2$ and $\imath^3$ are *isomorphisms* between the corresponding spaces, with $\imath^1$ and $\imath^2$ are the Piola transformations.

Exercise 38 *Write these matrices in an explicit form, using symbolic calculus or analyticaly.*

Matrix form for Poisson using mixed FEM: TODO

Matrix form for $\boldsymbol{H}(curl, \Omega)$-elliptic problem: TODO

Matrix form for $\boldsymbol{H}(div, \Omega)$-elliptic problem: TODO

Part IV

Appendices

List of Figures

List of Tables

Bibliography

[1] Q.-X. Huang, S.-M. Hu, and R. R. Martin. Fast degree elevation and knot insertion for b-spline curves. *Computer Aided Geometric Design*, 22(2):183 – 197, 2005.